NUREG/CR-0195
ANL-78-55

Distribution
Code: R-2

ARGONNE NATIONAL LABORATORY
9700 South Cass Avenue
Argonne, Illinois 60439

POST-CHF HEAT TRANSFER DURING STEADY-STATE AND TRANSIENT CONDITIONS

by

K. K. Fung*

Reactor Analysis and Safety Division

Published: June 1978

Prepared for the Systems Research Branch
Division of Reactor Safety Research
U. S. Nuclear Regulatory Commission
Washington, D. C. 20555
Under Interagency Agreement DOE 40-550-75

NRC FIN No. A2014

*University of Ottawa. Temporarily attached to
Atomic Energy of Canada Limited, Chalk River, Ontario, Canada

LIST OF CONTENTS

LIST OF FIGURES

LIST OF TABLES

POST-CHF HEAT TRANSFER DURING STEADY-STATE AND TRANSIENT CONDITIONS

by

K. K. Fung

ABSTRACT

This review extends previous reviews of steady-state post-CHF literature by Groeneveld, Gardiner, and Fung by including more recent data. A review of the literature on transient post-CHF data is also included by extending the work of Yadigaroglu.

INTRODUCTION

Post-CHF heat transfer is frequently encountered in the safety analysis of nuclear reactors. It corresponds to the boiling curve section to the right of the CHF as shown in Fig. 1a. As the wall temperature is increased beyond the CHF, the surface will be wetted intermittently. This regime is termed the "transition boiling". At temperatures above T_{min}, only the vapor phase will be in contact with the heated surface. This is the film boiling regime.

During film boiling the heated surface is cooled by radiation, forced convection to the vapor and liquid-wall interaction. The vapor can become highly superheated. The liquid is thought to be in the form of

(a) a dispersed spray of droplets, usually encountered at void fractions in excess of 80%. The corresponding flow regime is referred to as the "liquid-deficient regime" (Fig. 1b (i)).

(b) a continuous liquid core surrounded by vapor annulus. This is the inverted annular flow regime usually encountered at void fractions below 30% (Fig. 1b (ii)).

(c) a transition between the above two cases, usually in the form of slug flow (Fig. 1b (iii)).

Steady-state post-CHF heat transfer has been the subject of several review reports. Reviews of transition boiling were covered by Groeneveld and Fung [1976], high quality liquid deficient regime by Groeneveld [1975] and low quality and subcooled film boiling by Groeneveld and Gardiner [1977]. An exhaustive review of transient post-CHF heat transfer during the reflood phase of the LOCA was made by Yadigaroglu et al. [1975].

The purpose of this report is to consolidate the subject information and to review the more recent developments.

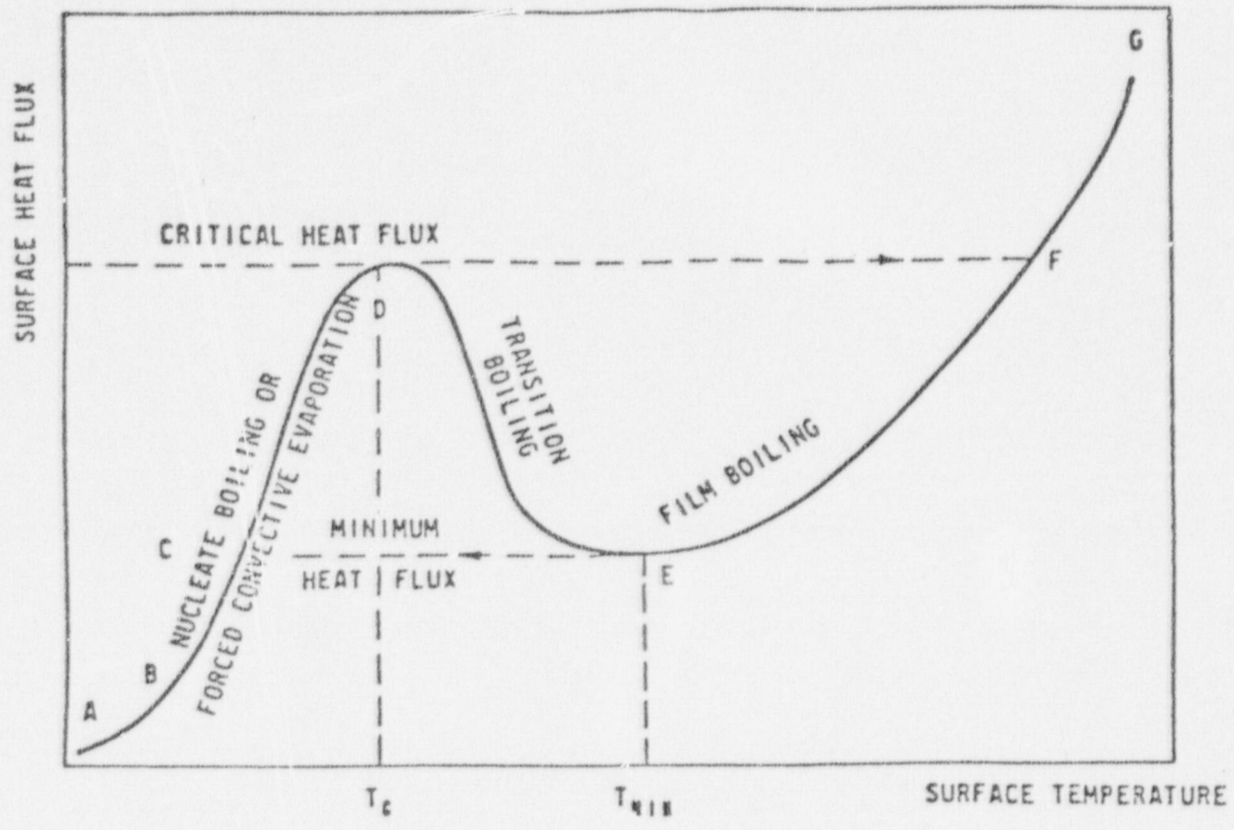

FIGURE 1a: BOILING CURVE

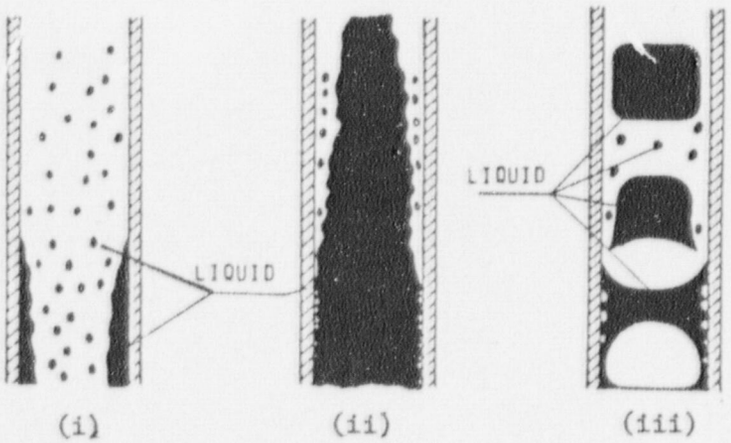

FIGURE 1b: FLOW REGIMES DURING FILM BOILING
(i) liquid deficient, (ii) inverse annular, (iii) slug flow

I. STEADY-STATE POST-CHF HEAT TRANSFER STUDIES

The most recent studies are listed in Table I.1. They are separated by boiling regimes and are reviewed in the following sections. For completeness, studies which were reviewed in previous reports are listed in Appendix 1.

I.1 TRANSITION BOILING

I.1.1 Recent Experimental Studies

Experimental studies were recently carried out in [illegible] and Britain, using a transient heat conduction quenching technique. Since the transients are very slow, the heat transfer process can be considered as semi-steady-state. This method, as originally used by Newbold [1976], Cheng [1976] and Fung [1976], consists of a short copper test block having a central flow passage. The test section was heated initially to a high temperature and then water at preset conditions was introduced. The temperature transient of the block is recorded by thermocouples located near the heat transfer surface. One of the drawbacks of this simple set-up is that high axial temperature gradients, sometimes comparable to the radial gradient (Fung [1976]), exist due to the presence of dryout and rewetting fronts at the entrance and exit. This renders the one-dimensional assumption used in the data reduction questionable. Nevertheless, these data still give some indication of the parametric trends. Improvements have since been made by Newbold et al. [1976], Cheng et al. [1978] and Ralph et al. [1977]. Newbold and Ralph used a composite test section formed from four copper cylinders separated by thin plated nickel-chromium alloy seals. In this way, the radial conductivity was much improved with respect to the axial conductivity. Cheng installed guard heaters just upstream of the test section to arrest the propagation of the quench front.

To establish the relationship between these transient data and those that would be obtained in a steady-state situation, Fung [1976] and Cheng et al. [1978] carried out some steady-state runs in the film boiling and nucleate boiling regions. In these tests, the test section power was carefully adjusted so that the surface temperature remained constant.

TABLE I.1: RECENT STEADY-STATE POST-CHF STUDIES [1978]

Authors	Geometry	Flow Conditions	Comments
Cheng et al. [1977]	Upflow in vertical tube ID = 12 mm nominal Inconel-copper and SS-copper composite test sections Length = 57 mm	136 $kg \cdot m^{-2} \cdot s^{-1}$ of water at subcoolings of 0 - 28°C; atm pressure	Study of surface effect on transition boiling
Ralph et al. [1977]	Vertical tube upward and downward flow ID = 10 mm Length = 77 mm Composite blocks	47 - 2170 $kg \cdot m^{-2} \cdot s^{-1}$ 0.2 MPa & 0.3 MPa 10°C & 30°C subcooling	Continuation of Newbold's experiment
Ragheb [1977]	ID = 12.7 mm Length = 105 mm Copper block	34 - 675 $kg \cdot m^{-2} \cdot s^{-1}$ of water at subcoolings of 0 to 20°C and atm pressure	Determination of transition boiling boundaries
Gardiner & Groeneveld [1977]	ID = 11.8 mm OD = 12.7 mm Heated length = 55.64 cm Inconel tube	50 - 250 $kg \cdot m^{-2} \cdot s^{-1}$ of water at subcoolings of 5 to 50°C; atm pressure	Steady-state low quality film boiling
Bailey [1977]	ID = 15 mm t = 1.5 mm Length = 5.4 m Inconel tube	50 - 1350 $kg \cdot m^{-2} \cdot s^{-1}$ of water at P = 14, 41 & 69 bar	High quality film boiling
Turner [1977]	21 & 25 rod bundles De = 1.5 & 1.35 cm Length = 2.13 m Inconel X-750	68 - 680 $kg \cdot m^{-2} \cdot s^{-1}$ P = 14 - 96 bar	High quality film boiling
Yates et al. [1975]	25 rod bundle 1.67 m heated length	135 - 540 $kg \cdot m^{-2} \cdot s^{-1}$ P = 35 bar X = 0.5 - 0.82	Only 5 points reported in film boiling
MacDonald [1977]	Zircaloy-clad, UO_2 fuel rod OD = 1.07 cm Shroud ID = 1.63 cm Length = 97 cm	775 - 2044 $kg \cdot m^{-2} \cdot s^{-1}$ P = 2.5 & 3.8 MPa	In-reactor tests of high quality film film boiling

Some of the results of Cheng et al. are shown in Figure 1.1. It can be seen that the transient and steady-state data are equivalent to each other. Fung further concluded that, although the assumption of the one-dimensional conduction in the data reduction method was not exact, the reduced data nevertheless represented an average heat flux over the entire length of the boiling surface.

Tests under a wide range of mass fluxes were carried out by Newbold, Fung and Ralph (typically from 10 - 1000 $kg \cdot m^{-2} \cdot s^{-1}$). Cheng concentrated only on the low flow range of 68 - 200 $kg \cdot m^{-2} \cdot s^{-1}$. It is found that the heat transfer improves with mass flux. A typical set of results of Newbold is shown in Figure 1.2. Fung [1976] noted that the increase was more significant in the low flow region of 135 - 675 $kg \cdot m^{-2} \cdot s^{-1}$. Ralph et al. [1977] also found that the increase was small above 400 $kg \cdot m^{-2} \cdot s^{-1}$ in the upflow tests. The higher rate of increase near the low flow region is probably due to the relatively higher increase of the inertial force over the buoyancy force.

The effect of inlet subcooling was investigated in the experiments of Fung [1976] and Cheng et al. [1978]. Figure 1.3 shows the recent results of Cheng et al. [1978]. The heat flux in the transition boiling region is found to increase with inlet subcooling. The results of Fung are somewhat different. The heat transfer coefficients for two mass fluxes are shown in Figures 1.4 and 1.5. They show that a saturated inlet condition has the highest heat transfer coefficient. Near the CHF, data at higher inlet subcoolings are lower than, and at best, approach this curve. Fung suggested that the better heat transfer at saturated inlet conditions was due to the higher vapor generation rate which resulted in a higher mixture velocity.

All of the recent studies have been carried out in vertical flow. In addition to the upflow tests common to all references cited above, Newbold and Ralph also carried out some tests with downflow. They found that, for the condition of higher subcooling, there was no significant difference between upflow and downflow. Newbold further noted that for conditions where saturation boiling existed, the heat transfer coefficients were lower in downflow. The lowest coefficient was observed

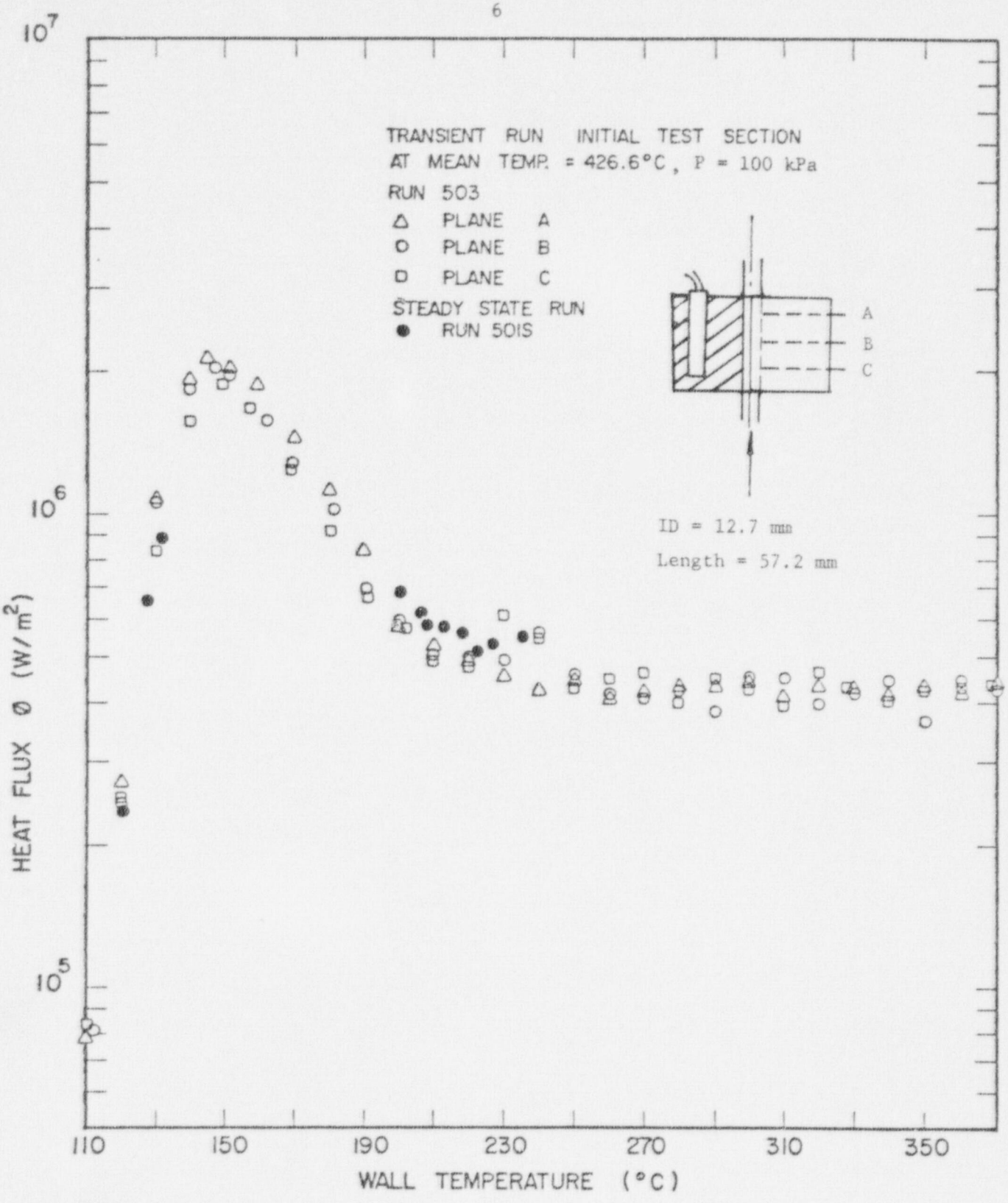

FIGURE 1.1: BOILING CURVES OF DISTILLED WATER FOR G = 136 $kg \cdot m^{-2} \cdot s^{-1}$ and ΔT_{sub} = 13.9°C (Cheng et al. [1978])

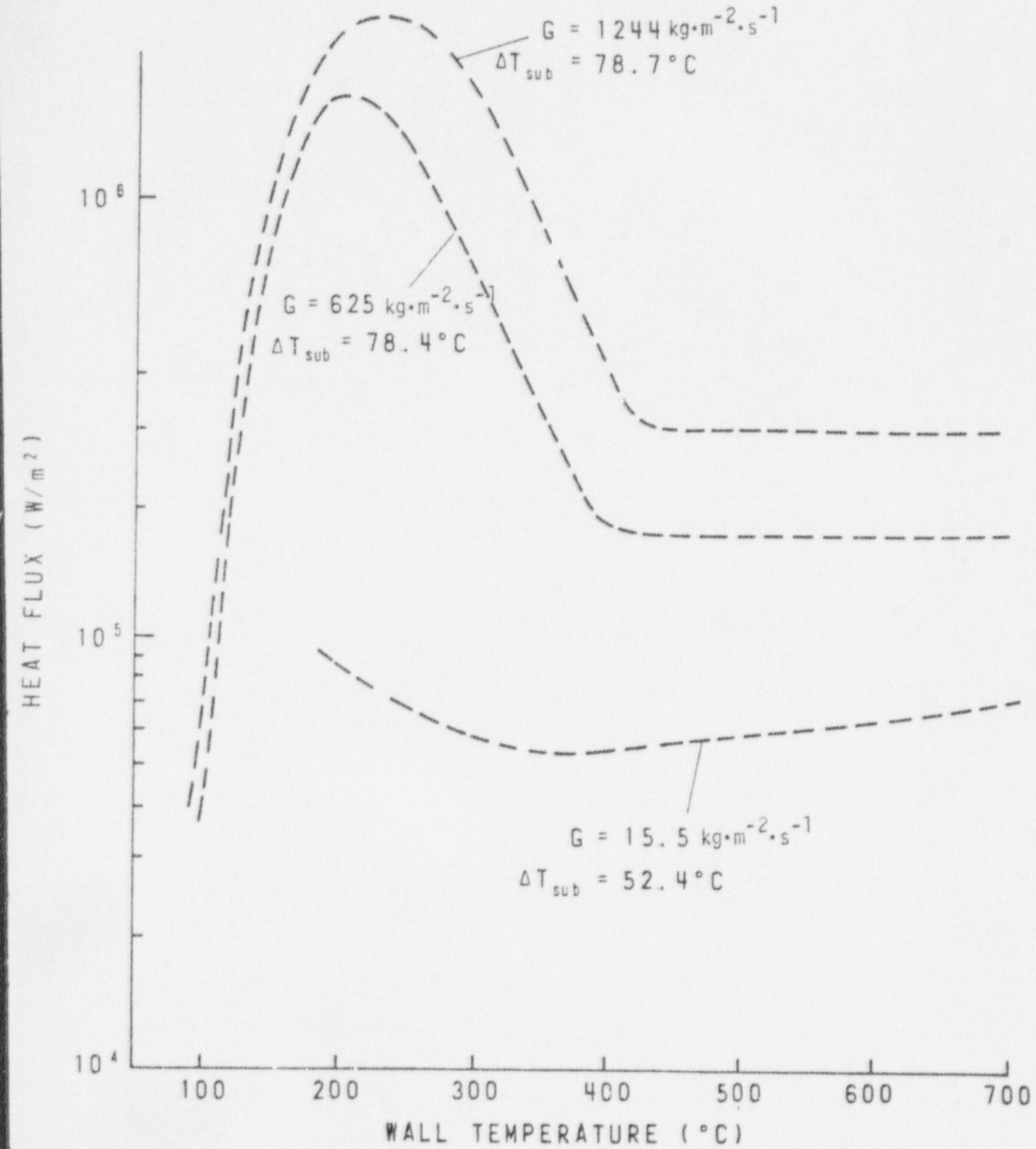

FIGURE 1.2: DATA OF NEWBOLD [1976] SHOWING THE EFFECT OF MASS FLUX FOR UPWARD FLOW OF WATER IN A 10 mm DIAMETER TEST SECTION 77 mm LONG (TRANSIENT TESTS). (PRESSURE = 300 kPa)

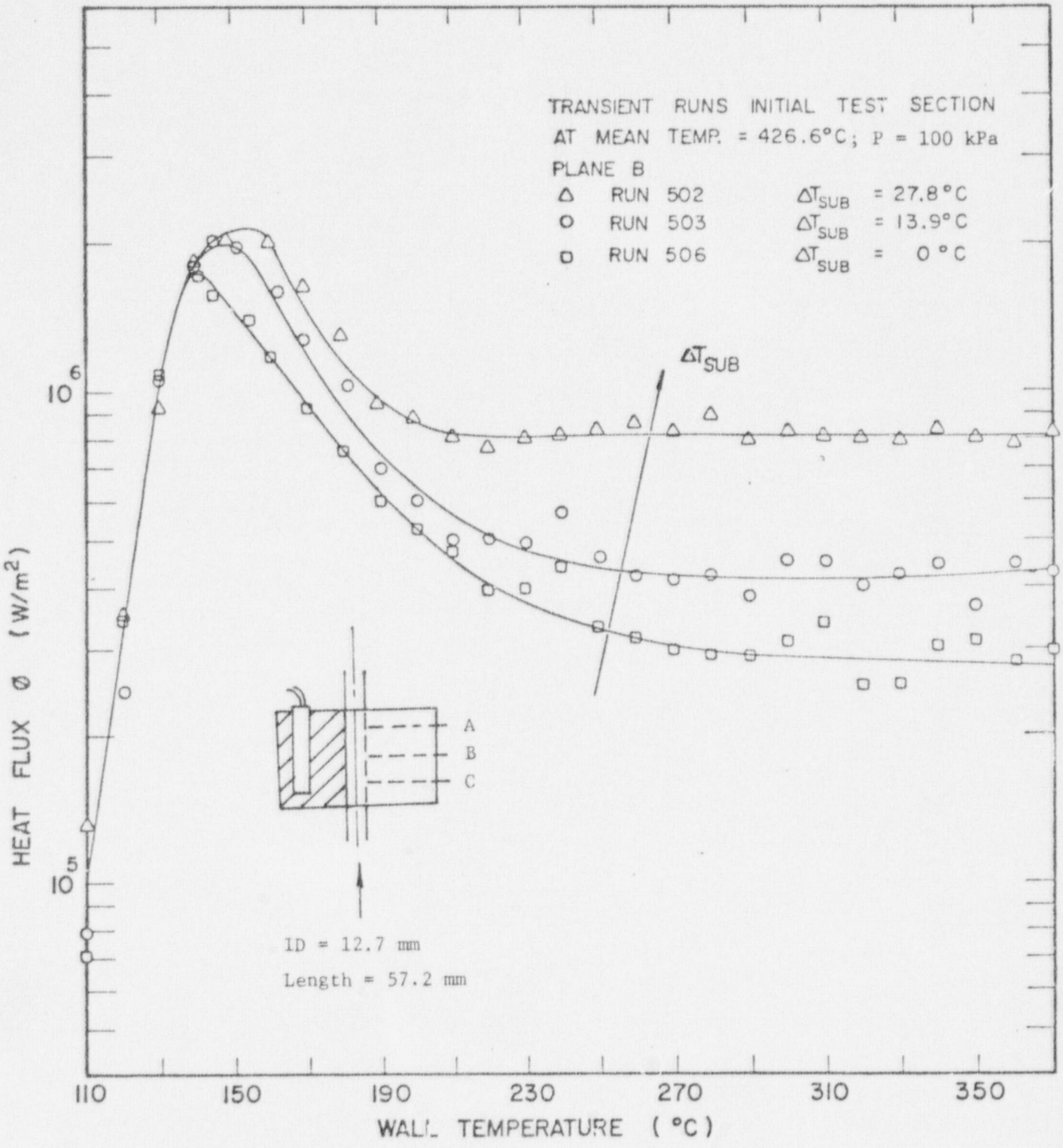

FIGURE 1.3: EFFECT OF SUBCOOLING ON BOILING CURVES OF DISTILLED WATER FOR G = 136 $kg \cdot m^{-2} \cdot s^{-1}$ (Cheng et al. [1978])

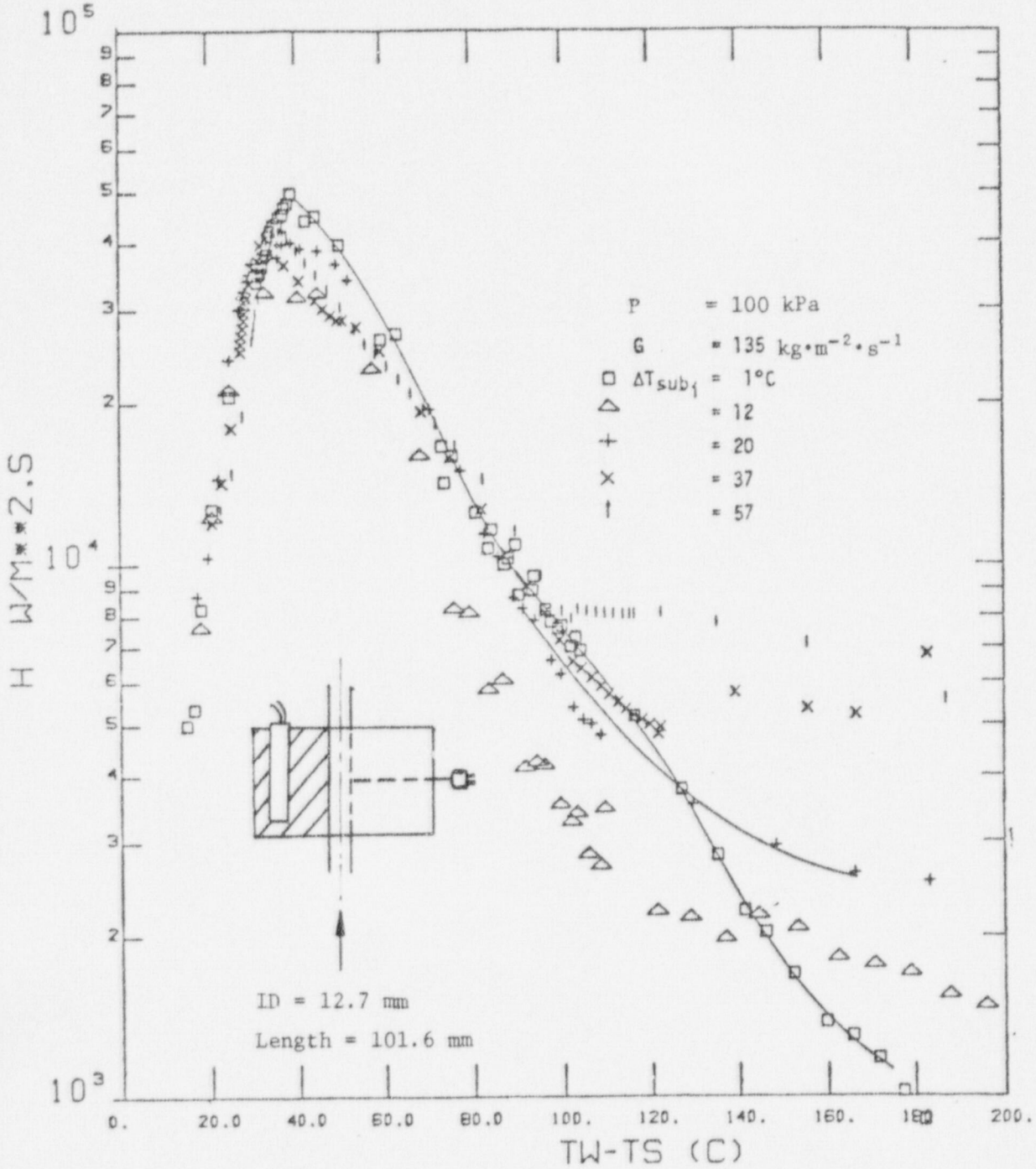

FIGURE 1.4: EFFECT OF SUBCOOLING ON THE HEAT TRANSFER COEFFICIENT AT MASS FLUX OF 135 $kg \cdot m^{-2} \cdot s^{-1}$ (Fung [1976])

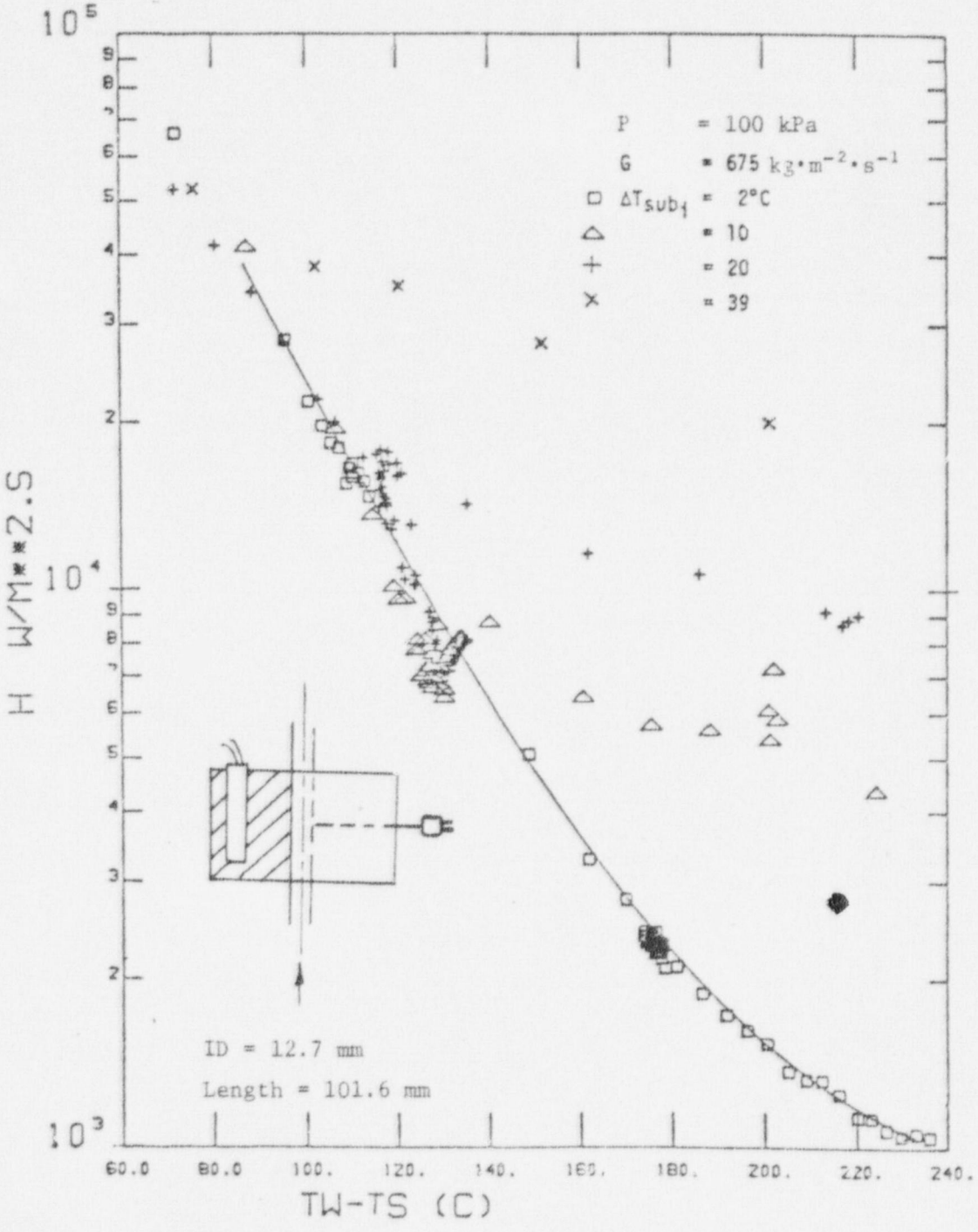

FIGURE 1.5: EFFECT OF SUBCOOLING ON THE HEAT TRANSFER COEFFICIENT AT MASS FLUX of 675 $kg \cdot m^{-2} \cdot s^{-1}$ (Fung [1976])

when the downward liquid velocity was very close to the rise velocity of a single isolated bubble.

The effect of different surface materials has been studied in a recent series of tests by Cheng et al. [1977]. In order to retain the long transition boiling period they,used a composite test section which consisted of the usual thick copper cylinder, with a thin stainless steel or Inconel tube soldered to the central bore. Some of the results are compared in Figure 1.6. Several observations can be made:

(1) The boiling curves are shifted to higher superheat.

(2) There is a difference in the boiling curves B and C obtained with stainless steel cladding of thickness 1.27 and 0.41 mm. Since in the data reduction the interface was taken as a nodal point and the boiling surface as the next one, discrepancies in representing the temperature gradient might probably arise as the cladding became thicker. This is even more evident by comparing the boiling curves A and C, which are obtained with stainless steel and Inconel claddings of comparable thickness. Here the transition regions of the two curves are very close to each other.

(3) The T_{CHF} and T_{min} depend on the surface material.

The above observations are tentative, pending further verification by experiments underway.

The boundary between the film boiling and transition boiling has been assumed to be the T_{min} (Groeneveld and Fung [1976]). However, the data of Newbold, Cheng and Fung show that just beyond the transition boiling region the film boiling heat flux is independent of the surface temperature. This casts much difficulty in locating the T_{min}. A recent experiment by Ragheb et al. [1978] demonstrated the relative extent of liquid-surface contact in transition boiling with respect to film and nucleate boiling. The test section used was similar to the one used by Cheng et al. The liquid-wall contact was indicated by an electric probe built into the boiling surface. The construction and installation details of the probe are shown schematically in the insert of Figure 1.8.

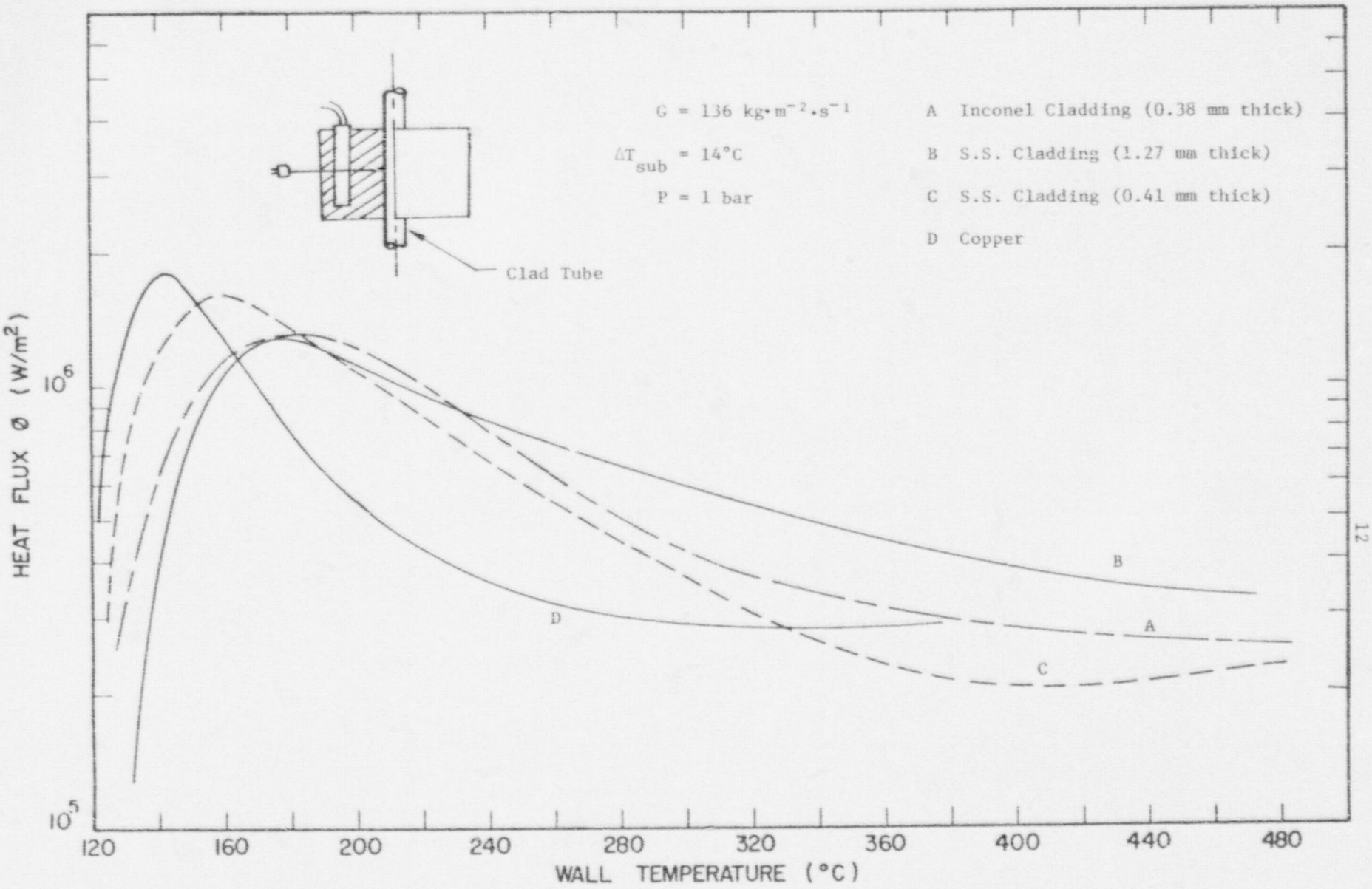

FIGURE 1.6: EFFECT OF SURFACE MATERIAL ON THE BOILING CURVE (Replot of data from Cheng et al.[1977])

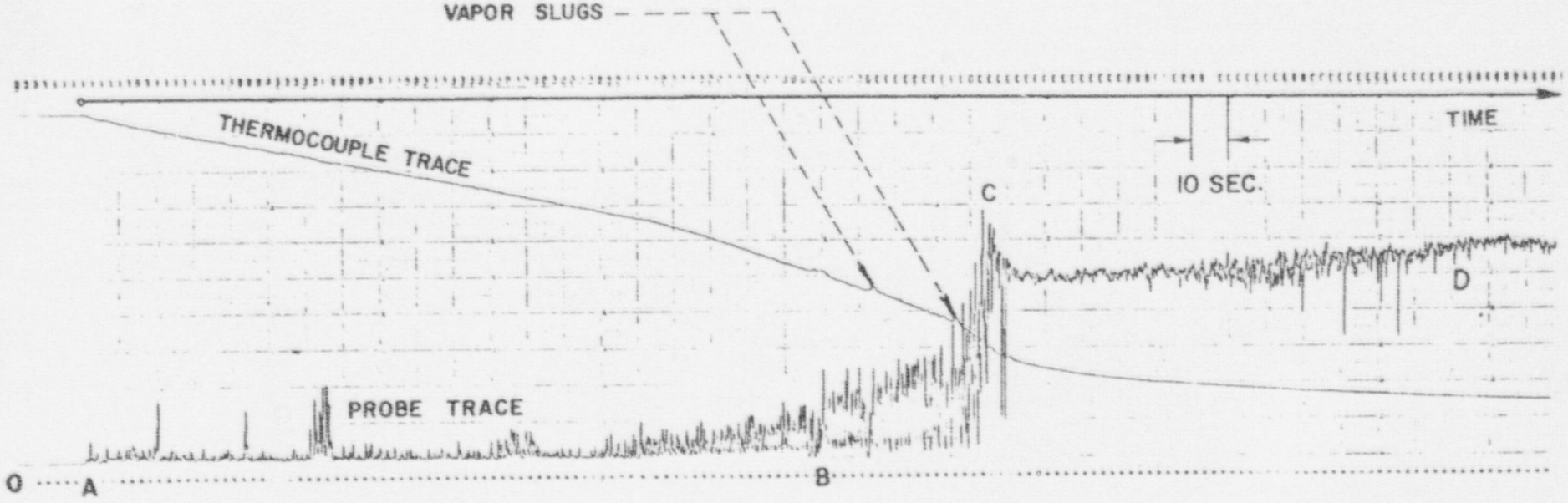

FIGURE 1.7: SIGNAL RECORDED FROM ZIRCONIUM--PLATINUM PROBE IN FLOW BOILING (Ragheb [1977])

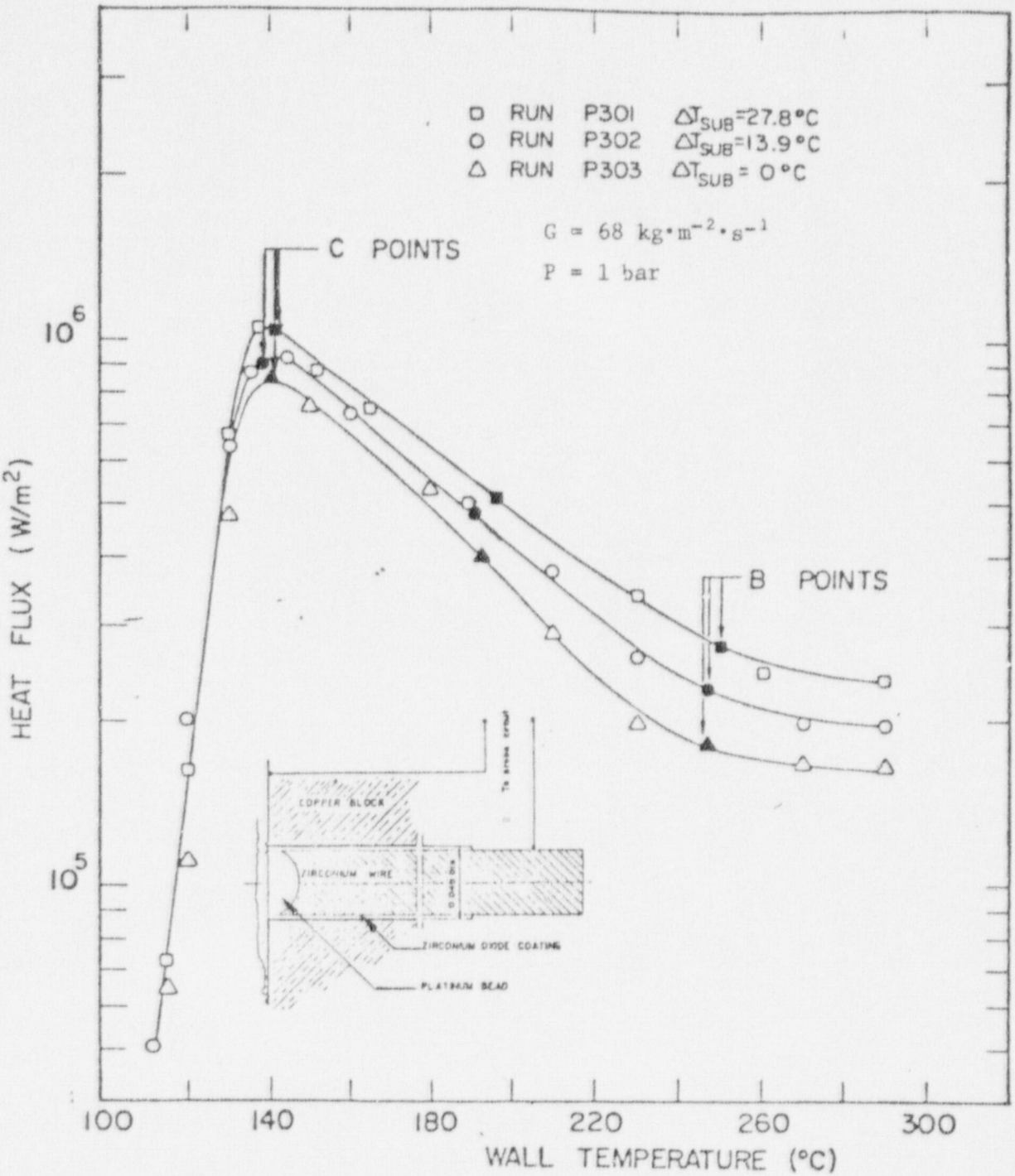

FIGURE 1.8: BOILING CURVES OF WATER (Ragheb [1977])

It consisted of a 1 mm zirconium wire insulated electrically from the test section by a zirconium-oxide film formed by autoclaving. A platinum coating was applied to the tip in order to avoid corrosion in the high temperature steam environment.

The signal from the probe during a quench of the test section is shown in Figure 1.7. The reduced data are shown as boiling curves in Figure 1.8. Ragheb et al. interpreted the signal as follows:

(i) Film boiling existed from A to B, with intermittent dry collisions showing up as spikes in the trace.

(ii) The region B to C characterized the transition boiling mode. Liquid-wall contact area and duration increased as the wall temperature decreased.

(iii) Beyond point C nucleate boiling was restored.

I.1.2 Prediction Methods

Most of the recent research efforts on transition boiling have been concentrated on obtaining reliable data. Fung [1976] and Cheng et al. [1978] compared their data with available correlations (Groeneveld and Fung [1976]) and found that their data were best correlated by the Berenson type correlation* with CHF and T_{CHF} obtained from the data and n varying from -1 to -1.5. A typical comparison is shown in Figure 1.9.

To the knowledge of this author, only two new prediction methods have come up since the review of Groeneveld and Fung [1976]. They are briefly outlined below.

(i) Bjornard and Griffith [1977]

In this proposed correlation, the transition boiling heat transfer is assumed to be composed of both nucleate boiling (wet wall) and film boiling (dry wall) heat transfer. They are weighted by δ, the fraction of wall area that is wet, to give

---

* $\frac{\phi}{CHF} \left(\frac{T_w - T_s}{T_{CHF} - T_s} \right)^n$

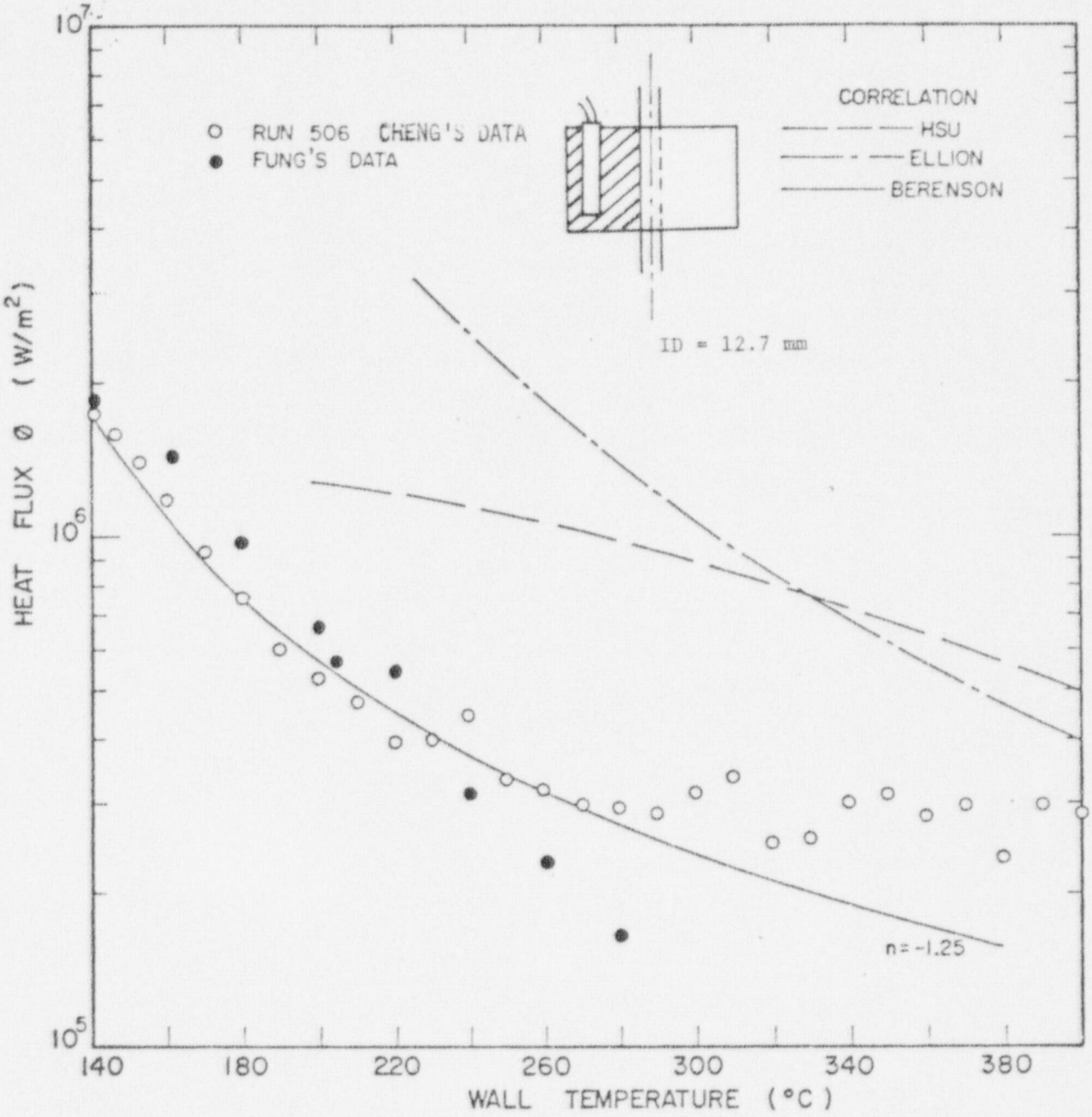

FIGURE 1.9: COMPARISON OF DATA IN THE TRANSITION AND FILM BOILING REGIMES FOR G = 136 $kg \cdot m^{-2} \cdot s^{-1}$, ΔT_{sub} = 0°C and P = 100 kPa (Cheng et al. [1978])

$$q''_{TB} = \delta q''_{CHF} + (1 - \delta) q''_{min}$$

$$\delta = \left(\frac{T_w - T_{min}}{T_{CHF} - T_{min}} \right)^2$$

(ii) Baum et al. [1977]

This is a theoretical model based on the oscillatory motions of a liquid-vapor interface normal to a vertical heat transfer surface and is applicable to low flow regime. The heat transfer during the liquid-wall contact period is assumed to be due to conduction and convection rather than by nucleate boiling. Solving the energy transport equation for the liquid in the direction normal to the wall, subjected to a constant temperature boundary condition, they found the following expression for the wall heat flux during one contact:

$$q'' = k_\ell (T_w - T_\ell) \left[\frac{v}{2\alpha_\ell} \left(1 + \operatorname{erf}\left(\frac{v}{2} \sqrt{\frac{t}{\alpha_\ell}} \right) \right) + \frac{1}{\sqrt{\pi \alpha_\ell t}} \exp\left(- \frac{v^2 t}{4\alpha_\ell} \right) \right]$$

The heat transfer during the off-contact period is assumed to be by conduction across the vapor film and is given by

$$q'' = k \frac{T_w - T_\ell}{\kappa_v}$$

where

$$k = k_v \left[1 + \left(\frac{Re - Re_o}{Re_o} \right)^{0.8} \right]$$

k_v = thermal conductivity of vapor

Re_o = transition between laminar and turbulent film flow (chosen to be 500)

$$Re = \frac{2\kappa_v K (T_w - T_\ell)}{i_{fg} \mu_v \eta}$$

$K = 1000$

κ_v = distance from wall to oscillating surface

η = distance from wall to valley of wave.

The average heat flux is determined by integrating the two components over the area and duration of the oscillation, which are obtained from a wave mechanics analysis.

They noted that their (pool) transition boiling data are best predicted by doubling the heat transfer component during contact. Agreement between the prediction and the data of Ramu et al. [1975] is shown to be satisfactory (Figure 1.10).

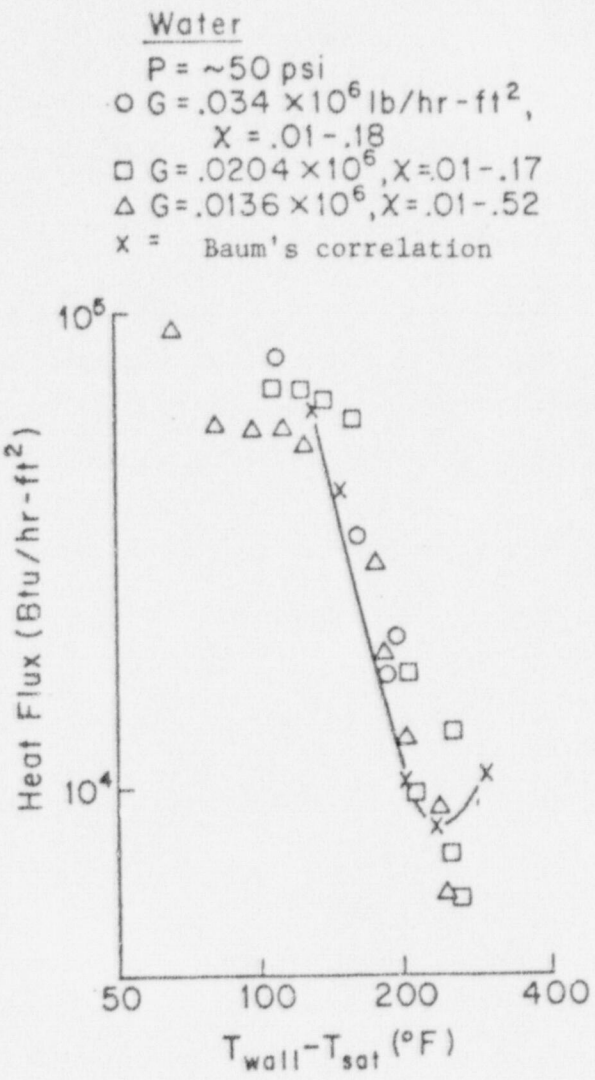

FIGURE 1.10: COMPARISON OF BAUM'S MODEL TO DATA OF RAMU & WEISMAN (BAUM [1977])

I.2 SUBCOOLED AND LOW QUALITY FILM BOILING

I.2.1 Recent Experimental Studies

In the transition boiling experiments of Newbold [1976], Cheng [1976], Fung [1976] and Ralph [1977], some film boiling data near the minimum temperature were also obtained. They observed that just beyond the minimum temperature, the film boiling heat flux was independent of the wall temperature. This implies a decrease in the heat transfer coefficient.

The technique of using a thick-walled copper cylinder is limited to short test sections, due to the axial conduction problem. Another method of obtaining flow film boiling data for subcooled water has recently been used by Groeneveld and Gardiner [1978]. This is the so called hot patch technique originally used by Groeneveld [1974] to study the effect of flux spikes on the CHF in Freon. It was discovered that, after steady film boiling was attained at the hot patch and the test section power raised gradually, the dry patch propagated downstream into the heated tube. It was immediately realized that this method could be used to obtain film boiling for subcooled water.

The test section used by Gardiner and Groeneveld [1977] is shown in Figure 2.1. The hot patch clamp was silver-soldered to the directly heated test section. The original purpose of the hot patch was to provide a dry patch location from which the vapor blanket could propagate downstream along the directly heated test section where steady-state heat transfer measurements could be made. It was found, however, that the spreading process was very slow in water and that excessive axial temperature variations occurred. This approach was therefore abandoned in favor of a much quicker and safer method.

The modified method employed the hot patch to stop and anchor a rewetting front rather than to initiate a spreading dry patch. Initially, the test section and the copper block were heated to temperatures well above the minimum film boiling temperature. When the flow was introduced, the high thermal inertia of the hot patch prevented the quench front from propagating further downstream. As a result the downstream portion of the

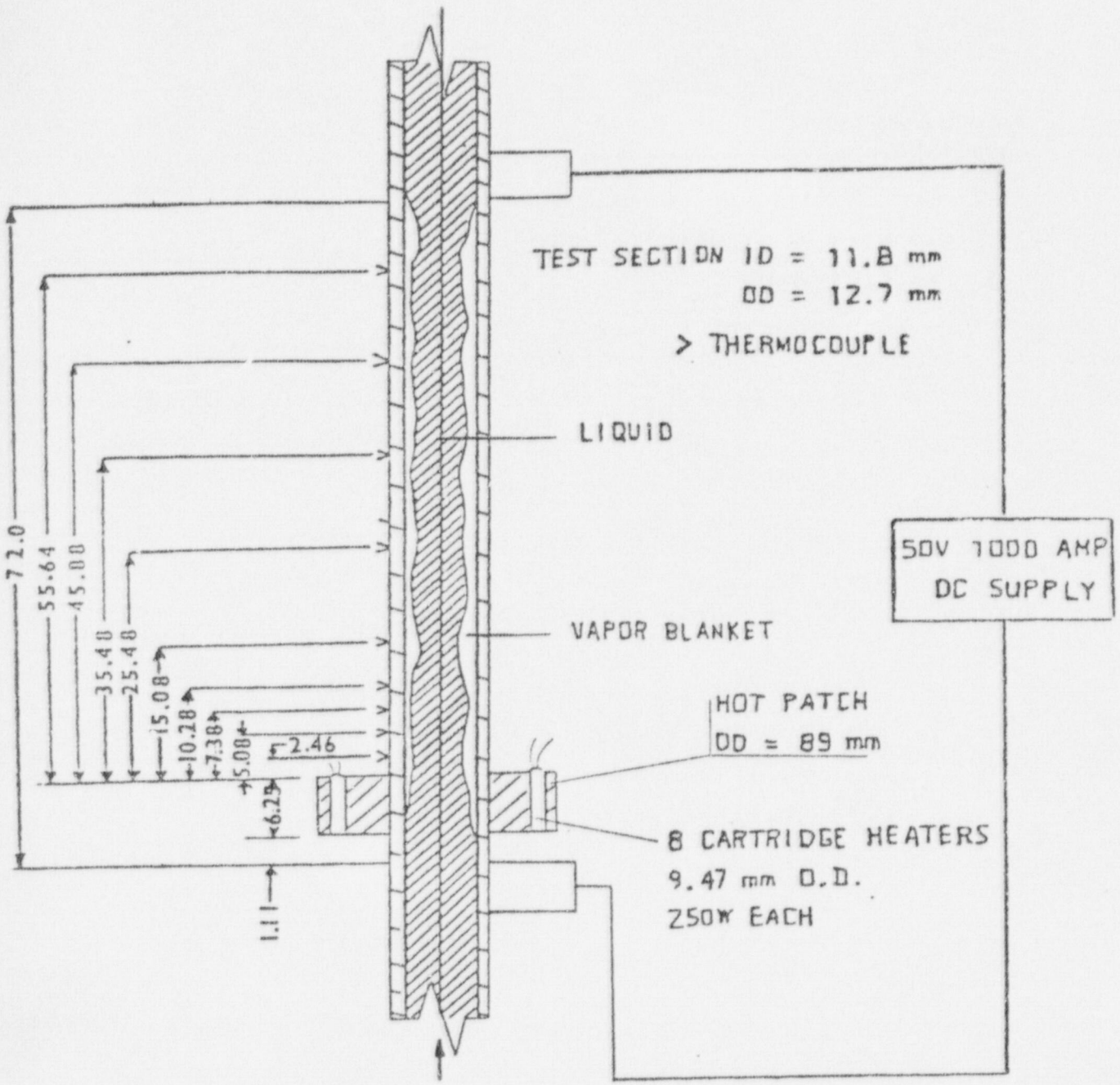

FIGURE 2.1: SCHEMATIC OF TEST SECTION
DIMENSIONS IN CM UNLESS INDICATED OTHERWISE
(Gardiner and Groeneveld [1977])

test section continued to experience film boiling at heat flux levels well below the CHF for uniform heating, thus permitting the measurement of steady-state film boiling temperatures.

The experiment of Gardiner and Groeneveld [1977] covered a wide range of wall temperatures. They found that the wall superheat might have a strong effect on the film boiling coefficient, h_{FB}, depending on the flow rate. Figures 2.2 and 2.3 show their data for two different flow rates. Note that the scatter in the data is very small. It can be seen that, at the low flow of 50 $kg \cdot m^{-2} \cdot s^{-1}$, h_{FB} was independent of wall superheat. At the high flow of 125 $kg \cdot m^{-2} \cdot s^{-1}$, h_{FB} at the 5.08 cm downstream location decreased initially with wall superheat, but the trend was reversed later. The decrease near the lower wall superheat range seems to confirm the observation in the quenching experiments of Newbold, Cheng and Fung. The increase in the higher wall superheat range is thought to be partly due to the increased radiation heat transfer.

In general, an increase in mass flux is found to increase the heat transfer in the film boiling region. Figure 2.4 shows the effect of mass flux at two different locations. It indicates that the film boiling heat flux increases with mass flux for all axial locations. The effect of mass flux, however, is coupled with the effect of local subcooling through the heat balance equation. The measurement of the local liquid temperature is planned in the new phase of tests by Fung.

Figure 2.5 shows the effect of inlet subcooling. In general, a strong effect was observed near the upstream end of the heated length, but this effect diminished near the end, where the liquid probably had become saturated. The positive effect of subcooling on h_{FB} is thought to be due to the thinning of the vapor film when heat is being transferred from the vapor annulus to heat up the subcooled liquid core.

Another observation that can be made from Figures 2.2 to 2.5 is that the axial position has some bearing on the heat transfer rate. This is suggested to be due to the cumulative influences of (a) local liquid subcooling, (b) vapor film characteristics, and (c) hydrodynamic and thermal boundary layers.

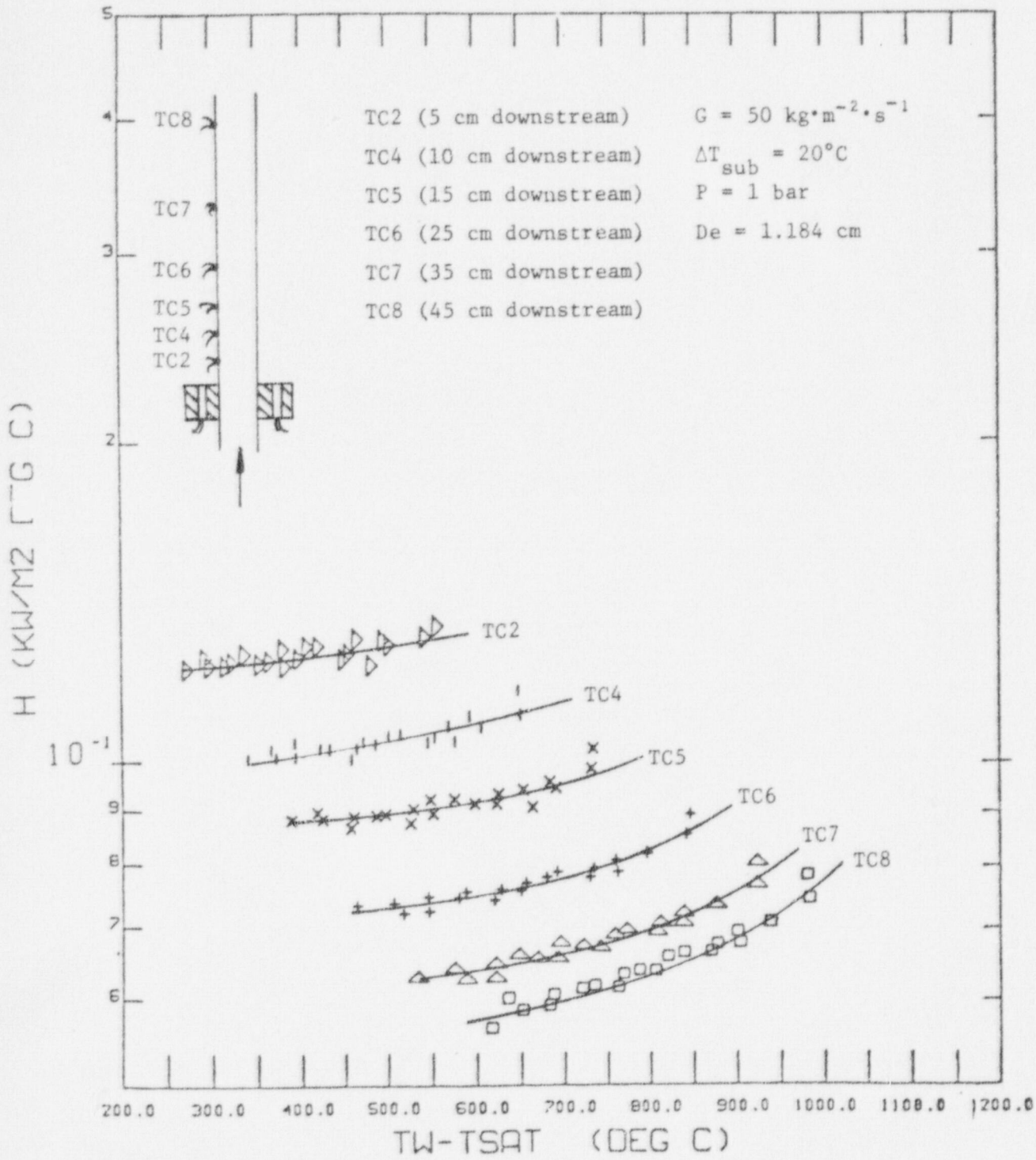

FIGURE 2.2: EFFECT OF WALL TEMPERATURE ON THE HEAT TRANSFER COEFFICIENT AT G = 50 $kg \cdot m^{-2} \cdot s^{-1}$ (Gardiner and Groeneveld [1977])

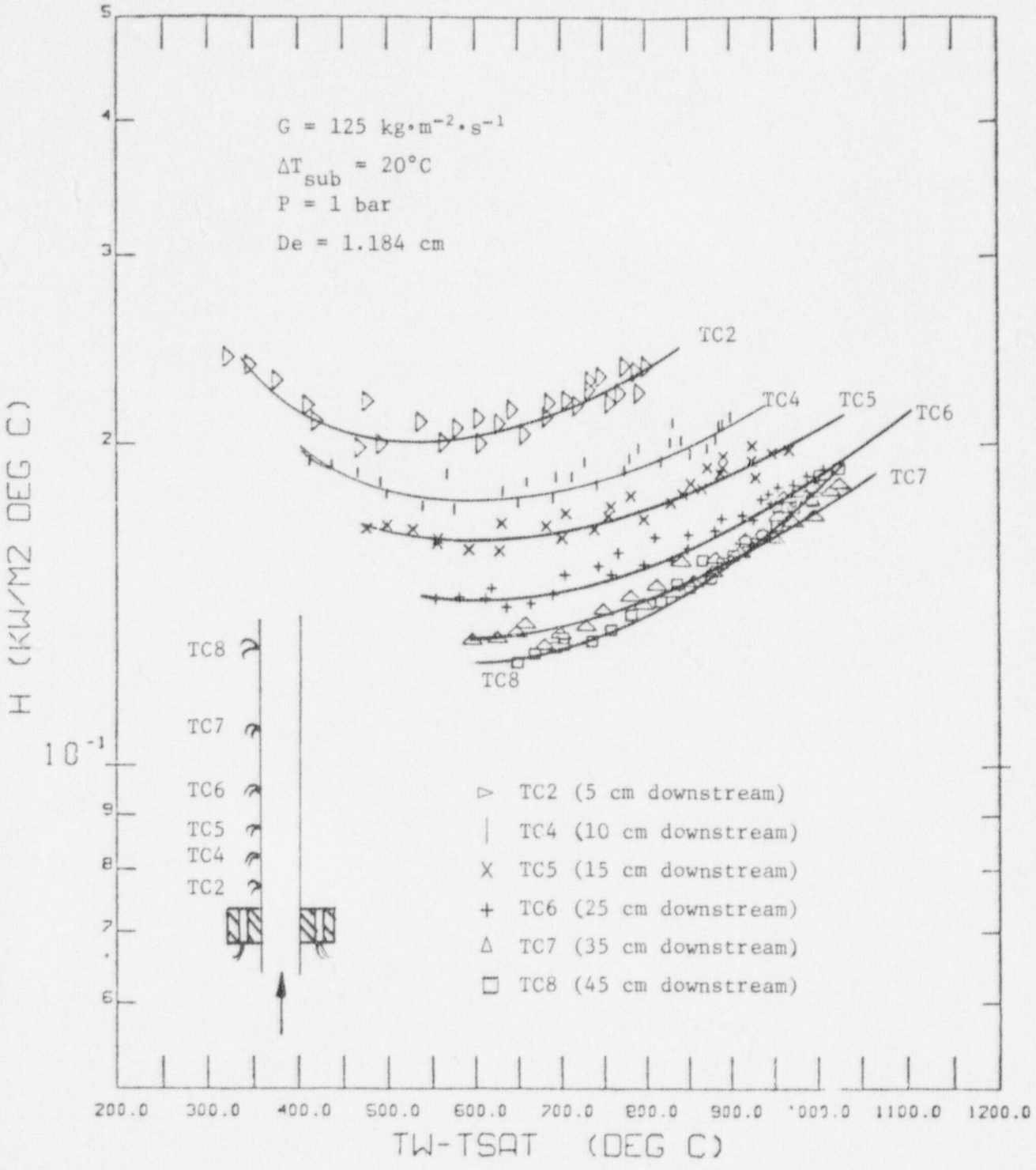

FIGURE 2.3: EFFECT OF WALL TEMPERATURE ON THE HEAT TRANSFER COEFFICIENT AT G = 125 kg•m^{-2}•s^{-1} (Gardiner and Groeneveld [1977])

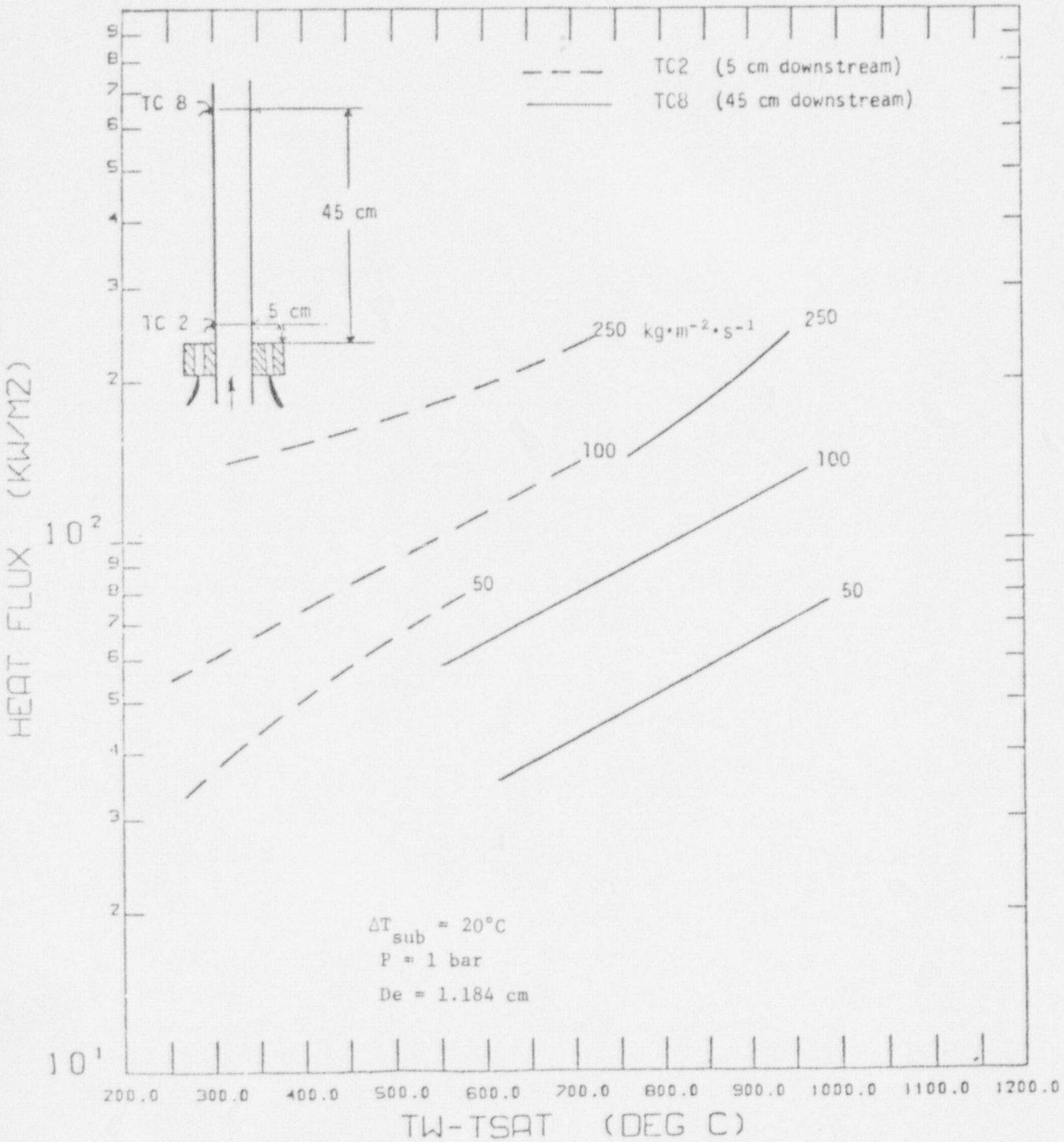

FIGURE 2.4: EFFECT OF MASS FLUX AND AXIAL LOCATION ON FILM BOILING (Groeneveld [1977])

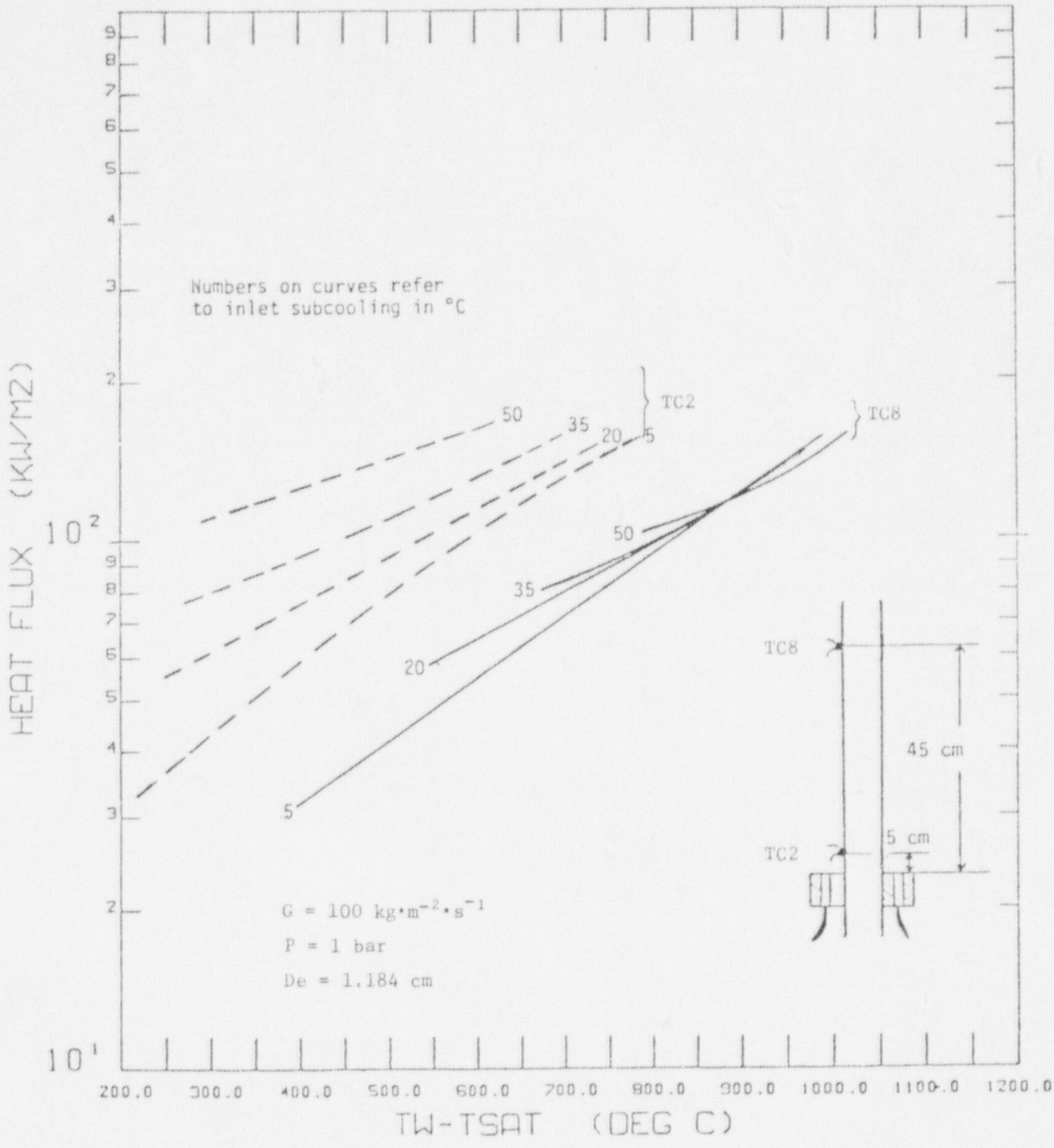

FIGURE 2.5: EFFECT OF INLET SUBCOOLING AND AXIAL LOCATION ON FILM BOILING (Groeneveld [1977])

Smith [1976] also adopted the hot patch technique to obtain data in the inverted annular and dispersed flow film boiling regimes, but he was unable to maintain film boiling in his test tube using a single hot patch. Instead, he had several copper blocks clamped to the tube. The upstream part of the tube was heated to serve as a preheater. The copper blocks, each of which was independently heated by cartridge heaters, acted as heat sources to the test section. By trial and error, he spaced the hot patches so that the tube was not rewetted in between.

Most of the data Smith obtained were in the dispersed flow regime. He presented his results in plots of heat transfer coefficient against local equilibrium quality. As shown in Figure 2.6, the heat transfer coefficient first decreases to a minimum and then rises again. It was postulated, to the left of the minimum, inverted annular film boiling existed initially. Further downstream the vapor film thickness and the liquid core heated up to close to saturation, resulting in a decrease in h_{FB}. At higher quality the flows broke up into slugs, with a further decrease in h_{FB} due to the higher enthalpy of the flow. Smith surmised that the minimum corresponded to the onset of dispersed flow film boiling.

I.2.2 Prediction Methods

The low flow, low quality film boiling data are usually compared to pool film boiling correlations. Figure 2.7 shows a comparison between Newbold's [1976] data and several correlations. It can be seen that the predicted heat fluxes usually fall below the data. Ralph [1977] noted that, for upflow, the measured heat fluxes were generally larger than those predicted by Bromley's and Berenson's correlations for pool film boiling. However, the same correlations tend to overpredict the downflow data.

Analysis of the data of Gardiner and Groeneveld is still underway and no extensive comparison with correlation has been made.

There has not been any relevant new prediction method since the review by Groeneveld and Gardiner [1977]. The model of Baum et al. [1977] mentioned in the transition boiling section of this report is claimed to be applicable also to inverted annular film boiling.

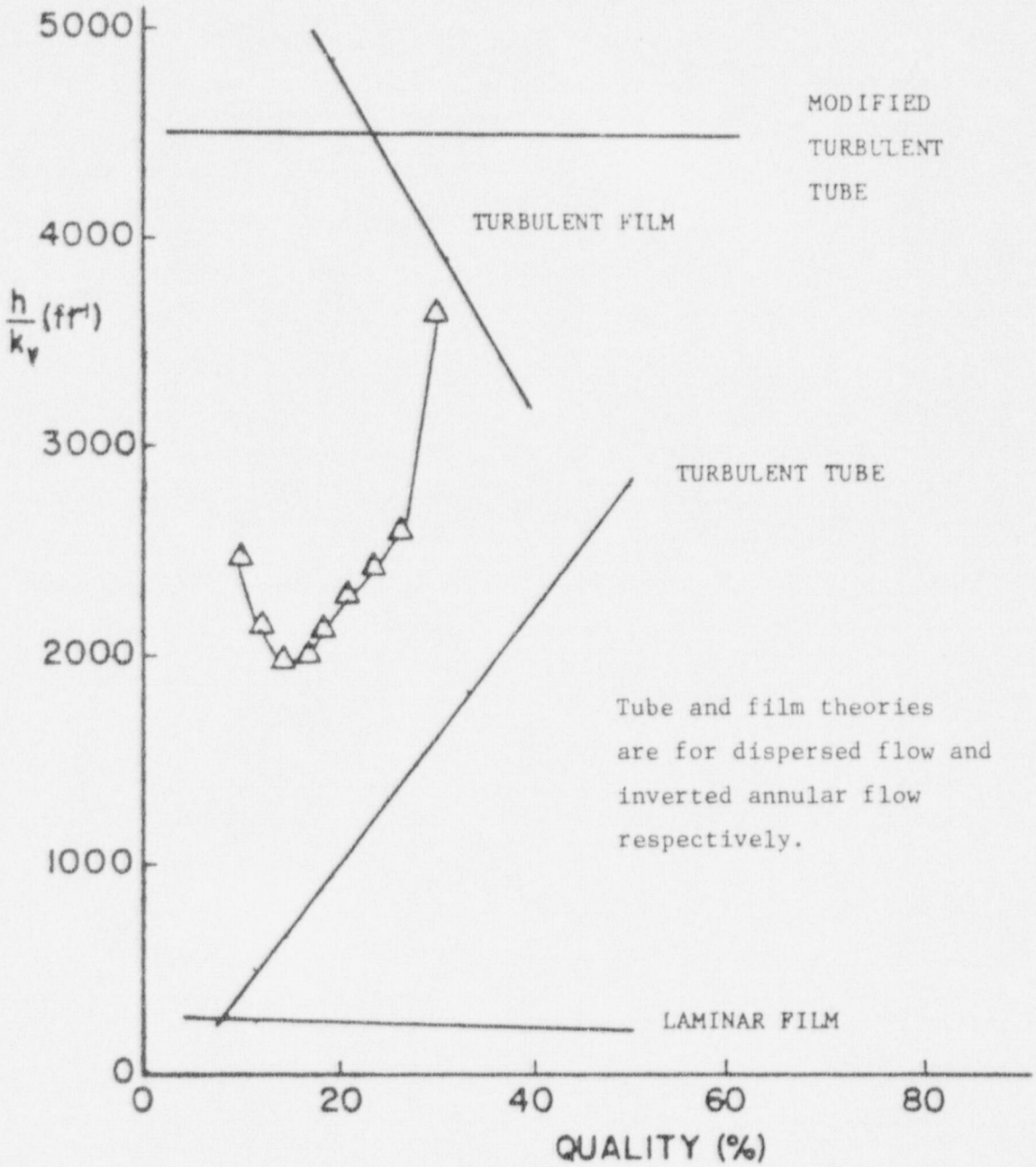

FIGURE 2.6: FILM BOILING DATA OF SMITH [1976] FOR WATER FLOWING IN A VERTICAL TUBE OF 12.5 mm ID. P = 462 kPa, V = 15.2 cm/s

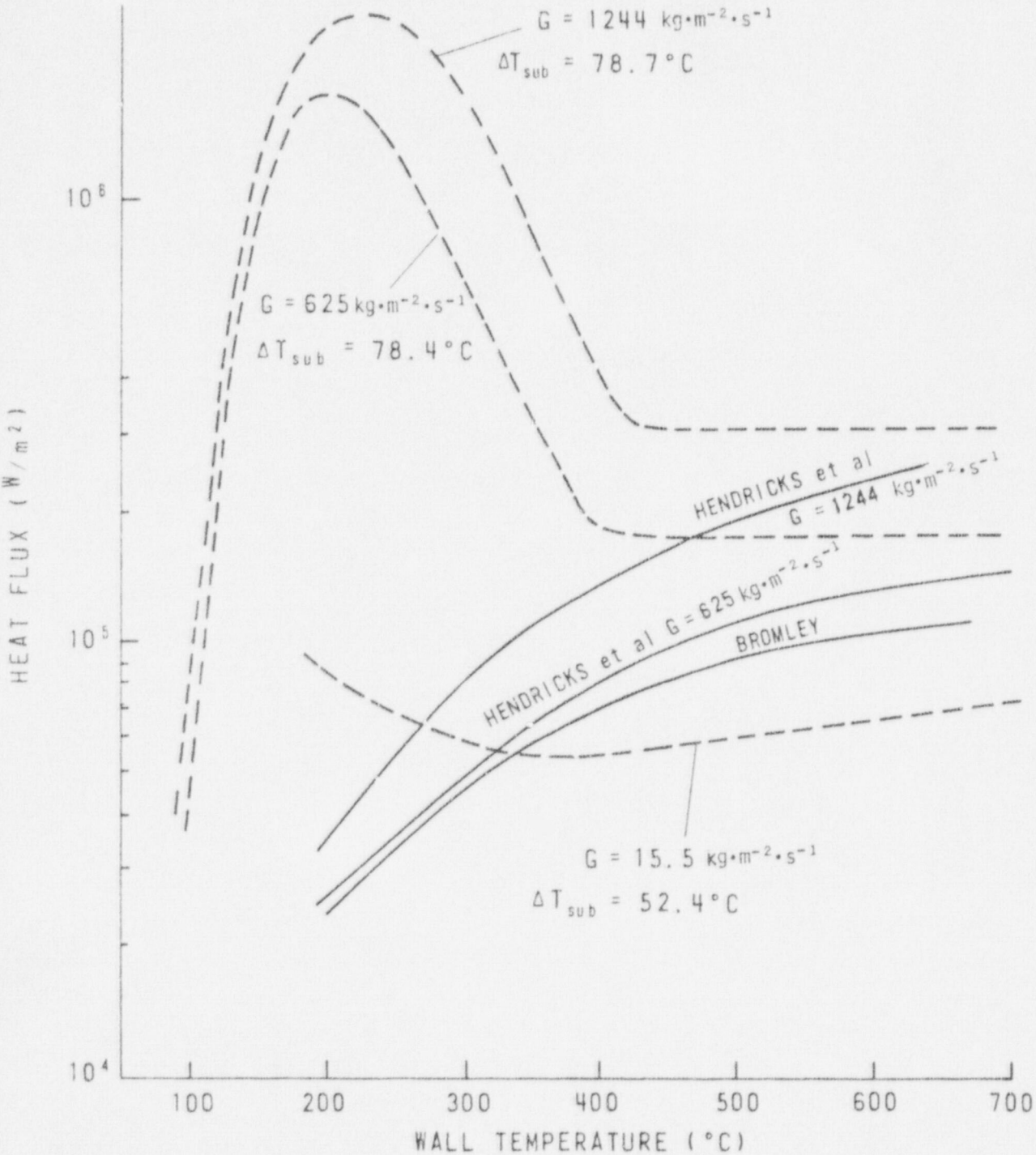

FIGURE 2.7: DATA OF NEWBOLD [1976] FOR TRANSIENT BOILING HEAT TRANSFER TO WATER FLOWING IN A VERTICAL TEST SECTION SHOWING THE THEORY OF BROMLEY [1950] AND THE CORRELATION OF HENDRICKS [1966]. (P = 300 kPa)

I.3 HIGH QUALITY FILM BOILING

I.3.1 Recent Experimental Studies

The dispersed flow film boiling regime has been investigated more thoroughly than the inverted annular and slug flow regimes. Consequently much effort is now concentrated on developing and refining prediction methods based on the accumulated data bank.

Four experimental studies were carried out recently, one in single tube (Bailey [1977]), two in simulated bundle strings (Turner [1977], Yates et al. [1977]) and one with actual fuel rods (MacDonald et al. [1977]). The experiment of Bailey was carried out in a 15 mm ID, 5.4 m long Inconel tube. He compared the post-dryout wall temperature with predictions by the Heineman and Dougall-Rohsenow correlations. Figure 3.1 shows a typical set of results. He noted that the Dougall-Rohsenow correlation with an assumption of thermal equilibrium yielded a trend in wall temperature that was different from the measured data. However, the prediction was much improved when used in conjunction with an assumption that there is no further droplet evaporation downstream of dryout. He therefore concluded that the droplets in the post-dryout region took very little part in the heat transfer processes, neither evaporating in the steam nor impinging directly on the tube wall.

The film boiling data of Turner were obtained in three simulated PWR 21 or 25 rod bundle assemblies. He compared the experimental heat transfer coefficient to those predicted by the Dougall-Rohsenow, modified Dougall-Rohsenow and Groeneveld correlations (Figure 3.2), and observed that the modified Dougall-Rohsenow and Groeneveld correlations consistently underpredict the bundle data.

As an adjunct to the 25-rod simulated bundle CHF tests, Yates et al. [1975] obtained five points in the film boiling region. They compared the experimental data with the correlations of Groeneveld [1969], Dougall-Rohsenow [1963], and Berenson [1961] and found that, in all cases, the heat transfer coefficient exceeded the predicted values.

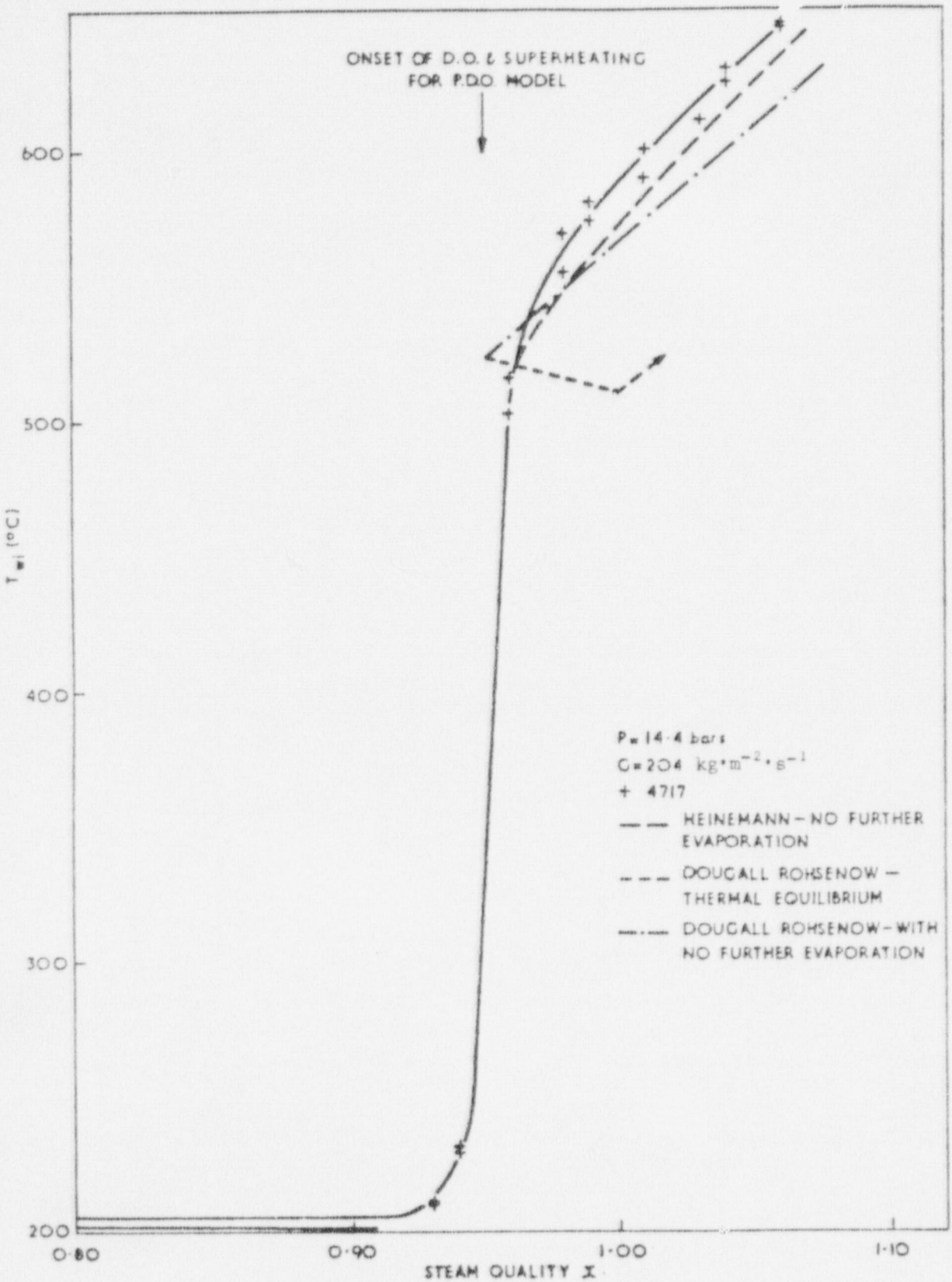

FIGURE 3.1: FILM BOILING DATA OF BAILEY [1977] FOR UPFLOW OF WATER IN A 15 mm ID, 5.4 m LONG INCONEL TUBE

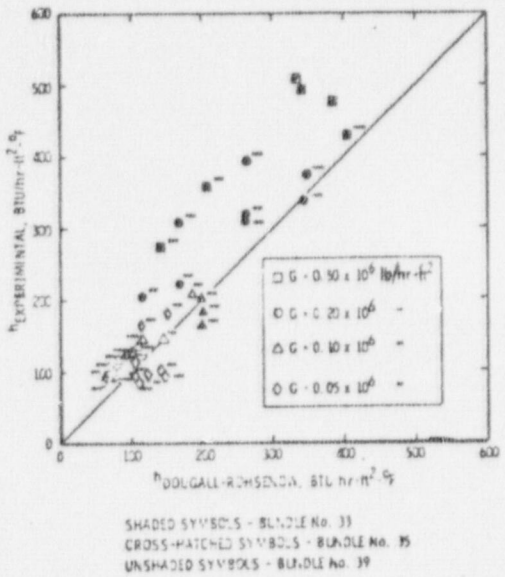

(a) Comparison with Dougall-Rohsenow correlation

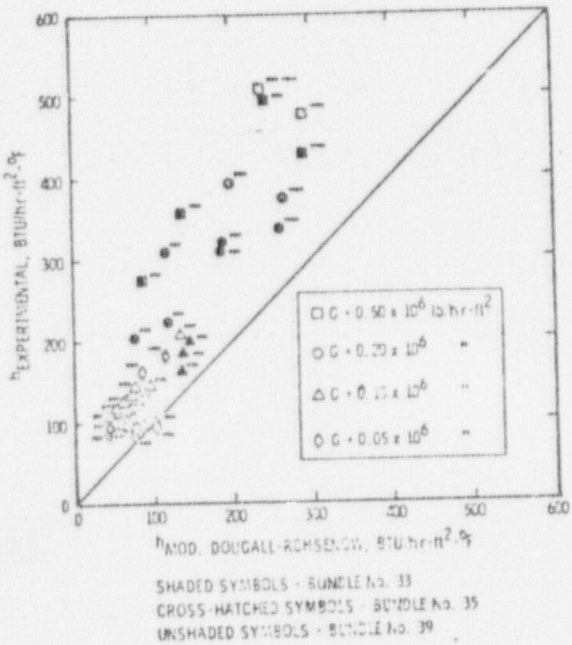

(b) Comparison with modified Dougall-Rohsenow correlation

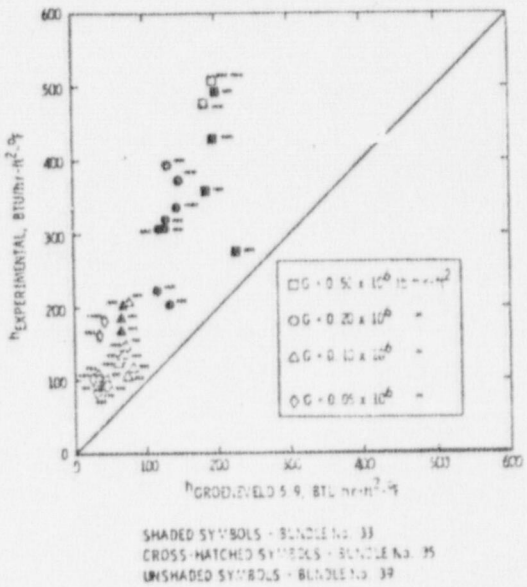

(c) Comparison with Groeneveld correlation

FIGURE 3.2: COMPARISON OF FILM BOILING COEFFICIENTS FROM SIMULATED BUNDLE ASSEMBLY TESTS WITH CORRELATIONS (Turner [1977])

Macdonald et al. [1977] carried out in-reactor tests with PWR type zircaloy-clad, 97 cm long, UO_2 fuel rods. Each rod was tested in its own coolant flow shroud. The results are shown in Figure 3.3. It indicates that the Groeneveld correlation for film boiling in annuli tends to serve as an upper bound for the measured wall temperature. The calculations either agree well with the data or overestimate the observed maximum cladding temperature. In three cases the correlation underpredicts by up to 9%.

I.3.2 Prediction Methods

Several phenomenological models to predict the heat transfer in dispersed film boiling have been developed recently. Jones & Zuber [1977] and Jones & Saha [1977] considered the vapor-droplet interactions as a first order relaxation process having a forcing function proportional to the local rate of heat input. A superheat relaxation number is correlated based on the data of Forslund & Rohsenow [1966] and Bennett et al. [1967]. They demonstrated that this model is capable of predicting actual quality (Figure 3.4a) and that it can be extrapolated to higher pressures as shown by the comparison with Swenson's data in Figure 3.4b.

Sergeyev et al. [1976] developed a governing equation for the change in actual quality by using a droplet heat transfer coefficient and taking the driving potential $(T_{va} - T_{sat})$ to be proportional to $(h_{va} - h_g)$. They derived the following equation

$$\frac{dX_a}{dX_e} = K(1 - X_e)(X_e - X_a)(X_e/X_a)^2$$

where K is a constant proportional to $(\rho U)^2/q''$ for a fixed pressure. Simultaneous solution of the above equation and the vapor heat transfer equation is shown to give good agreement with their experimental data (Figure 3.5).

Chen et al. [1977] adopted the two-step model but instead of solving the mechanistic equations they used a phenomenological approach. The wall-to-vapor heat transfer is calculated based on the momentum analogy and is expressed through the two-phase friction factor for the

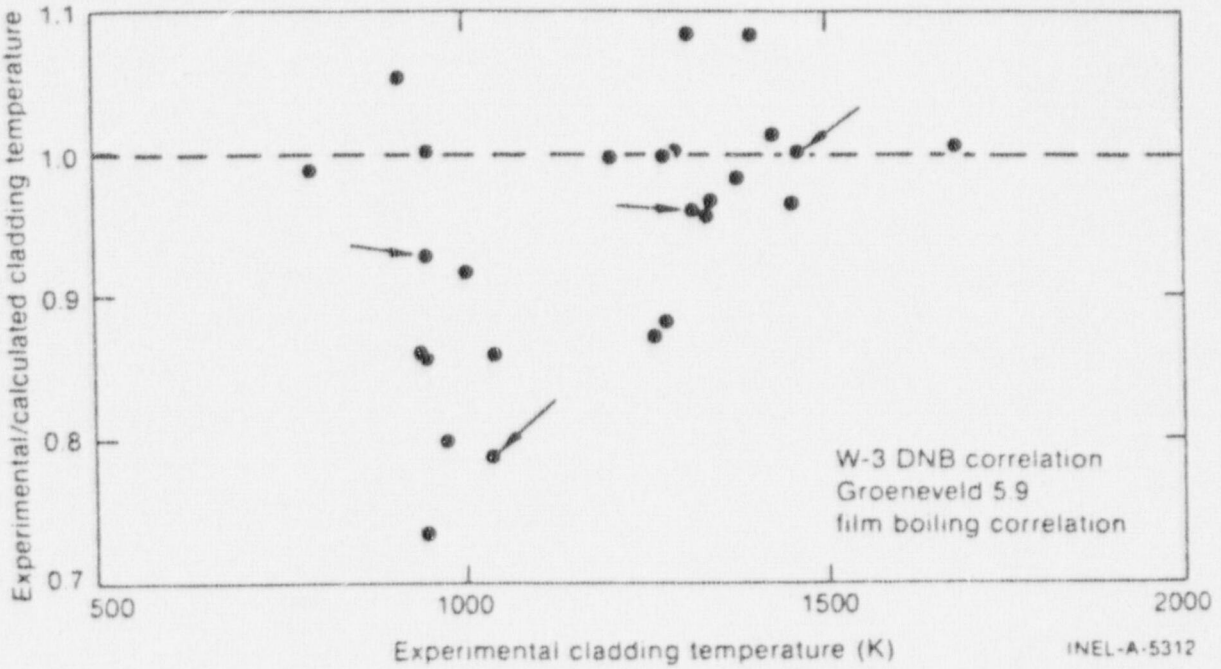

FIGURE 3.3: COMPARISON OF EXPERIMENTAL FILM BOILING TEMPERATURE IN THE IN-REACTOR TESTS OF MACDONALD ET AL. [1977] AND THOSE PREDICTED BY THE GROENEVELD CORRELATION

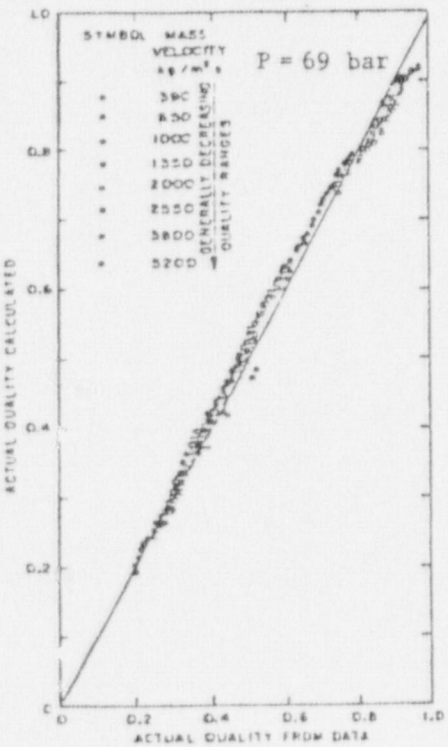

(a)

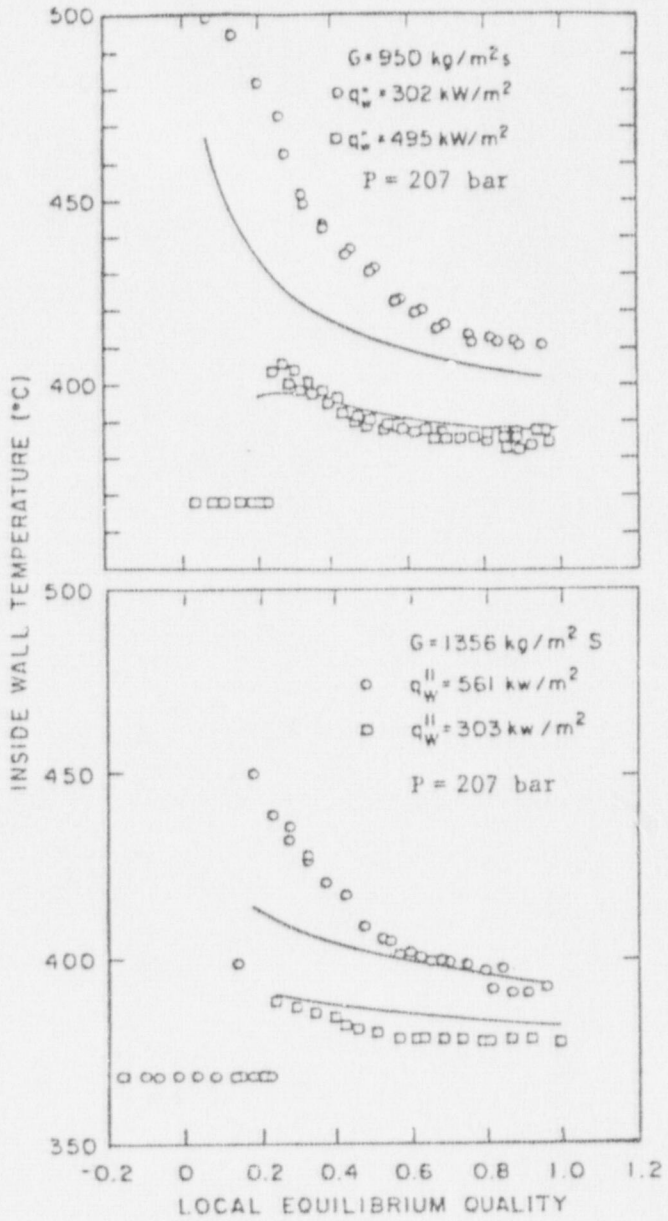

(b)

FIGURE 3.4 (a): COMPARISON OF NON-EQUILIBRIUM QUALITY PREDICTED BY Jones & Zuber [1977] WITH THAT DERIVED FROM THE DATA OF Bennett et al. [1967]

(b): COMPARISON OF WALL TEMPERATURES PREDICTED BY Jones & Zuber WITH THOSE MEASURED BY Swenson et al. [1967]

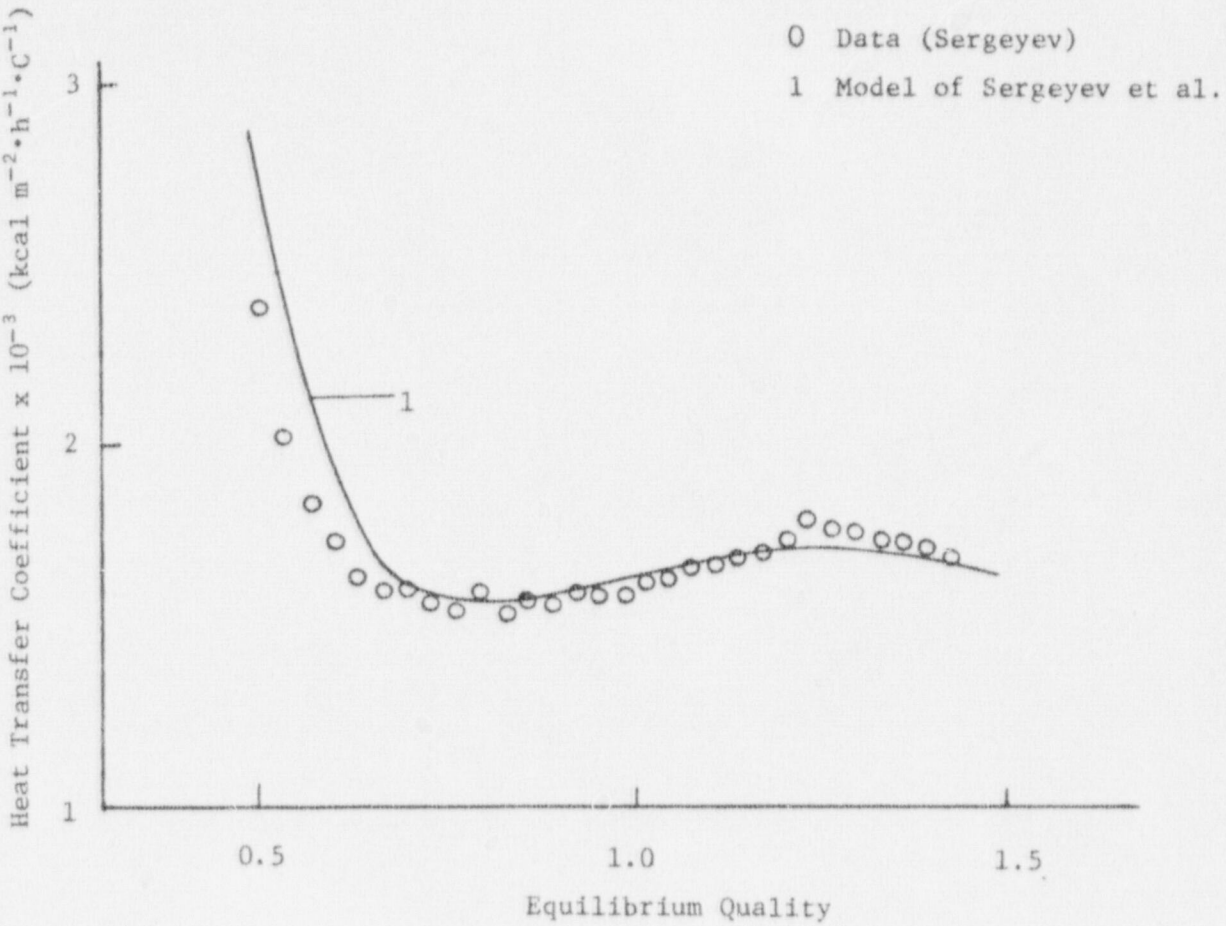

P = 13.73 MPa

G = 697 $kg \cdot m^{-2} \cdot s^{-1}$

X_{CHF} = 0.5

q" = 557 kW/m^2

FIGURE 3.5: COMPARISON OF CALCULATIONS WITH EXPERIMENTAL DATA (Sergeyev et al. [1976])

appropriate flow regime. The heat transfer to impinging liquid is considered to take place in three stages: pre-nucleation stage, bubble growth and disruption stage and finally the residual liquid film evaporation stage. The two components are weighted according to the liquid contact area fraction, which is empirically correlated. Agreement between data from several sources and the correlation is reasonably good, as shown in Figure 3.6.

One of the premises in the development of this model is that liquid-wall contacts exist throughout the dispersed flow regime. This seems to contradict the belief that only dry collisions take place beyond the Leidenfrost temperature. It is true that the contribution to the total heat transfer due to liquid wall interaction is small at high wall temperature. Nevertheless the mechanism needs to be identified correctly. Probably the component of heat transfer due to droplet entering the thermal boundary layer should be incorporated to make this model more compatible with the physical phenomena.

A modification to the Groeneveld correlation has been proposed by Bjornard and Griffith [1977]. In the original Groeneveld correlation, the vapor velocity is calculated by using the homogeneous void fraction model, which is probably appropriate in the proposed mass flux range of 0.8 to 4 $Mg \cdot m^{-2} \cdot s^{-1}$. In order to extend the applicability of this correlation to low mass fluxes, Bjornard and Griffith used the drift flux model, which, besides properly accounting for the influence of mass flux and flow direction on the void fraction, will automatically transform into the homogeneous model at high mass fluxes. The modified correlation becomes

$$h = 0.052 \frac{k_g}{De} \left(\frac{G\ De\ X}{\mu_g\ \alpha_{dfm}} \right) Pr_w^{1.26}\ Y^{-1.06}$$

where α_{dfm} = drift flux void fraction (see the same reference for method of evaluation).

In addition, to circumvent the singularities of this correlation at low pressure, they proposed that a modified Dittus-Boelter correlation be used for pressures below 1.38 MPa.

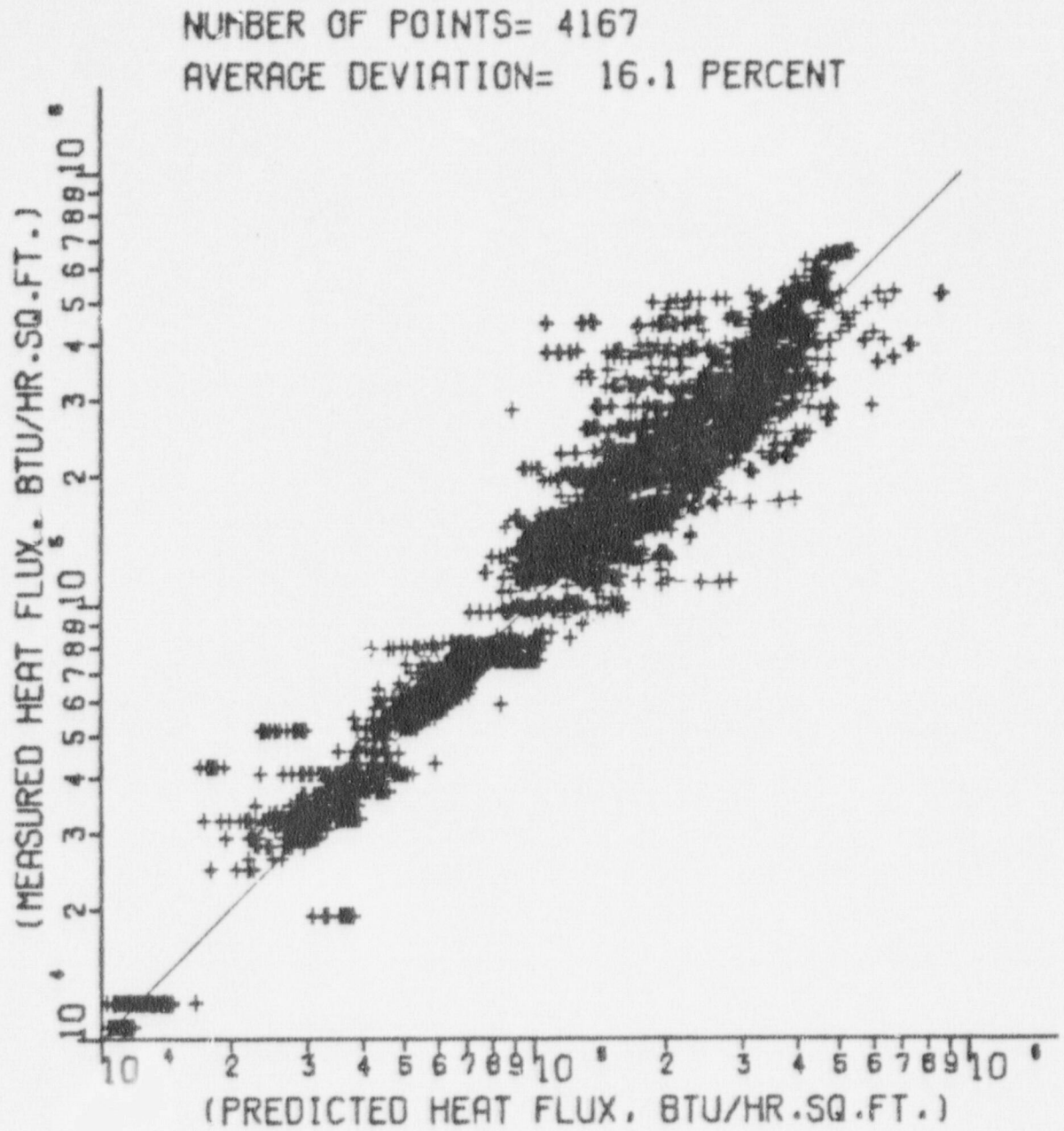

FIGURE 3.6: COMPARISON OF CHEN'S CORRELATION WITH POST-CHF DATA UP TO PRESSURE OF 2830 psia (Chen [1977])

I.4 DISCUSSION

The recent researches in steady-state post-dryout heat transfer have been summarized in the previous sections. In general, it can be seen that a large variety of correlations are available. However, each type has its own shortcoming.

Although theoretical models may eventually predict post-dryout heat transfer for simple geometries, the requirement of the simultaneous solution of several differential equations under well defined initial conditions renders them impractical for use in thermohydraulic codes.

Purely empirical correlations have a limited range of applicability. Their application beyond the bounds of their original data base is usually questionable. Empirical correlations which take into account the thermal non-equilibrium are more accuate but still have limited applicable range.

Phenomenological correlations seem to be a compromise. They are developed based on physical phenomena, with some empirically correlated factors. They are less cumbersome to apply than the mechanistic model, and should have a wider applicability, particularly to transient conditions, than the empirical correlations.

Prediction methods based on tube data have frequently been found to overestimate sheath temperatures in fuel bundles (Groeneveld and Gardiner [1977]). This has been suggested to be due to (a) improved heat transfer due to the presence of rod spacing devices, (b) intersubchannel flow oscillations, and (c) not fully developed film boiling. Present subchannel codes are not yet capable of predicting the local flow and enthalpy in partially dry bundles and therefore caution should be exercised when using the local conditions correlations. The use of experimental bundle data, whenever available, is advised.

II. TRANSIENT POST-CHF HEAT TRANSFER

II.1 GENERAL

Transient post-CHF heat transfer is generally investigated in the context of blowdown and reflooding. During a transient the heat transfer not only depends on the instantaneous local conditions, but also on the history of the development of the flow and boiling regimes. Furthermore, it also depends on the thermal and hydrodynamic feedback between the heat transfer surface and the rest of the system.

Experiments have been carried out both on simulated fuel strings and on single channels. The bundle tests generated data that were required for the safety analysis of reactors. Due to the complexity of the geometry, local conditions are generally unknown and these data can only be correlated based on system parameters. The single channel tests are aimed at gaining more basic understanding of the heat transfer mechanisms.

An extensive review of reflood heat transfer was given by Yadigaroglu et al. [1975]. Appendix II, taken from their paper, lists the available data at the time of their reviews. More recent experiments are listed in Table II.1

II.1.1 Bundle Data

Most of the simulated bundle experiments were of the transient quenching type with steady or stepwise-variable flooding rate. The heater power was either kept constant or varied to simulate the power decay after a LOCA. In most of these tests cooling water was introduced under forced flow conditions, which essentially decoupled the system hydraulics from the heat transfer. In order to study this feedback effect some of the primary heat transport system components were also simulated in the FLECHT-SET (Blaisdell et al. [1973]) and Siemens (Riedle & Winkler [1972]) experiments.

TABLE II.1: RECENT TRANSIENT† POST-CHF STUDIES (1978)

Reference	Geometry*	Heater Design	Pressure (MPa)	Initial Temperature (°C)	Peak Power	Inlet Coolant Temp. (°C)	Flooding Rate	Comments
Farman & Cermak [1972]	Tube ID = 12.7 mm x 91 cm	Stainless Steel t = 3.18 mm Hastelloy C t = 2.54 mm	Initial 17.24 Blowdown rate 1.38 - 69 MPa/s	~ 590	2 - 3.47 MW/m^2	250 - 290	1.35 - 3.375 $kg \cdot m^{-2} \cdot s^{-1}$ decay rate 0.34 - 1.55 $kg \cdot m^{-2} \cdot s^{-1}$	Blowdown tests with constant or decaying flow rate
Morgan et al. [1972]	9-rod bundle OD = 11 mm 3 x 3 array pitch = 14.4 mm	resistance heated	Initial 15	≈ 370	962 kW/m^2 step-varying	290	3.375 $Mg \cdot m^{-2} \cdot s^{-1}$	Blowdown tests
Lauer & Hufschmidt [1977]	Rod 45 mm OD	t = 11 mm heated by radiation furnace	.10	300 - 700	0	5 - 73	5 - 15 cm/s	Bottom flooding tests
Groeneveld & Young [1978]	Tube ID_1 = 16.07 mm ID_2 = 12.70 mm x 1.68 m	Inconel 600 t_1 = 0.76 mm t_2 = 1.59 mm	.10	400 - 700	Voltages: V_1 = 0 V_2 = 0, 3, 5	54, 35, 17	34 - 1500 $kg \cdot m^{-2} \cdot s^{-1}$	Vertical upflow tests
Lee, Chen & Groeneveld [1978] Chen, Lee & Groeneveld [1978]	Tube ID_1 = 19.1 mm ID_2 = 19.1 mm ID_3 = 15.9 mm L_1 = 4 m L_2 = 3.5 m L_3 = 4 m	t_1 = 1.65 mm SS t_2 = 0.89 mm SS t_3 = 1.02 mm Inconel	.10	270 - 800	Up to 5 kW/m^2	10 - 80 subcooling	100 - 400 $kg \cdot m^{-2} \cdot s^{-1}$	Horizontal and vertical upflow reflooding tests

†Slow transient tests of Newbold, Cheng, Fung and Ralph are included in the "steady state" section of this report.

*Subscripts designate different test sections.

II.1.2 Single Channel Data

In these experiments, resistance heating of the test section was used. After the test section had been heated up to a high temperature, coolant was introduced and quenching was achieved by the propagation of a rewetting front. During quenching, all three boiling regimes existed simultaneously along the channel. The principal information extracted from these tests is the rate of rewetting during a reflood condition. Most authors did not report explicitly the PDO heat transfer coefficients. The experiment of Chen et al. [1978] contained a more systematic study of the parametric effects on the heat transfer coefficient. Their report will be reviewed in greater detail in the following section.

In the single rod reflooding experiment of Lauer & Hufschmidt [1977] a thick-walled cylinder was used as test section. However, the wall thickness was not as large as those used in the transition boiling experiments of, for example, Cheng et al. Therefore, it is expected that the effect of transient will be more significant.

II.2 PARAMETRIC EFFECTS

II.2.1 Effect of System Pressure

In general, the effect of pressure in reflooding heat transfer is found to be in agreement with the observation that two-phase heat transfer improves at higher pressure. Riedle & Winkler [1972] and Martini & Premoli [1973] found that, at low pressure, a relatively small increase of the pressure resulted in a large reduction of the quench time. This suggests that the PDO heat transfer coefficients improved more significantly at low pressure. The BWR-FLECHT data (Fig. 2.1) show that the heat transfer coefficient increased significantly with pressure up to some pressure in the vicinity of 1.4 MPa (200 psia). Beyond this pressure, the trend seemed to be reversed. The increase of the PDO heat transfer coefficient with increasing pressure has been attributed to the increases in vapor density and specific heat (McConnell [1972]), and to the higher entrainment with increasing pressure (Cadek et al. [1971]). The reduced influence at higher pressure has not been explained satisfactorily.

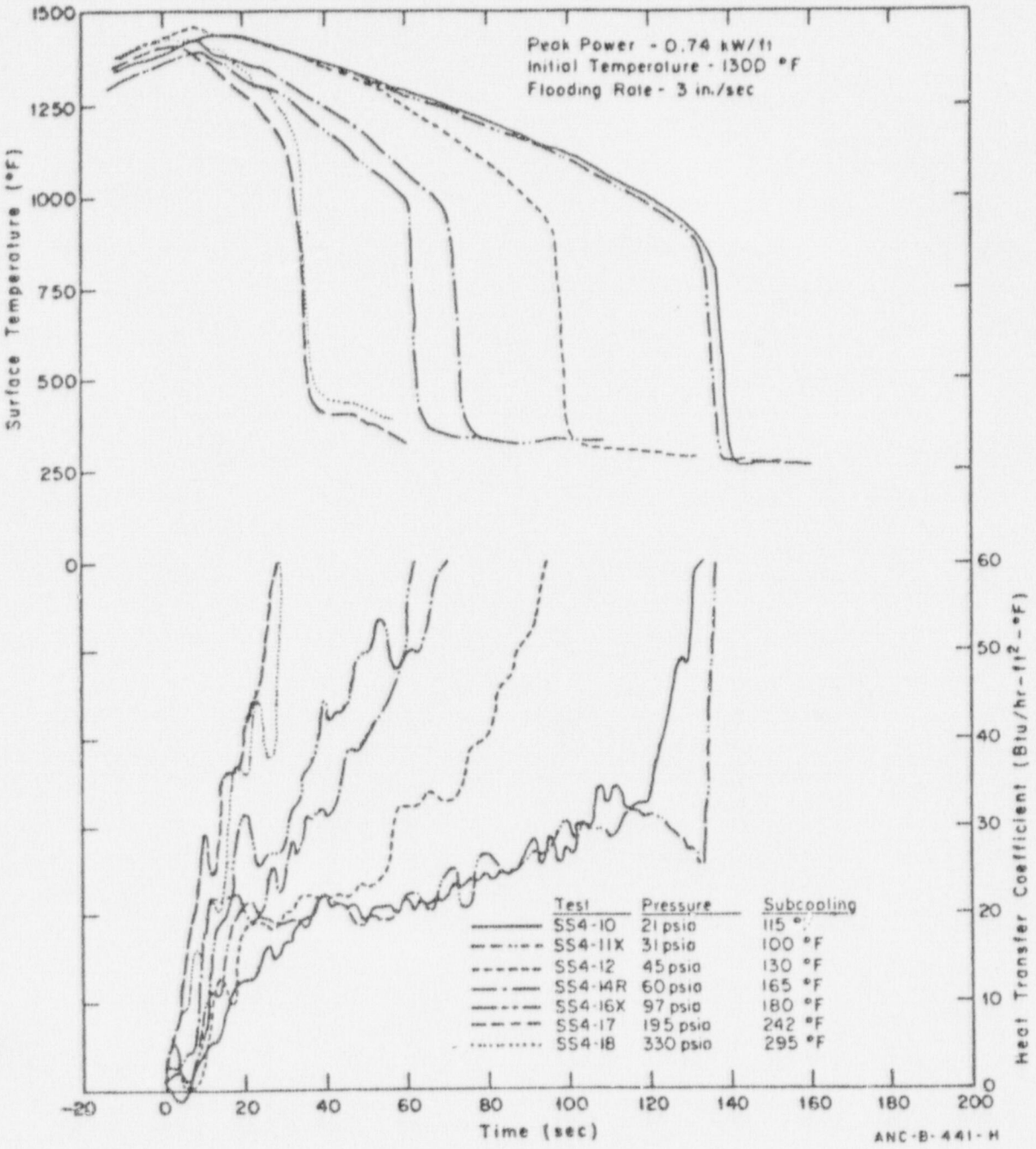

FIGURE 2.1: EFFECT OF PRESSURE ON SURFACE TEMPERATURE AND HEAT TRANSFER COEFFICIENT - BWR-FLECHT, SIX-FOOT ELEVATION ON THE HOTTEST ROD (McConnell [1972])

II.2.2 Effect of Inlet Subcooling

In general, it was found that the quench time decreased with increasing inlet subcooling. This implies a higher average heat transfer coefficient over the film and transition boiling regions. However, the effect of inlet subcooling on different boiling modes may not be the same. For example, during the initial reflooding stage in the PWR-FLECHT tests, the mid-level of the bundle assembly was cooled by liquid deficient film boiling and the heat transfer coefficient was found to increase with decreasing inlet subcooling. This is shown in the initial 0.4 dimensionless time in Fig. 2.2. The increase was attributed to the higher vapor generation rate at the upstream location. Later when the quench front propagated to near the mid-level, the heat transfer mode changed to transition and inverted annular film boiling. At this stage, the lower subcooling retarded the propagation of the rewetting front and therefore the heat transfer coefficients decreased.

Lauer & Hufschmidt [1977] observed a very significant increase in the heat flux with increasing fluid subcooling in both transition and film boiling regimes in their reflooding test with a heated rod. Their data are shown in Fig. 2.3. There is a sharp minimum film boiling temperature, which increases with increasing inlet subcooling.

Chen et al. [1978] also found that the PDO heat flux increased with inlet subcooling (Fig. 2.4). However, the difference during film boiling was found to be relatively small.

II.2.3 Effect of Depressurization

The effect of depressurization is a combined effect of change in pressure and subcooling* In the two blowdown studies (Farman [1972] and Morgan et al. [1972]), the PDO heat transfer coefficients were found to be significantly higher than those at steady-state.

Farman [1972] measured post-CHF heat transfer coefficients during a blowdown test in a tubular geometry. The system was depressurized while the flow rate was kept at an approximately constant value. He found that the transition and film boiling heat transfer coefficients were higher than those at steady-state conditions. No explanation for

*If the coolant is at saturation temperature, depressurization will result in flashing.

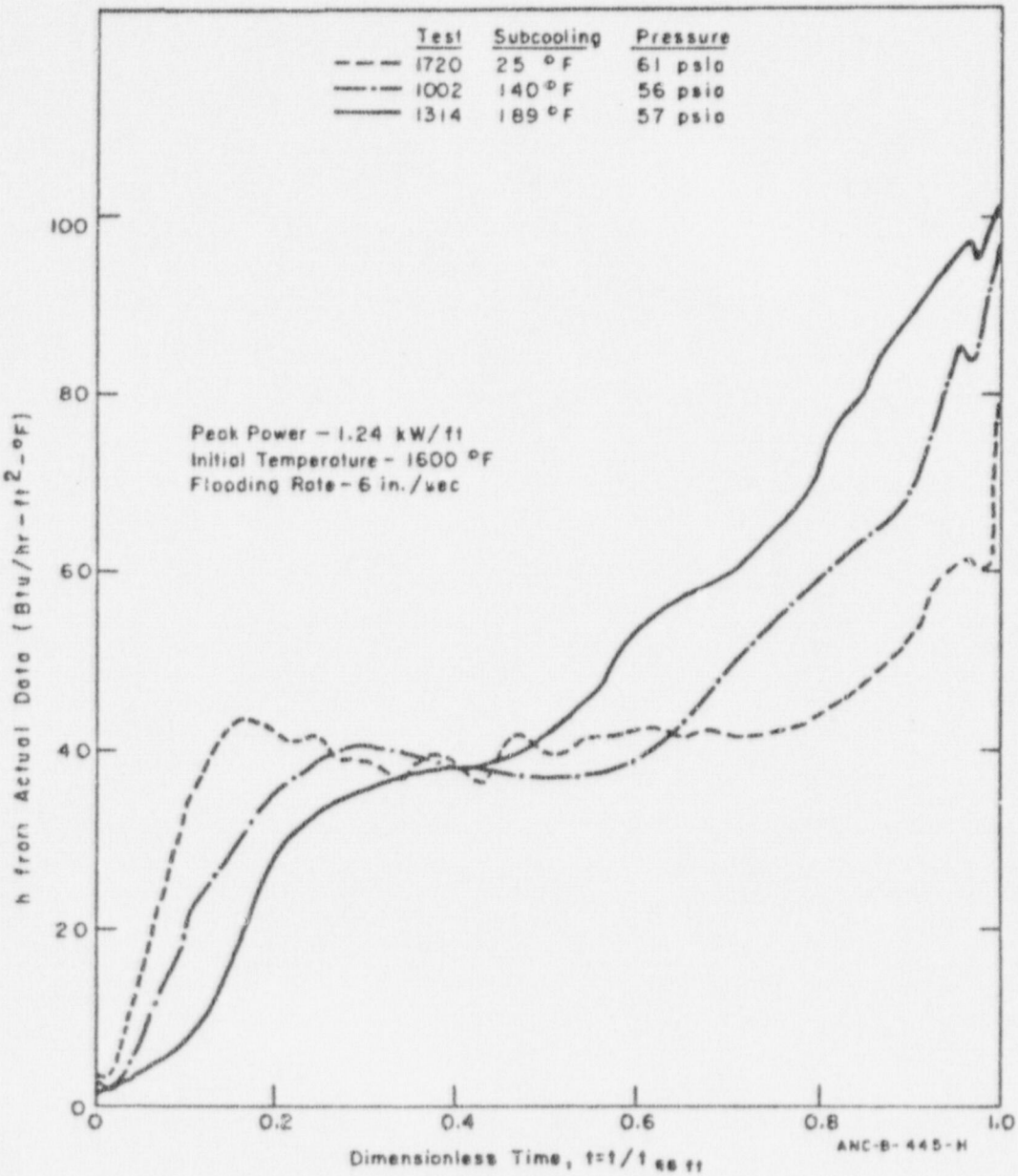

FIGURE 2.2: VARIATION OF HEAT TRANSFER COEFFICIENT WITH SUBCOOLING, DIMENSIONLESS TIME BASE — PWR-FLECHT, SIX-FOOT ELEVATION ON THE HOTTEST ROD (McConnell [1972])

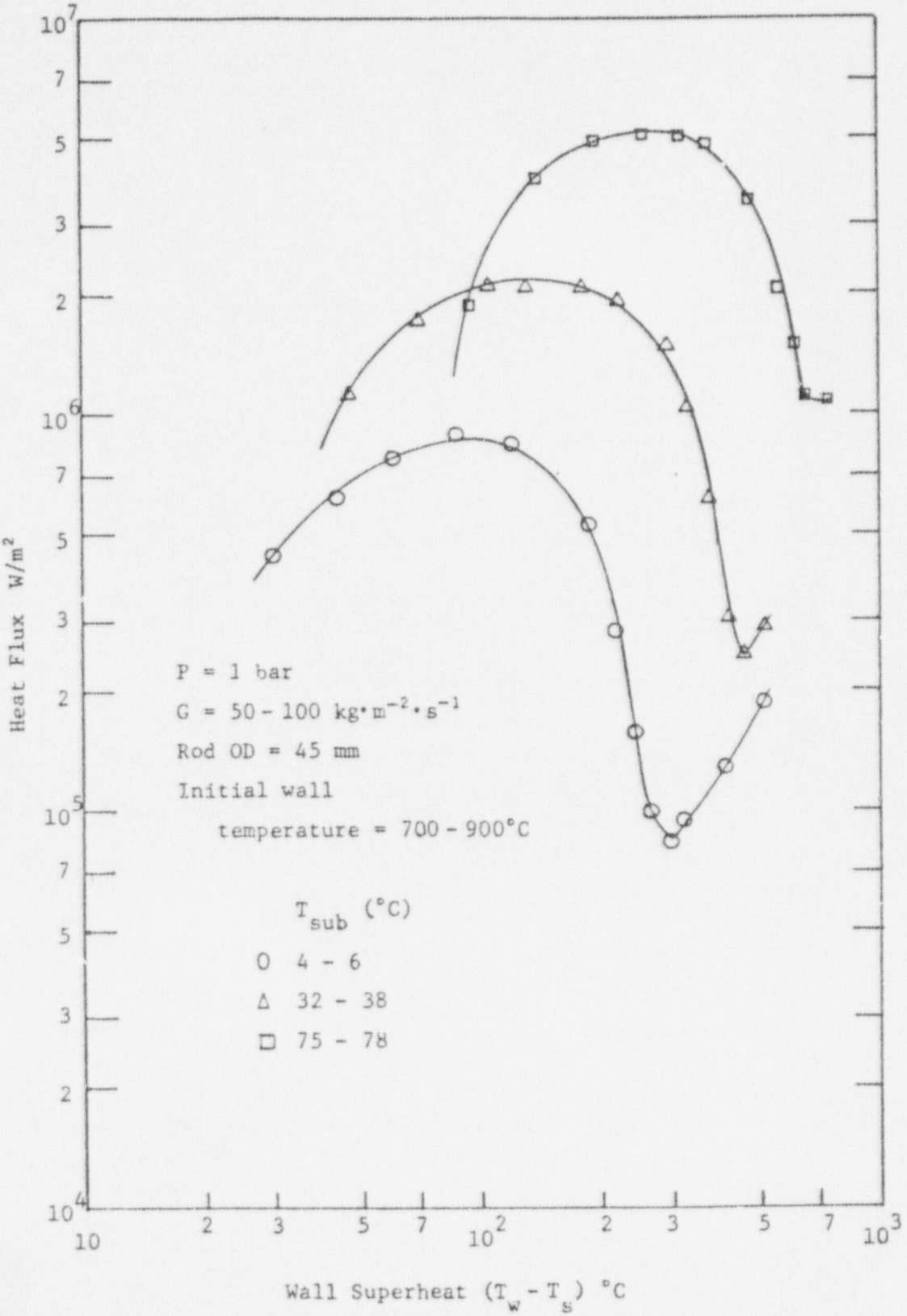

FIGURE 2.3: THE EFFECT OF SUBCOOLING ON THE PDO HEAT FLUX DURING REFLOODING OF A HEATED ROD

(Lauer & Hufschmidt [1977])

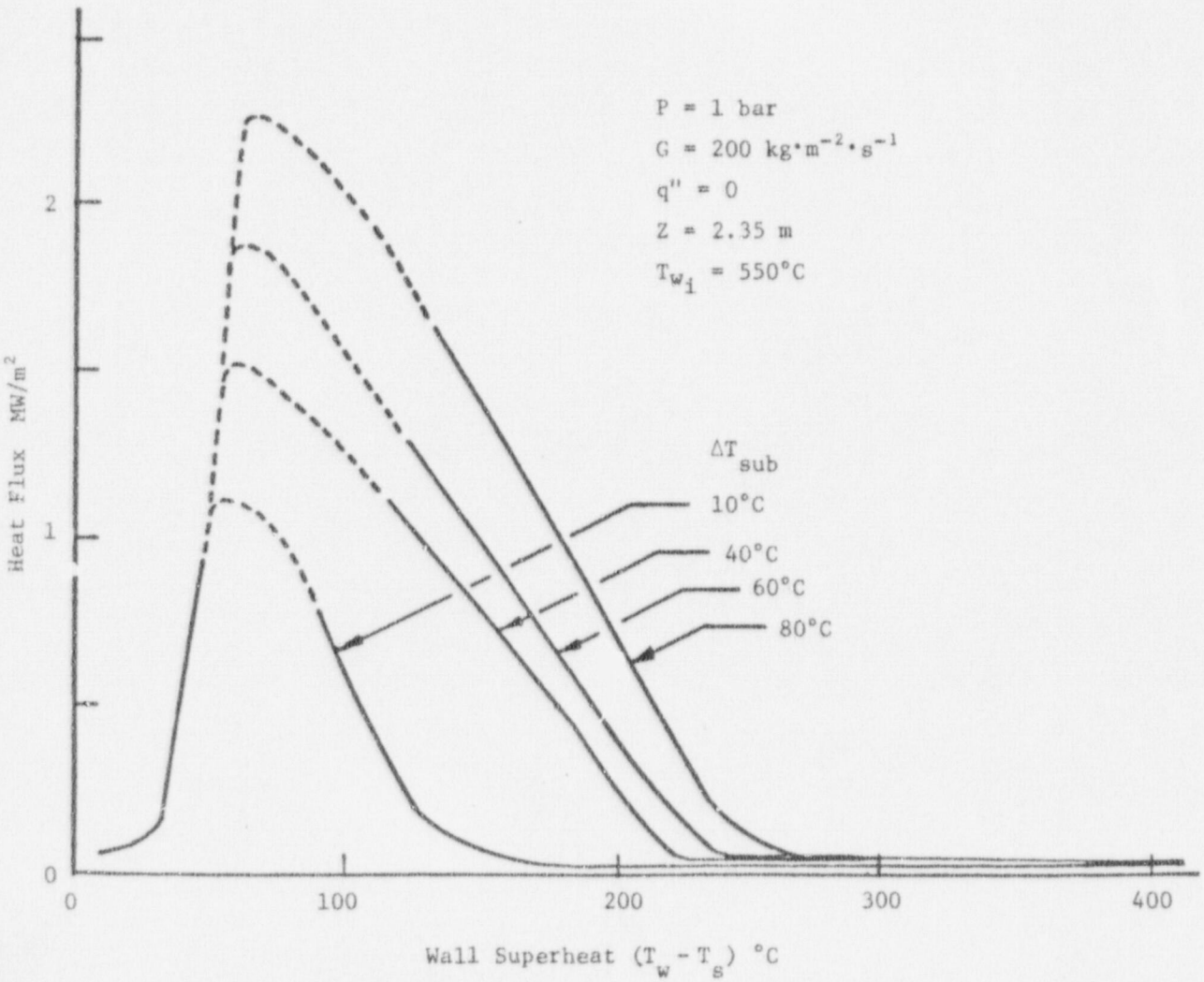

FIGURE 2.4: EFFECT OF INLET SUBCOOLING ON THE SURFACE HEAT FLUX DURING REFLOODING OF A 19.1 mm ID, 3.5 m LONG TUBE ORIENTED VERTICALLY (Chen et al. [1978])

the increase was given. In this author's opinion, this is probably due to the higher vapor generation rate and higher turbulence as a result of flashing.

Morgan et al. [1972] carried out blowdown tests with a 9-rod bundle. They compared the measured wall temperatures with those predicted by a computer code (CRAFT) and found that the best agreement was obtained by using a film boiling heat transfer coefficient about twenty times larger than those predicted by the steady-state correlation of Quinn [1966]. They suggested that the heat transfer process early in the blowdown phase was dominated by a high degree of turbulence generated by bulk nucleation rather than by a flow-dominated, boundary-layer phenomenon such as film boiling.

II.2.4 Effect of Flow Rate

The effect of flow rate is coupled with the effect of subcooling. At higher flow rates, the convective component of the heat transfer will increase. Also the local subcooling at a fixed location will decrease with increasing mass flux, resulting in a further improvement in heat transfer. However, during a transient, the heat transfer process might be dominated by the turbulence level.

In most of the tests, only the quench time was reported. It is therefore not straightforward to deduce the effect of flow rate on the heat transfer coefficients. Riedle & Winkler [1972] reported that the heat transfer coefficient in the transition and film boiling regions in their tests with a 340-rod simulated bundle assembly did not depend strongly on the flooding rate. Chen et al. [1978] found that, during reflooding of a heated tube, the critical heat flux and surface heat flux in the transition and film boiling regions increased slightly with mass flux (Fig. 2.5). Comparing Figs. 2.4 and 2.5, it seems that the effect of mass flux (in the range tested) is less than that of subcooling.

In the PWR-FLECHT program, some tests were carried out at stepwise variable flooding rates. It was found that, with a step reduction in flow rate as shown in the insert of Fig. 2.6, the variable flow heat transfer coefficient was between the 6 and 10 in./s curve during the high flow part

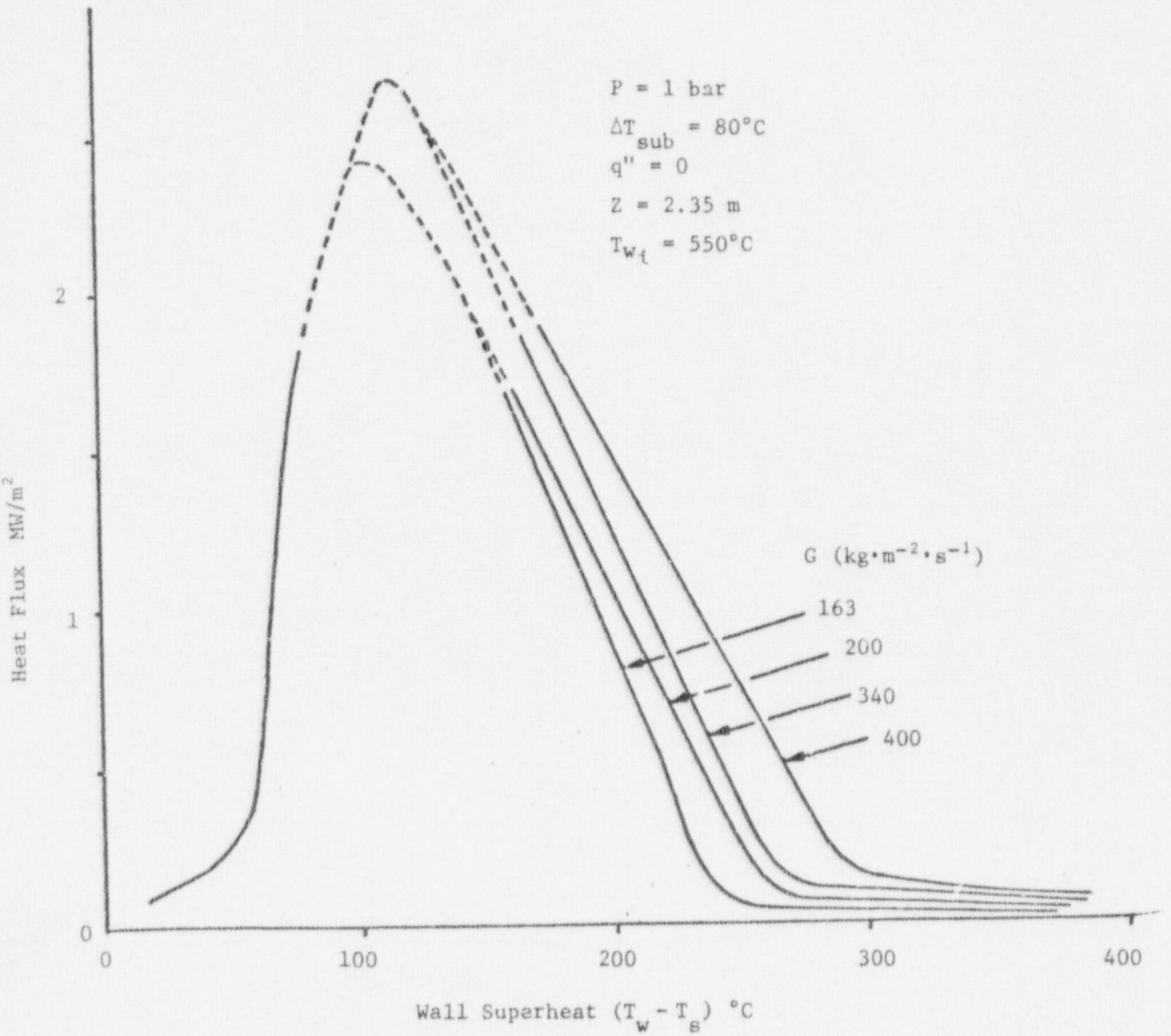

FIGURE 2.5: EFFECT OF MASS FLUX ON THE SURFACE HEAT FLUX DURING A REFLOODING OF A 19.1 mm ID, 3.5 m LONG TUBE ORIENTED VERTICALLY (Chen et al. [1978])

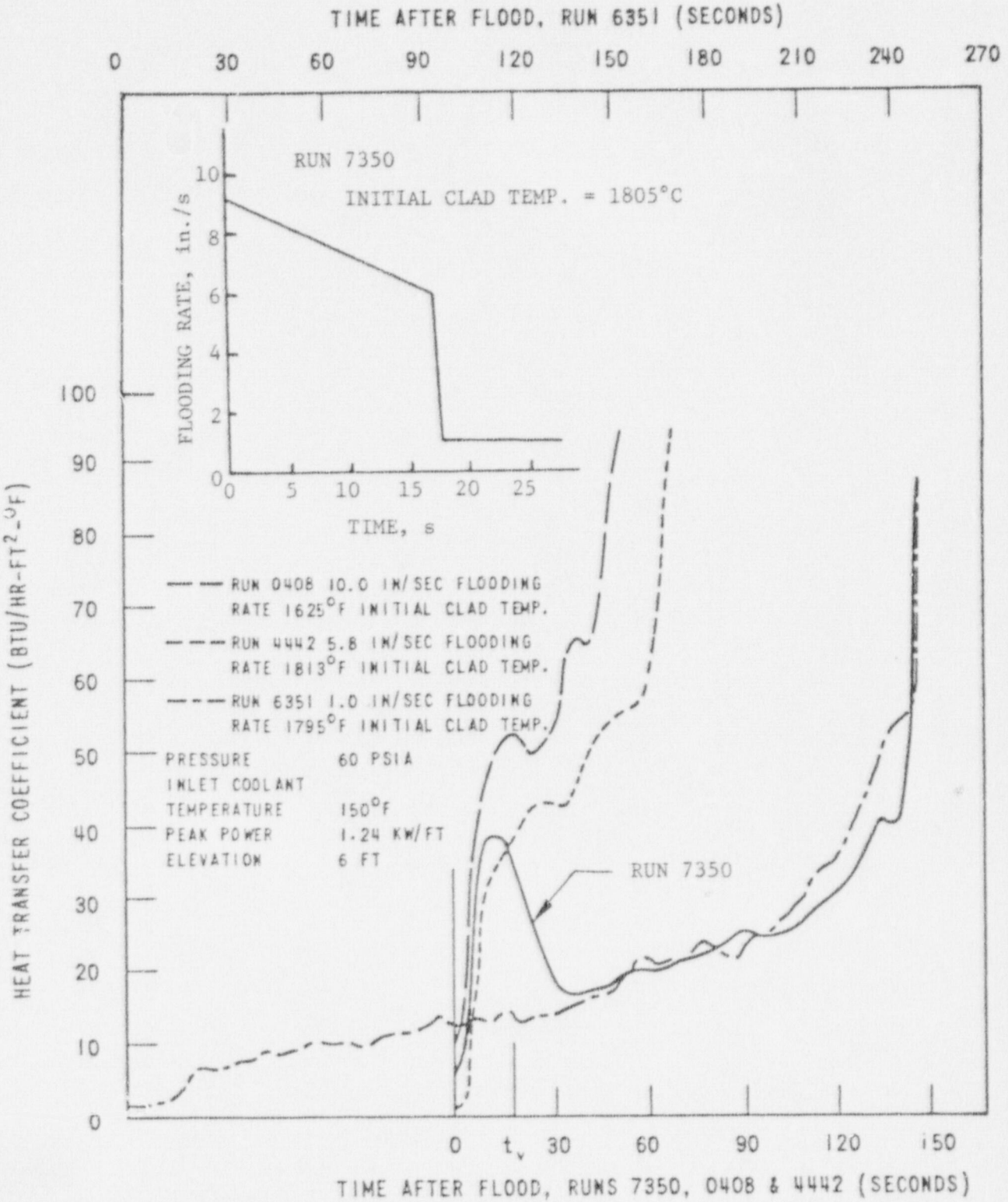

FIGURE 2.6: COMPARISON OF HEAT TRANSFER COEFFICIENTS FOR CONSTANT AND VARIABLE FLOODING RATE TESTS (Cadek et al. [1971])

of the run. For the later low flow part of the run, the heat transfer coefficient of the variable flow runs agreed with those of the comparable 1 in./s constant flow runs when the time coordinate was shifted as stipulated by Cadek et al. [1971]. However, as can be seen in Fig. 2.6, there was a lag between the time of flow reduction and that of attainment of heat transfer corresponding to the lower flow. In this author's opinion, the lag is probably due to the use of time instead of wall temperature as the independent variable.

Farman [1972] carried out some blowdown tests in tubes with a flow decay rate ranging from 0.34 to 1.55 $Mg \cdot m^{-2} \cdot s^{-2}$. He noted that nc significant effect on the relationship between the predicted and measured heat transfer coefficients was incurred because of flow decay.

Flow oscillations observed in the FLECHT-SET A tests (Blaisdell et al. [1973]) and the annular tests of Martini & Premoli [1972] and White & Duffey [1974] had been found to enhance the heat transfer coefficient. The origin of these oscillations had been traced back to the intense vapor generation downstream of the quench front, and to the onset of slug flow.

II.2.5 Effect of Initial Wall Temperature

Lauer & Hufschmidt [1977] found that the initial wall temperature generally did not affect the quenching boiling curve unless the initial wall temperature was lower than the rewetting temperature. It can be seen in Fig. 2.7 that the boiling curve corresponding to an initial wall temperature of 314°C is shifted to lower wall superheat, while others at higher initial temperature are not significantly different from each other. This suggests that if sufficient time is allowed for the transient hydrodynamic forces (e.g. due to the injection of coolant) to die down in the film boiling region, then no effect will be felt in the transition boiling region.

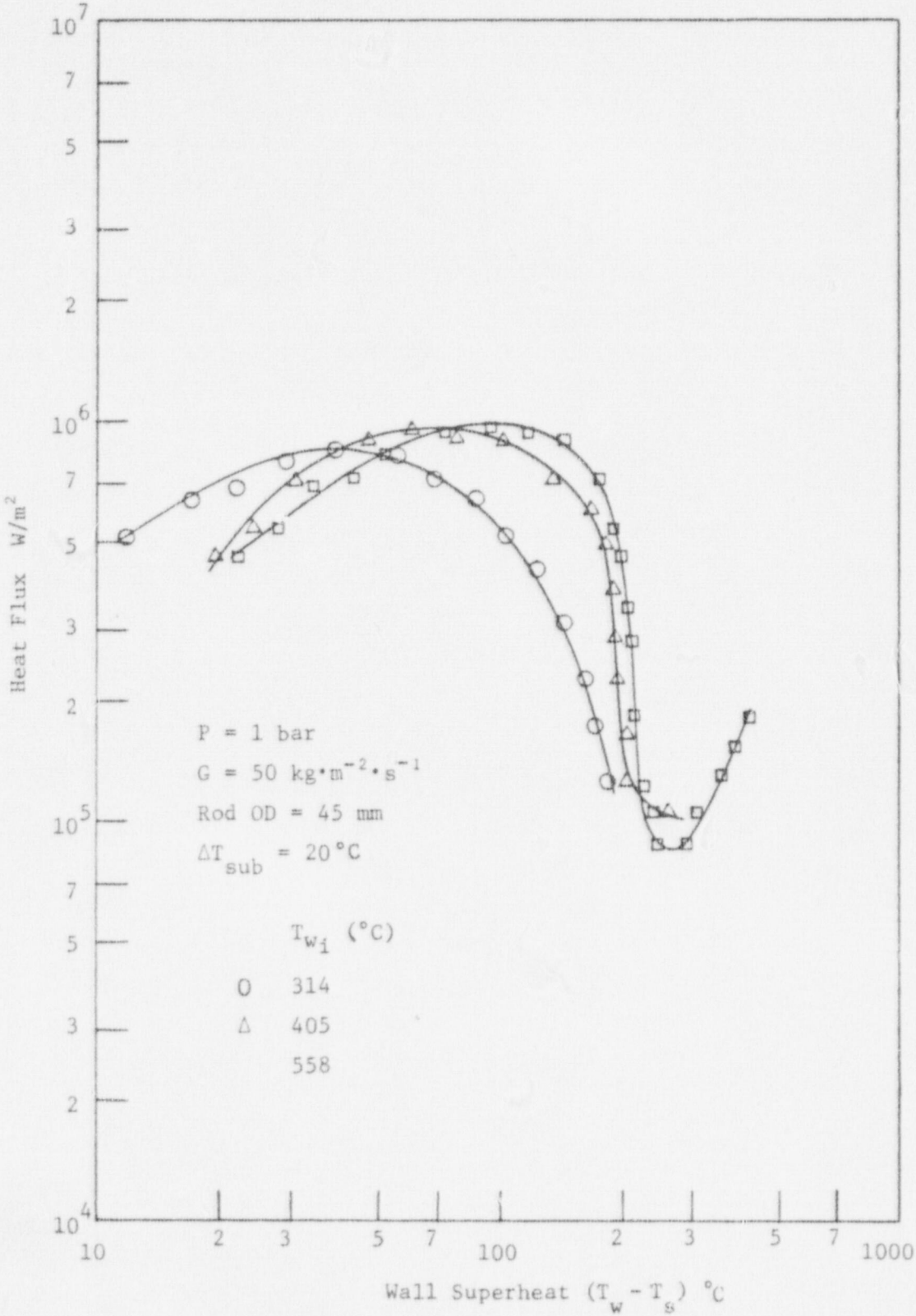

FIGURE 2.7: EFFECT OF INITIAL WALL TEMPERATURE ON THE PDO HEAT FLUX DURING REFLOODING OF A HEATED ROD

(Lauer & Hufschmidt [1977])

Fig. 2.8 shows the effect of initial wall temperature in the reflooding test of a heated tube of Chen et al. [1978]. Here a strong effect of initial wall temperature can be seen. However, the boiling curves corresponding to initial wall temperatures of 650°C and 750°C coincide with each other. This seems to agree with the observations of Lauer & Hufschmidt that, at sufficiently high initial wall temperature, there was no significant difference in the boiling curve.

II.2.6 Effect of Power Level

In all of the transient PDO experiments the power was either kept constant (including zero) or programmed to decay. In the 21-rod simulated bundle assemblies tests of Campanile & Pozzi [1972], the PDO heat transfer coefficient was found to increase with power level.

Siemens et al. [1973] also reported that, at low flow (8.64 cm/s), the average PDO heat transfer coefficient downstream of the one-third elevation of their tubular test section improved with higher power level.

Chen et al. [1978] observed that the major difference caused by the power input during the reflooding process was the shift of the boiling curve to higher temperature, as shown in Fig. 2.9. The shift was thought to be due to the power generation rate but not to the change in local subcooling because, as can be evidenced from Fig. 2.4, the influence of subcooling on the nucleate boiling region was negligibly small.

In some of the PWR-FLECHT tests, Cadek et al. [1971] investigated the effect of different power generation rate on the heat transfer coefficient. Their results were plotted against time after flood (Fig. 2.10). It cannot be deduced from this figure alone whether the boiling curves (heat flux vs. wall temperature) are different. At higher peak power, we would expect that the wall temperature also increases. This will tend to bring the curves shown in Fig. 2.10 closer to each other, if they are plotted against wall temperature.

The effect of power decay rate was also studied in the PWR-FLECHT tests. It was found that, with exponential decay rates differing in time constants by a factor of 2, no measurable effect on the heat transfer was observed. Cadek et al. inferred from this that the vapor generation rate was not significantly affected by the power decay rate.

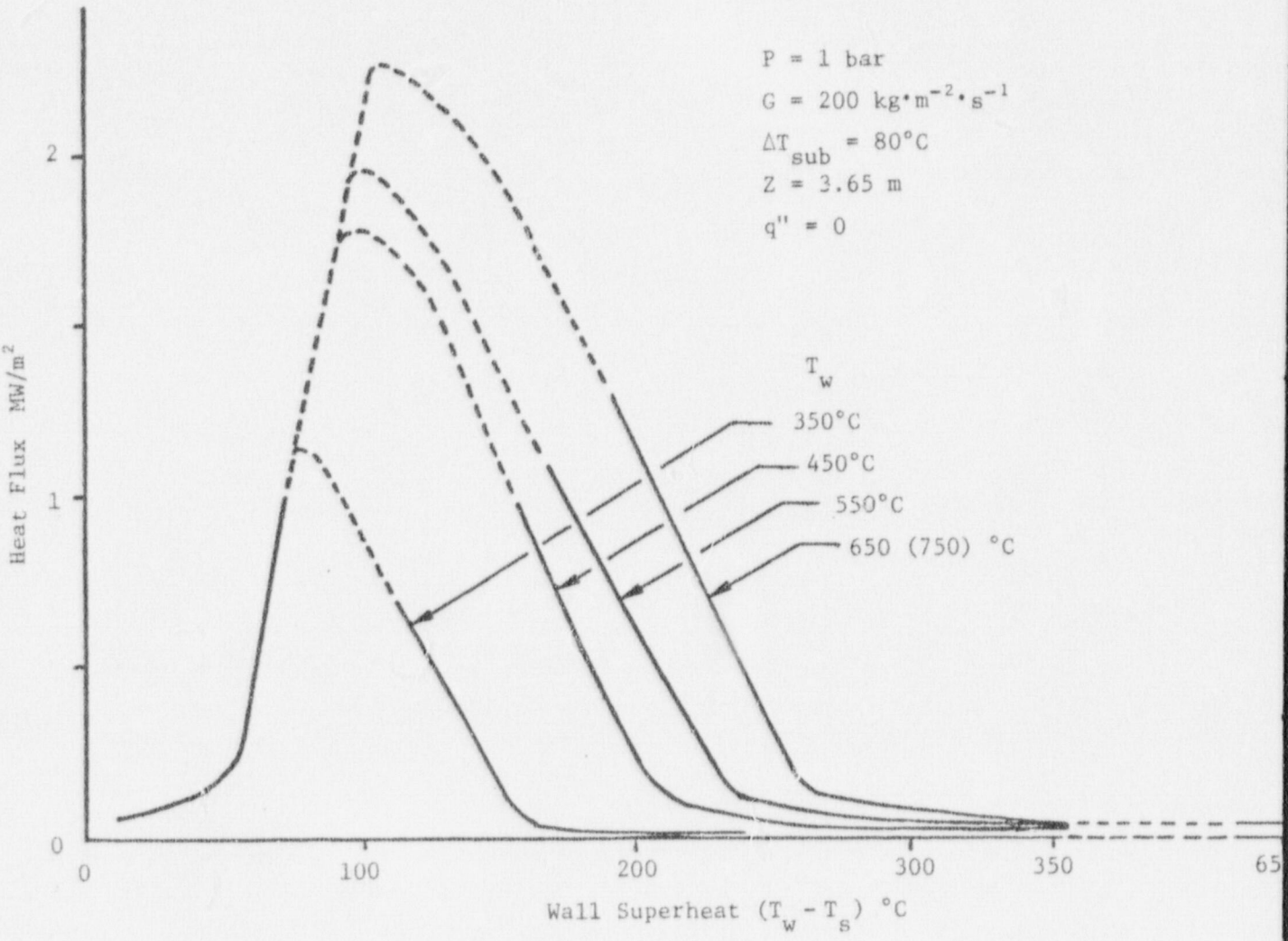

FIGURE 2.8: EFFECT OF INITIAL WALL TEMPERATURE ON THE SURFACE HEAT FLUX DURING A REFLOODING OF A 19.1 mm ID, 4 m LONG TUBE ORIENTED VERTICALLY (Chen et al. [1978])

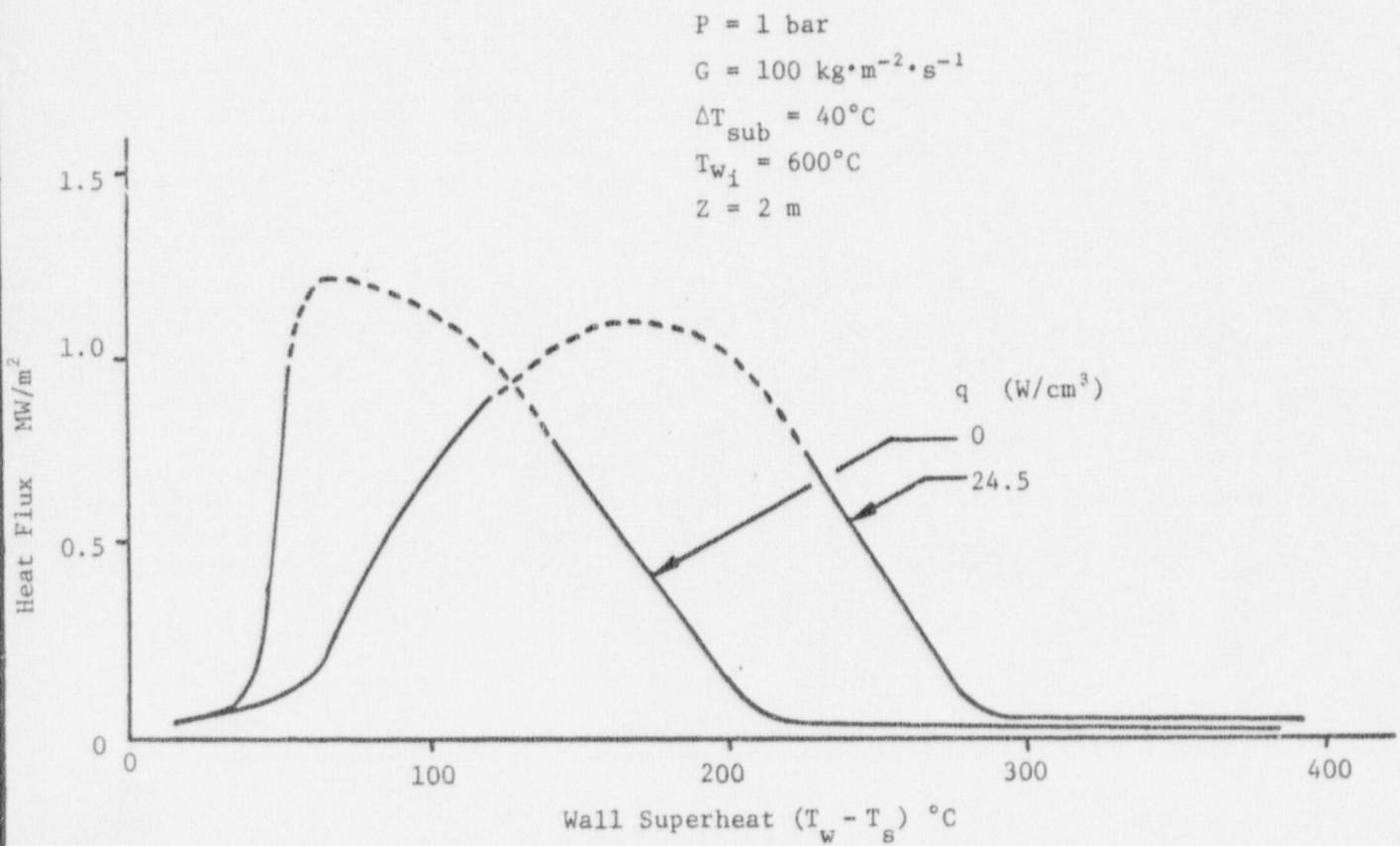

FIGURE 2.9: EFFECT OF HEAT GENERATION RATE ON THE SURFACE HEAT FLUX DURING A REFLOOD OF A 15.9 mm ID, 4 m LONG INCONEL TUBE ORIENTED VERTICALLY (Chen et al. [1978])

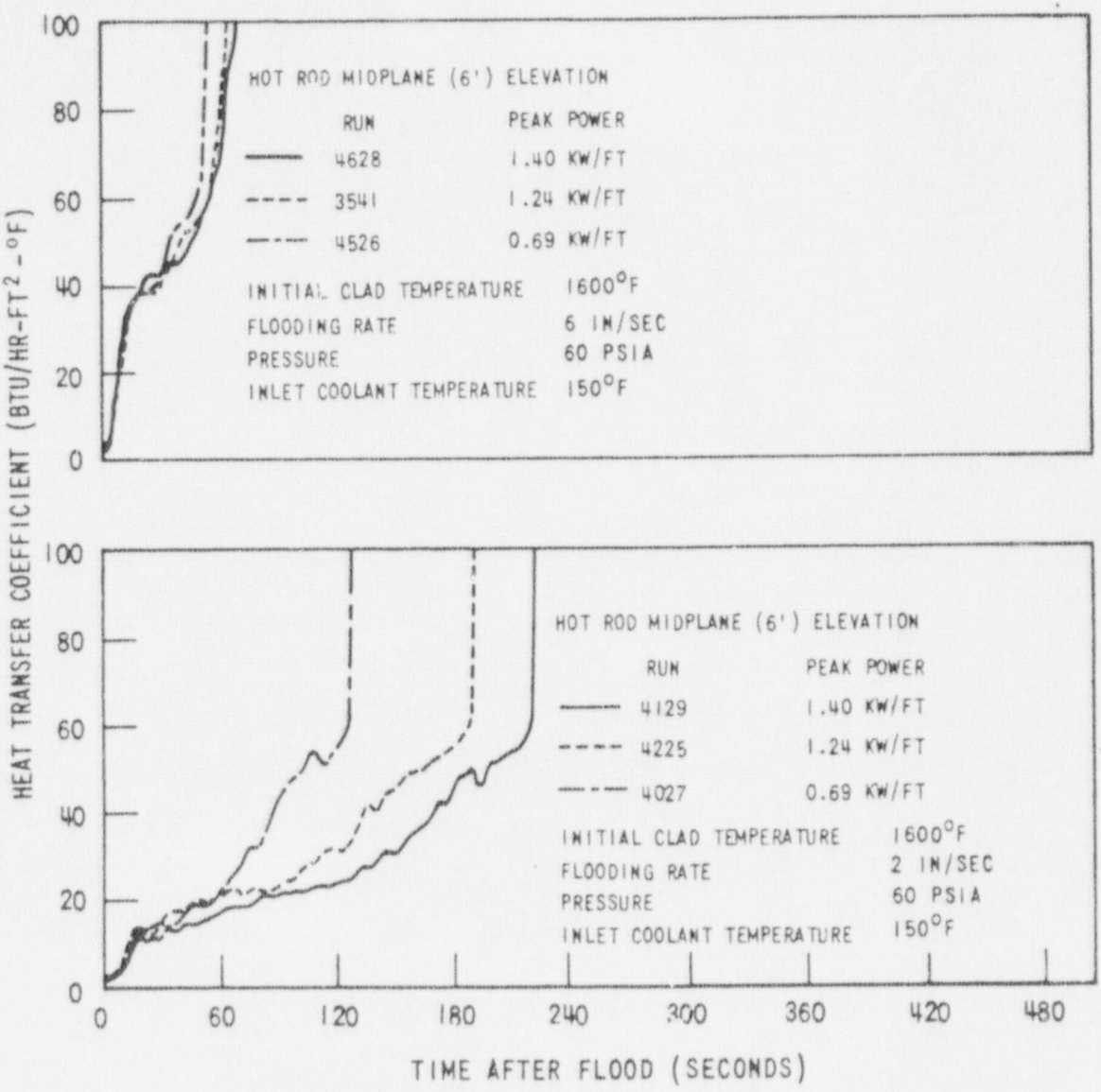

FIGURE 2.10: EFFECT OF PEAK POWER ON HEAT TRANSFER COEFFICIENT FOR 6 AND 2 in./s FLOODING RATE IN A 10 X 10 SIMULATED PWR-BUNDLE (Cadek et al. [1971])

II.2.7 Effect of Flow Blockage

A comparison of the findings of several studies on the effect of flow blockage during reflood is given by Lee [1977]. A typical set of data from the PWR-FLECHT program is shown in Fig. 2.11. It can be seen that the flow blockage simulated by flat plates resulted in higher heat transfer at the 1 in. downstream location from the blockage. Contrary to this observation, Davis' [1971] data show that, at 0.5 in. downstream, no flow blockage gave the best heat transfer, while a sleeve blockage resulted in a worse heat transfer than a flat plate blockage (Fig. 2.12). In the FLECHT tests, the positive effect of flow blockage on heat transfer extended as far as two feet upstream and four feet downstream of the blockage location, whereas in Davis' tests, the negative effect became unnoticeable beyond 5.5 - 10.5 in. downstream.

The improvement in heat transfer in the FLECHT test is attributed to droplet atomization and increased turbulence. The discrepancies between the PWR-FLECHT and Davis' data were thought to be due to the differences in bundle geometry and operating conditions. Lee [1977] concluded that Davis' experiment was not a representative simulation of a low velocity reflooding.

II.3 PREDICTION METHODS

Two approaches are currently being taken to predict the post-CHF boiling heat transfer during blowdown and reflood. The first is the global parameter approach in which empirical correlations derived from data obtained in simulated bundle tests are used. Invariably, the correlation based on FLECHT data has been used in the U.S. due to licensing requirements. The other approach is the so-called "instantaneous local conditions hypothesis" in which the local conditions are calculated by a loop code and then the heat transfer correlations are chosen accordingly. The correlations used are generally derived from single channel data obtained in steady-state experiments. Table II.2 summarizes the approaches taken by different authors.

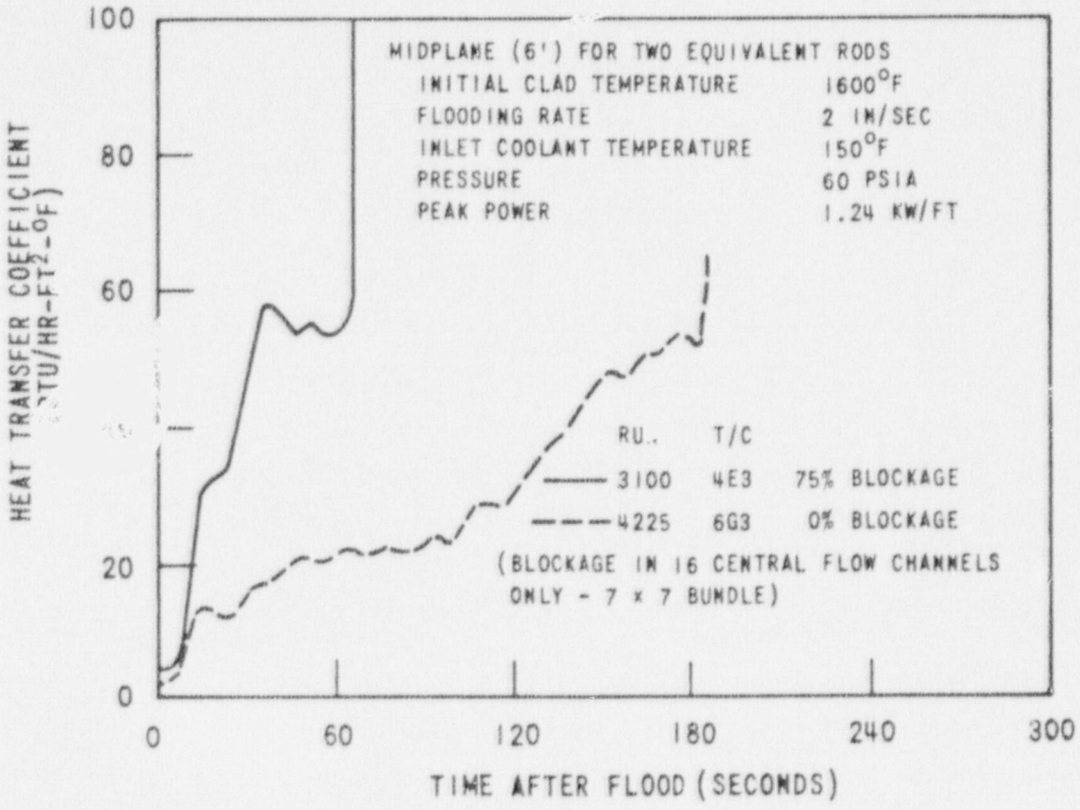

FIGURE 2.11: EFFECT OF FLOW BLOCKAGE WITH BYPASS FLOW ON MIDPLANE HEAT TRANSFER COEFFICIENTS IN A 7 X 7, 12 ft. LONG SIMULATED PWR-BUNDLE (Cadek et al. [1971])

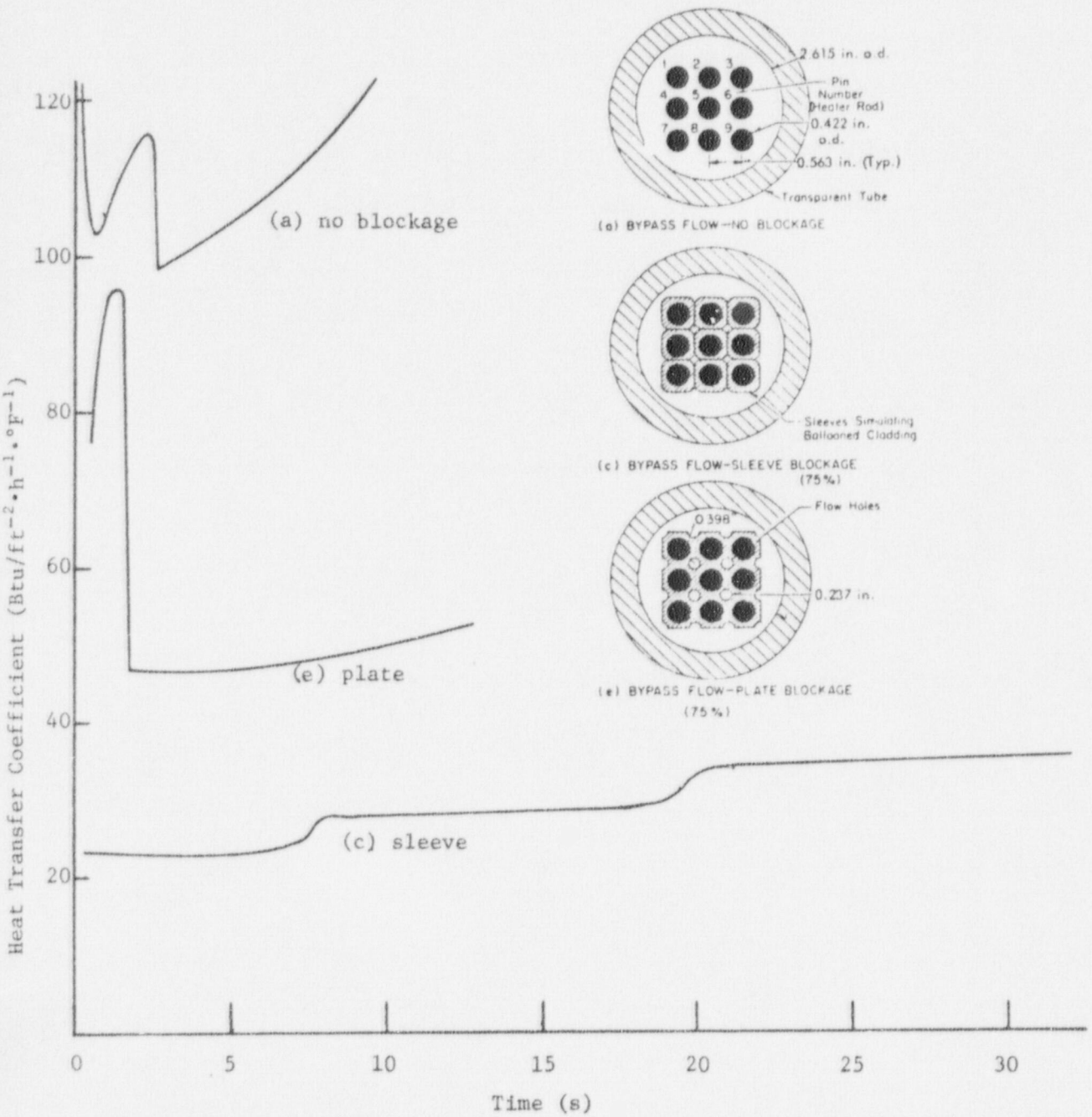

FIGURE 2.12: EFFECT OF FLOW BLOCKAGE ON HEAT TRANSFER COEFFICIENT IN A 3 X 3, 30 in. LONG SIMULATED PWR-BUNDLE (Lee [1977])

TABLE II.2: PREDICTION METHODS FOR TRANSIENT POST-CHF HEAT TRANSFER

Reference	Type of Transient	Correlations	Comments
Hsu [1977]	Blowdown	For low flow $h = (1-\alpha)[h_{mod,Bromley} + h_{Hsu,TB}] + \alpha\, h_{steam}$ $h_{mod,Bromley} = 0.62\left[2\pi\sqrt{\frac{g_c\sigma}{g(\rho_L-\rho_g)}}\right]^{-\frac{1}{4}}\left[\frac{k_g^3\rho_g(\rho_L-\rho_g)h_{fg}\,g}{De\,\mu_g\,\Delta T_s}\right]^{0.25}$ Btu·h^{-1}·ft^{-2}·F^{-1} $h_{Hsu,TB} = 1456\,P^{0.558}\exp[-0.003758\,P^{0.1733}\,\Delta T_s]$ Btu·h^{-1}·ft^{-2}·F^{-1} $h_{steam} = \max\begin{Bmatrix}h_{Rohsenow-Choi}\\ h_{natural\ conv}\end{Bmatrix}$ all evaluated with steam properties at saturation temperature For high flow $q'' = q''_{LC}\,F_L + q''_{FB}\,(1-F_L)$ (Chen 1977)	Applicable to both transition and film boiling; see reference for definition of low flow rate; units are British Engineering
Bjornard & Griffith [1977]	Blowdown	Transition boiling $q''_{TB} = \delta q''_{CHF} + (1-\delta)q''_{min}$ $\delta = \left(\frac{T_W - T_{min}}{T_{CHF} - T_{min}}\right)^2$ Film Boiling (a) For high flow use modified Groeneveld correlation: $h = 0.052\,\frac{k_g}{De}\left(\frac{G\,De\,X}{\mu_g\,\alpha_{dfm}}\right)^{0.688} Pr_W^{1.26}\,Y^{-1.06}$ $Y = 1 - 0.1\left(\frac{\rho_f}{\rho_g} - 1\right)^{0.4}(1-X)^{0.4}$ if $p \leq 1.38$ MPa use modified Dittus-Boelter $h = 0.023\,\frac{k_g}{De}\left(\frac{G\,De\,X}{\mu_g\,\alpha_{dfm}}\right) Pr_g^{0.4}$ (b) For low flow $h = (1-\alpha)\,h_{mod,Bromley} + \alpha\, h_{conv}$ (Hsu's recommendation) $h_{conv} = \max$ of $\begin{Bmatrix}\text{McAdams corr. for turbulent natural convection}\\ \text{h from (a)}\end{Bmatrix}$	Used in computer code "BEEST" α_{dfm} is void fraction evaluated from drift flux model (see reference)
Solbrig & Shumway [1976]	Reflood	Transition $\frac{CHF - \phi}{T_W - T_{CHF}} = 730\,e^{576/p}$ (McDonough et al.) (heat flux in Btu·h^{-1}·ft^{-2}, T in °F and P in psia) Film Low flow and high quality: Modified Bromley High flow and high quality: Groeneveld	Used in computer code "RELAP4"

TABLE II.2: PREDICTION METHODS FOR TRANSIENT POST-CHF HEAT TRANSFER (Cont'd)

Reference	Type of Transient	Correlations	Comments
Griffith & Kirchner [1976]	Reflood	Transition Log-log interpolation between CHF & minimum film boiling temperature Film (a) Inverted Annulus Modified Bromley (b) Dispersed Flow 2-step model of Laverty & Forslund	Used in computer code "REFLUX"
Westinghouse, Babcock & Wilcox, Combustion Engineering, Aerojet Nuclear Co.	Reflood	Correlations derived from PWR-FLECHT data	Empirical correlation used for licensing purpose
BNDC (Goldmuid [1972])	Reflood	Transition Boiling $h = \left(\frac{k_g^3 \rho_g \rho_f h_{fg} g}{12\mu_g \Delta T_s L}\right)^{0.25} \cdot \left(\frac{1}{x}\right)^{0.33\sqrt{V_{in}}}$ Btu·h^{-1}·ft^{-2}·°F^{-1} (modified Ellion) Film Boiling Dittus-Boelter	Used in computer code "CLADFLOOD"
CISE (Martini & Premoli [1972])	Reflood	Film Boiling (a) Annular $h = h_o + h_{rad}$ $\frac{1}{h_o} = \frac{1}{h_f} + \frac{1}{h_{conv}}$ h_{conv} — Dittus-Boelter $h_f = 7.72 \frac{k_g G}{(G X)^{0.672}}$ (h in W/cm^2°C, k in W/cm°C and G in g/cm^{2}s) (b) Dispersed flow $h = h_{conv} + h_{rad}$ h_{conv} — Dittus-Boelter modified on the basis of CISE data	Transition boiling ignored; used in computer code "TRE"
Hsu [1977]	Reflood	Transition & Inverted Annular Film Boiling Same as in blowdown phase Dispersed Flow Film Boiling For $V_{steam} < V_{entrainment}$ $q'' = h'_{steam} (T_w - T_g)$ $h_{steam} = \max \begin{Bmatrix} h_{Dittus-Boelter} \\ h_{Rohsenow-Choi} \end{Bmatrix}$ For $V_{steam} > V_{entrainment}$ $q''_w = h_{steam} (T_w - T_g) + q_{rad, wall-to-drop} + q_{rad, wall-to-vapor}$	

II.4 DISCUSSION

There has been very little effort to incorporate the effect of transient in post-dryout heat transfer coefficient. During a transient, the heat transfer mechanism is probably dominated by the turbulence level rather than by the boundary layer phenomenon. Evidences reviewed in this report suggest that significant improvement in heat transfer will occur during depressurization and flow oscillation. Therefore, we can expect that correlations based on steady-state data will tend to underestimate the heat transfer coefficient, resulting in an overconservatism in the safety analysis of reactors.

Empirical correlations such as the one based on the PWR-FLECHT data have only been correlated by the system parameters, due to a lack of information on the local conditions. As such, they have a very limited range of applicability.

Most of the single-channel experiments have been concentrated on the measurement of the rewetting rate. Future experiments should consider the measurement of local conditions and the heat transfer coefficients.

REFERENCES

Bailey, N.A., "Dryout and post-dryout heat transfer at low flow in a single tube test section," AEEW-R 1068, 1977.

Baum, A.J., Purcupile, J.C., Dougall, R.S., "Transition and film boiling heat transfer for vertical surfaces," ASME paper 77-HT-82, 1977.

Bennett, A.W., Hewitt, G.F., Kearsey, H.A., Keeys, R.F.K., "Heat transfer to steam-water mixture flowing in uniformly heated tubes in which the critical heat flux has been exceeded," AERE-R 5373, 1967.

Berenson, P.J., "Film boiling heat transfer from a horizontal surface," J. of H.T., 83, 351-358, 1961.

Bjornard, T.A., Griffith, P., "PWR blowdown heat transfer," Symposium on the Thermal and Hydraulic Aspects of Nuclear Reactor Safety, Vol. 1, Light Water Reactors, ASME, 1977.

Blaisdell, J.A., Hochreiter, L.E., Waring, J.P., "PWR FLECHT-SET Phase A Report," WCAP-8238, 1973.

Bromley, L.A., Heat transfer in stable film boiling," Chem. Eng. Prog., 46, 221-227, 1950.

Cadek, E.F., Dominicis, D.P., Leyse, R.H., "PWR FLECHT - Final Report," WCAP-7665, 1971.

Campanile, A., Pozzi, G.P., "Low rate emergency reflooding heat transfer tests in rod bundle," Proceedings of the CREST Specialist Meeting on Emergency Core Cooling for Light Water Reactors, Garching/Munchen, MRR 115, Vol. 1, 1972.

Chen, J.C., Sundaram, R.K., Özkaynak, F.T., "A phenomenological correlation for post-CHF heat transfer," Dept. of Mech. Eng'g. and Mechanics, Lehigh U., Bethlehem, Pa., TS-774, 1977.

Chen, W.J., Lee, Y., Groeneveld, D.C., "An experimental study on the heat transfer mechanisms during rewetting," Paper to be published, 1978.

Cheng, S.C., Ng, W., "Transition boiling heat transfer in forced vertical flow via a high thermal capacity heating process," Letters in Heat Transfer, 3, 333-342, 1976.

Cheng, S.C., Ng, W.W.L., Heng, K.T., "Transition boiling heat transfer in forced vertical flow," University of Ottawa Quarterly Progress Report to Argonne National Laboratory, No. 6, 1977.

Cheng, S.C., Ng, W.W.L., Heng, K.T., Groeneveld, D.C., "Measurements of transition boiling data for water under forced convective conditions," Paper accepted for publication, ASME J. of H.T., 1978.

Davis, P.R., "Experimental studies of the effect of flow restrictions in a small rod bundle under emergency core coolant injection conditions," Nucl. Technology, II, 551-556, 1971.

Dhir, V.K., Purdhit, G.P., "Subcooled film-boiling heat transfer from spheres, ASME 77-HT-78, 1977.

Farahat, M.M., Armstrong, D.R., Eggen, D.T., "Transient heat transfer between hot metal spheres and subcooled water," Atomkernergie (ATKE) Bd. 29, Lfg. 1, 1977.

Farman, R.F., Cermak, J.O., "Post DNB heat transfer during blowdown," WCAP-7837, 1972.

Forslund, R.P., Rohsenow, W.M., "Thermal non-equilibrium in dispersed flow film boiling in a vertical tube," MIT Report 75312-44, 1966.

Fung, K.K., "Forced convective transition boiling," M.A.Sc. Thesis, U. of Toronto, 1976.

Gardiner, S.R.M., Groeneveld, D.C., "Subcooled and low quality film boiling," Progress Report submitted to USNRC, Sept. 1977.

Goldemund, M.H., "CLADFLOOD - An analytical method of calculating core reflooding and its application to PWR loss of coolant analysis," Proceedings of the CREST Specialist Meeting on Emergency Core Cooling for Light Water Reactors, Garching/Munchen, MRR 115, V. 2, 1972.

Griffith, P., Kirchner, W., "Reflood heat transfer in a light water reactor," Paper presented at 16th National Heat Transfer Conference, St. Louis, 1976.

Groeneveld, D.C., "An investigation of heat transfer in the liquid deficient regime," AECL-3281, 1968, Revised 1969.

Groeneveld, D.C., "Effect of a heat flux spike on the downstream dryout behavior," ASME J. of H.T., 96, 121-125, 1974.

Groeneveld, D.C., "Post-dryout heat transfer: Physical mechanisms and a survey of prediction methods," Nuc. Eng. & Des., 32, 283-294, 1975.

Groeneveld, D.C.. "Post-CHF heat transfer studies," Presentation at Fifth Water Reactor Safety Research Information Meeting, Gaithersburg, Md., 1977.

Groeneveld, D.C., Delorme, G.G.J., "Prediction of thermal non-equilibrium in the post-dryout regime," Nuc. Eng. & Des., 36, 17-26, 1976.

Groeneveld, D.C., Fung, K.K., "Forced convective transition boiling: Review of literature and comparison of prediction methods," AECL-5543, 1976.

Groeneveld, D.C., Gardiner, S.R.M., "Post-CHF heat transfer under forced convective conditions," Symposium on the Thermal and Hydraulic Aspects of Nuclear Reactor Safety, V. 1, Light Water Reactors, ASME, 1977.

Groeneveld, D.C., Gardiner, S.R.M., "A method of obtaining flow film boiling data for subcooled water," accepted for publication, Int. J. of H.T., 1978.

Groeneveld, D.C., Young, J.M., "Film boiling and rewetting heat transfer during bottom flooding of a hot tube," Paper submitted to Sixth Int. H.T. Conf., Toronto, Ontario, Aug. 7-11, 1978.

Hendricks, R.C., Graham, R.W., Hsu, Y.Y., Friedman, R., "Experimental heat transfer results for cryogenic hydrogen flowing in tubes at subcritical and supercritical pressures to 800 psia," NASA TN D-3095, 1966.

Hsu, Y.Y., "Proposed heat transfer 'Best Estimate' packages," Nov. 1977.

Jones, O.C., Jr., Saha, P., "Non-equilibrium aspects of water reactor safety," Symposium on the Thermal and Hydraulic Aspects of Nuclear Reactor Safety, V. 1, Light Water Reactors, 249-288, ASME, 1977.

Lauer, H., Hufschmidt, W., "Heat transfer and surface rewet during quenching," Proceedings of NATO Advanced Safety Institute, Aug. 16-27, 1976, Istanbul, Turkey, V. III, 1309-1326.

Lee, N., "Evaluation of Davis' data and movies," Attachment to Progress Report to USNRC, 1977.

Lee, Y., Chen, W.J., Groeneveld, D.C., "Rewetting of very hot vertical and horizontal channels by flooding," Paper to be published, 1978.

MacDonald, P.E. et al., "Performance of unirradiated and irradiated PWR fuel rods tested under power-coolant-mismatch conditions," EG&G Idaho Inc., Report presented at the Fifth Water Reactor Safety Research Information Meeting, 1977.

Martini, R., Premoli, A., "A simple model for predicting ECC transients in bottom flooding conditions," Proceedings of the CREST Specialist Meeting on Emergency Core Cooling for Light Water Reactors, Garching/Munchen, MRR 115, V. 2, 1972.

Martini, R., Premoli, A., "Bottom flooding experiments with simple geometries under different ECC conditions," Energia Nucleare, 20, 1973

McConnell, J.W., "Effect of geometry and other parameters on bottom flooding heat transfer associated with nuclear fuel bundle simulators," ANCR-1049, 1972.

Morgan, C.D. et al., "Analytical and experimental investigation of heat transfer during simulated cold-leg blowdown accidents," Babcock & Wilcox, TP-L89, presented at CREST Specialist Meeting on Emergency Core Cooling for Light Water Reactors, Garching/Munchen, 1972.

Newbold, F.J., Ralph, J.C., Ward, J.A., "Post dryout heat transfer under low flow and low quality conditions," Paper presented at the European Two Phase Flow Group Meeting, Erlangen, 1976.

Quinn, E.P., "Forced flow heat transfer to high-pressure water beyond the critical flux," ASME 66-WA/HT-36, 1966.

Ragheb, H.S., "Development of electric probes to detect phase change at a heated surface," M.A.Sc. Thesis, U. of Ottawa, 1977.

Ragheb, H.S., Cheng, S.C., Groeneveld, D.C., "Measurement of transition boiling boundaries in forced convective flow," Paper to be published, 1978.

Ralph, J.C., Sanderson, S., Ward, J.A., "Post-dryout heat transfer under low flow and low quality conditions," Paper presented at the Symposium on the Thermal and Hydraulic Aspects of Nuclear Reactor Safety, Winter Annual ASME Meeting, Atlanta, Ga., Nov. 27 - Dec. 2, 1977.

Ramu, K., Weisman, J., "Transition boiling heat transfer to water in a vertical annulus," Paper presented at Heat Transfer Conference, AIChE, ASME, St. Francis Hotel, San Francisco, Aug. 1975.

Riedle, K., Winkler, F., "ECC-reflooding experiments with a 340-rod bundle," Proceedings of the CREST Specialist Meeting on Emergency Cooling for Light Water Reactors, Garching/Munchen, MRR 115, V. 1, 1972.

Sergeyev, V.V., Remisov, O.V., Vorobyev, V.A., "Thermal non-equilibrium and heat transfer in post-dryout region," Paper presented at Soviet-Canadian Heat Transfer Seminar, Moscow, 1976 (Translated by A.S. Borodin, AECL).

Siemens, A.G. et al., "Further development of the technology of light water-cooled reactors - Project 2b - Cooling conditions of the reactor core in the case of the maximum credible accident during refilling by the safety feed system - final report," AEC-tr-7396, 1973.

Smith, T.A., "Heat transfer and carryover of low pressure water in a heated vertical tube," M.Sc. Thesis, MIT, 1976.

Solbrig, C.W., Shumway, R.W., "Prediction of reflood heat transfer with standard loop programs," ASME 76-WA/HT-54, 1976.

Swenson, H.S., Carver, J.R., Szoeka, G., "The effects of nucleate boiling vs. film boiling on heat transfer in power boiler tubes," J.Eng. Power, Transactions ASME, 84, 365-371, 1965.

Turner, D.M., "Rod bundle film boiling heat transfer experiments," ASME 77-HT-94, 1977.

White, G.P., Duffey, R.B., "A study of the unsteady flow and heat transfer in the reflooding of water reactor cores," Central Electricity Generating Board Report RD/B/N3134, 1974.

Yadigaroglu, G., Yu, K.P., Arrieta, L.A., Greif, R., "Heat transfer during the reflooding phase of the LOCA - state of the art," EPRI 248-1, Topical Report, Sept. 1975.

Yates, J., Galbraith, K., Collingham, R., "DNB and post DNB heat transfer data in 25 rod bundles," Report XN-75-54, EXXON Nuclear Co. Inc., presented at Third Water Reactor Safety Information Meeting, Washington, D.C., Sept. 1975.

NOMENCLATURE

CHF	Critical heat flux
Cp	Specific heat
De	Hydraulic equivalent diameter, tube diameter
g	Acceleration due to gravity
g_c	Conversion factor
G	Mass flux
h	Enthalpy, heat transfer coefficient
i	Enthalpy
k	Thermal conductivity
L	Length
Nu	Nusselt number (h D/k)
P	Pressure
Pr	Prandtl number (μ Cp/k)
q"	Surface heat flux
Re	Reynolds number
t	Time; thickness
T	Temperature
U	Velocity
V	Velocity
v	Velocity component of wavy interface normal to solid surface
X	Quality
Y	Miropol'skiy two-phase flow factor
Z	Axial coordinate

Greek

α	Void fraction
α_ℓ	Thermal diffusivity of liquid
ϕ	Surface heat flux
δ	Droplet diameter, fraction of wet wall area
μ	Dynamic viscosity
ν	Kinematic viscosity
ρ	Density
σ	Surface tension

ΔH Local subcooling, $h_s - h$

ΔT Local subcooling, $T_s - T$

Subscripts

a Actual value

CHF Critical heat flux

conv Convection

e Equilibrium value

f Film temperature, (average of wall and bulk temperature)

fg Difference between saturated vapor and saturated liquid value

hom Homogeneous

g Saturated vapor

i Initial

in Inlet

ℓ Liquid

max Maximum

min Minimum

rad Radiation

s Saturation value

sub Subcooling

v Vapor

va Actual vapor conditions

w Heated wall

Abbreviations

CHF Critical heat flux

DNB Departure from nucleate boiling

FB Film boiling

TB Transition boiling

DO Dryout

PDO Post dryout

APPENDIX I

POST-CHF HEAT TRANSFER UNDER FORCED CONVECTIVE CONDITIONS

(A previous review which includes tables of steady-state post-CHF data)

AECL – 5883

Post-CHF Heat Transfer Under Forced Convective Conditions

D. C. GROENEVELD
S. R. M. GARDINER
(Attached Staff, Canadian General Electric Co. Ltd., Peterborough, Ontario)
Atomic Energy of Canada Limited
Chalk River, Ontario
Canada

ABSTRACT

This paper reviews the published information on transition boiling and film boiling heat transfer under forced convective conditions. Transition boiling data were found to be available only within limited ranges of conditions. The data did not permit the derivation of a correlation; however the parametric trends were isolated from these data.

A larger number of heat transfer experiments have been carried out in the liquid deficient regime. Most studies were concerned only with simple geometries (tubes, annuli) but recently the post-dryout behavior of reactor fuel bundles have also been studied. Prediction methods in the liquid deficient regime for simple geometries were found to be fairly reliable, especially for simple geometries at high flows and high pressures.

Little information on heat transfer in the inverted annular flow regime was found to be available; some data and correlations were available from cryogenic studies; extrapolation to reactor conditions is questionable. Data from transient studies are also considered and recommendations for prediction methods are made.

NOMENCLATURE

A	Constant
B	Constant
C	Constant
CHF	Critical heat flux
C_p	Specific heat
De	Hydraulic equivalent diameter, tube diameter

reprinted from
Symposium on the Thermal and Hydraulic Aspects of Nuclear Reactor Safety
Volume 1: Light Water Reactors
Edited by O. C. Jones, Jr. and S. G. Bankoff

published by
THE AMERICAN SOCIETY OF MECHANICAL ENGINEERS
345 East 47th Street, New York, N.Y. 10017
Printed in U.S.A.

f	Friction factor
g	Acceleration due to gravity
g_c	Conversion factor
G	Mass flux
Gr	Grashof number $\left[\frac{g \beta \Delta T D^3}{\nu^2}\right]$
h	Enthalpy
h	Heat transfer coefficient
k	Thermal conductivity
L	Length
Nu	Nusselt number (h D/K)
P	Pressure
Pr	Prandtl number (μ Cp/K)
Q	Surface heat flux
R	Gas constant
S	Slip ratio, suppression factor
T	Temperature
U	Velocity
X	Quality
Z	Axial coordinate
α	Void fraction
β	Thermal expansion coefficient
γ	Ratio of specific heats
ϕ	Surface heat flux
δ	Droplet diameter
ϵ	Roughness height, eddy diffusivity, emissivity
ν	Kinematic viscosity
μ	Dynamic viscosity
τ	Shear
ρ	Density
σ	Surface tension
ΔH	Local subcooling, h_s - h
ΔT	Local subcooling, T_s - T

Subscripts

a	Actual value
b	Bubble, bulk, boiling
c	Critical (thermohydraulic), convection
CHF	Critical heat flux
e	Equilibrium value
f	Film temperature, (average of wall and bulk temperature)
fg	Difference between saturated vapor and saturated liquid value
hom	Homogeneous
g	Saturated vapor
i	Inside, inlet
ℓ	Liquid
m	Maximum
max	Maximum
min	Minimum
o	Outside, outlet
rad	Radiation
s	Saturation value
sub	Subcooling
v	Vapor
va	Actual vapor conditions
ve	Equilibrium vapor conditions
w	Heated wall

Abbreviations

CHF	Critical heat flux
DNB	Departure from nucleate boiling
FB	Film boiling
TB	Transition boiling
DO	Dryout
PDO	Post Dryout

INTRODUCTION

Fuel sheath temperatures in water-cooled nuclear reactors are usually near the saturation temperature of water. During an accidental increase in power or decreases in flow and pressure, however, deterioration in heat transfer can occur when the surface temperature increases to such a high level that the heated surface temperature can no longer support continuous liquid contact. This phenomenon is usually referred to as the boiling crisis* and the corresponding heat flux as the critical heat flux or CHF. The boiling crisis is characterized either by a sudden rise in surface temperature, caused by the heated surface being covered by a stable vapor film (film boiling), or by small surface temperature spikes, corresponding to the appearance and disappearance of dry patches (transition boiling).

Due to the poor heat transport properties of the vapor, high heated surface temperatures are often encountered in the post-CHF or post-dryout region. Although nuclear reactors normally operate under conditions where dryout does not occur, accidents can be postulated where dryout occurrence is possible. The most serious of the postulated accidents is thought to be the loss-of-coolant accident (LOCA) caused by a rupture in the primary coolant system. Accurate prediction of the consequences of a LOCA requires precise calculation of fuel-coolant heat transfer during (1) the blowdown phase (when the fuel channel is voided), and (2) the subsequent emergency-core-cooling (ECC) phase.

Heat transfer regimes, encountered during a LOCA or any other incident where the fuel dries out, depend on the fuel sheath temperature. The boiling curve (fig. 1) illustrates this dependence. In general, the heated surface is wetted intermittently in the transition boiling region while in the film boiling region the heated surface is covered by a stable vapor blanket.

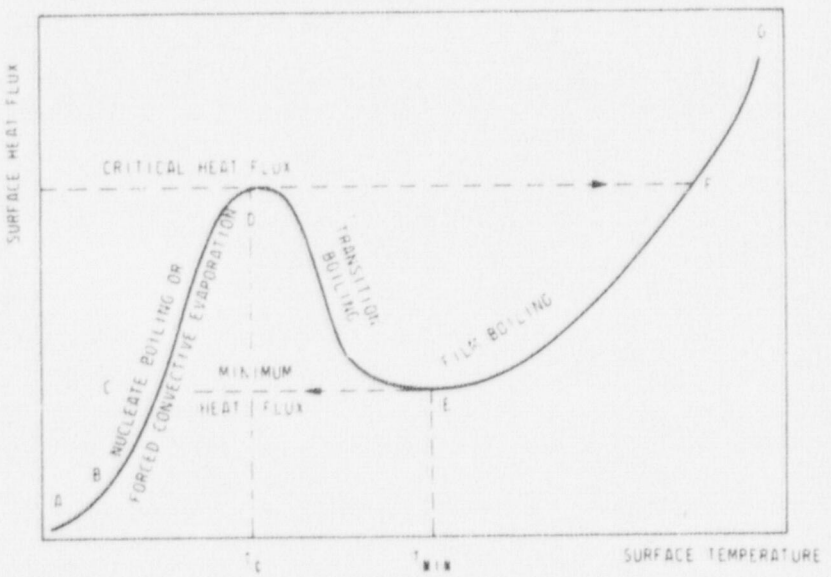

FIG. 1. BOILING CURVE

*Other terms frequently used to denote the boiling crisis: "dryout", "burnout" and "departure from nucleate boiling (DNB)."

Due to the scarcity of transition boiling data and the high inaccuracies associated with the available data, proposed transition boiling correlations are not considered reliable and cannot be extrapolated outside the range of data on which they are based. Instead, in a LOCA analysis it is usually assumed that, when the critical heat flux is exceeded, the heat transfer mode will change from the very efficient nucleate boiling mode directly to the inefficient film boiling mode (fig. 1). This assumption ignores the contribution of the intermediate transition boiling mode which is present due to the thermal inertia of the fuel. Also, in analyzing the thermal behavior of a hot surface which is being rewetted (such as may occur during emergency core cooling of a nuclear reactor) it is often assumed that film boiling is followed immediately by nucleate boiling, again ignoring the transition boiling heat transfer mode. In both cases, the assumption that film boiling rather than transition boiling occurs will result in an over-prediction of the calculated sheath temperature.

The post-CHF sheath temperature can be predicted from empirical correlations or from theoretical models. Since the theoretical models are rather complex and the physical mechanisms on which they are based are not yet fully understood, predictions are usually based on empirical correlations.

In this paper various physical mechanisms governing post-CHF heat transfer are discussed. A survey of experimental studies and prediction methods is also presented for each of the post-CHF regimes. Finally, our current knowledge of post-CHF heat transfer is discussed and recommendations are made for tentative prediction methods and for areas requiring further experimentation.

PHYSICAL MECHANISMS

Forced Convective Transition Boiling

As the name implies, transition boiling is an intermediate boiling region. Berenson [1] has provided a concise description of the transition boiling mechanism: *Transition boiling is a combination of unstable film boiling and unstable nucleate boiling alternately existing at any given location on a heating surface. The variation in heat transfer rate with temperature is primarily a result of a change in the fraction of time each boiling regime exists at a given location.*

The transition boiling section of the boiling curve is bounded by the critical heat flux at D and the minimum heat flux at E. The critical heat flux has been extensively studied and can be predicted by a variety of correlations. The minimum heat flux has undergone less study; it is known to be affected by flow, pressure, surface properties, fluid properties and heated surface parameters.

In pool boiling or low flow boiling systems the boiling crisis is reached when the flow of vapor leaving the heated surface is so large that it prevents a sufficient amount of liquid from reaching the surface to maintain the heated surface in the wet condition. The phenomenon that limits the inflow of liquid is the Helmholts instability which occurs when a counterflow of vapor and liquid becomes unstable. Zuber [2] and Kutateladze [3] have derived equations for the CHF based on the Helmholtz instability theory; their predictions agree with CHF values measured in pool boiling systems. At surface temperatures in excess of the boiling crisis temperature, the heated surface will be partially covered with unstable vapor patches (varying with space and time). The formation of such dry patches will be accompanied by a drastic reduction in heat transfer coefficient; the corresponding reduction in local vapor generation will permit the liquid to momentarily rewet the heat-

ed surface. Liquid contact with the heated surface will be frequent at low wall superheats but becomes less frequent at high wall superheats (Ruckenstein [4]). Bankoff [5] and Stock [6] have shown that liquid-solid contact is of very short duration at high wall superheats: an explosive formation of vapor occurred when the liquid contacted the heated surface; the subsequent vapor thrust forced the liquid away from the surface*. There is no agreement in the literature regarding the question of liquid-solid contact near the minimum of the boiling curve. Hesse [8] and Stock [6] believed that the vapor film, which may be in violent motion, will be maintained at wall superheats less than ΔT_{min} while Berenson [9] and Ruckenstein [4] believed that liquid-solid contact will occur up to ΔT_{min}.

In forced convective boiling the critical heat flux is no longer controlled by Helmholtz instability. Instead the boiling crisis is due to an agglomeration of bubble nucleation sites (Collier [10], high subcooling), bubble clouding (Tong [11], slight subcooling or low quality) or film depletion (Hewitt [12], annular dispersed flow). Ellion [13] studied forced convective transition boiling in subcooled water and observed frequent replacement of vapor patches by liquid. Although this may seem similar to transition pool boiling as described above, the introduction of the convective component will improve the film boiling component by reducing the vapor film thickness and changing the heat transfer mode, whether dry or wet, from free convection to forced convection. This will result in an increase in ϕ_{min} and might also increase ΔT_{min} (if ΔT_{min} is hydrodynamically controlled).

In the high quality region most of the heat transferred during transition boiling will be due to droplet-wall interaction. Initially, at surface temperatures just in excess of the boiling crisis temperature, a significant fraction of the droplets will deposit on the heated surface but at higher wall superheats the vapor repulsion forces would become significant in repelling most of the droplets before they can contact the heated surface. The repelled droplets will contribute to the heat transfer by disturbing the boundary layer sufficiently to enhance the heat transfer to the vapor. The heat transferred to the droplets was found to depend on droplet size (Wachters [14], droplet impact velocity (Pedersen [15]), impact angle (McGinnis [16]) and surface roughness (Wachters [14]). These variables also affect the minimum heat flux and corresponding surface temperature.

Minimum Film Boiling Temperature

Rewetting commences at the minimum film boiling temperature and, as a rule, rapidly proceeds until nucleate boiling is established at a much lower wall temperature. Predicting the minimum temperature as a function of the system parameters is thus very important since heat transfer coefficients on either side of the minimum film boiling temperature can differ by two orders of magnitude. Generally, the minimum film boiling temperature is defined as the temperature at the minimum heat flux.

Two theories have been proposed for the mechanism responsible for initiating transition boiling (or partial rewetting). One theory says that the minimum temperature is a thermodynamic property of the fluid (i.e. maximum liquid temperature) and thus is primarily a function of pressure. The other theory suggests that rewetting commences due to hydrodynamic instabilities which depend on the velocities, densities, and viscosities of both phases as well as the surface tension at the liquid-vapor interface. During fast transi-

*Westwater [7] did not believe that liquid-solid contact occurred in transition boiling; he did observe explosive formation of vapor when the liquid approached the heated surface.

tions, where insufficient time is available to fully develop the hydrodynamic forces, rewetting is expected to be thermodynamically controlled while for low flows and low pressures, where sufficient time is available and the volumetric expansion of the fluid near the wall is large, rewetting is more likely to be hydrodynamically controlled. Once rewetting has occurred locally, the rewetting front can then propagate at a rate which is primarily controlled by axial conduction (e.g. Thompson [17]). Both theories can be modified to include the thermal properties of the surface.

There is no general consensus on the effect of the various system parameters on the minimum film boiling temperature under forced convective conditions. These effects are included in correlations for the minimum temperature which have been tabulated by Gardiner and Groeneveld [18].

Film Boiling

General. During film boiling the heated surface is cooled by radiation, forced convection to the vapor and by interaction of the liquid and the heated surface. The vapor can become highly superheated; its temperature is controlled both by wall-vapor and vapor-liquid heat exchange. The liquid is thought to be in the form of:

(a) a dispersed spray of droplets, usually encountered at void fractions in excess of 80%. The corresponding flow regime is often referred to as the liquid-deficient regime as insufficient liquid is available to maintain a wet wall (figure 2a).

(b) a continuous liquid core (surrounded by a vapor annulus which may contain entrained droplets) usually encountered at void fractions below 30%. The corresponding flow regime is sometimes referred to as the inverted annular flow regime (figure 2b).

(c) a transition between the above two cases, usually in the form of slug flow (fig. 2c).

Of the above post-dryout regimes, the liquid-deficient regime is most commonly encountered and has been well studied. Its post-dryout temperature is moderate while for flow regimes (b) and (c) the boiling crisis frequently results in a failure of the heated surface.

Liquid Deficient Regime. In the liquid deficient regime the vapor temperature is controlled by wall-vapor and vapor-droplet heat exchange. Due to the low superheat of the

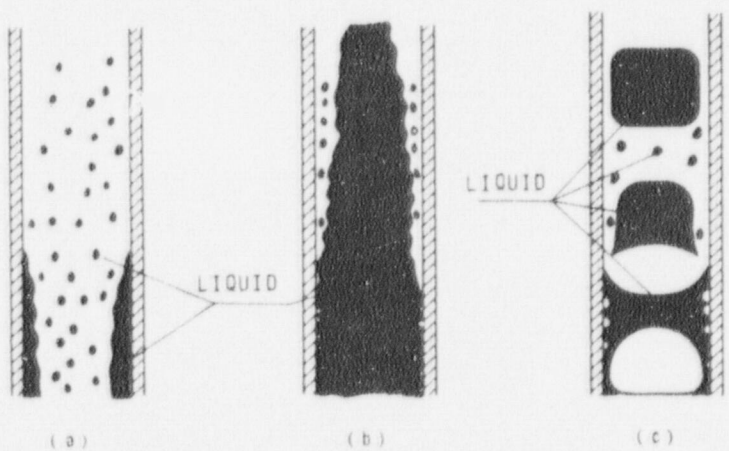

FIG. 2. FLOW REGIMES DURING FILM BOILING. (a) LIQUID DEFICIENT FLOW REGIME, (b) INVERTED ANNULAR FLOW REGIME, AND (c) SLUG FLOW REGIME

vapor near the dryout location or rewetting front the vapor-droplet heat exchange is small and most of the heat transferred from the wall is used for superheating the vapor. At distances further downstream, however, an "equilibrium" vapor superheat can be reached, i.e. the amount of heat transferred from the wall to the vapor may approximately balance the amount of heat absorbed by the droplets (from the vapor) and used for evaporation of the droplets.

Near a heated surface the heat exchange between vapor and droplets is enhanced due to the temperature in the thermal boundary layer being well above that of the vapor core (Cumo [19]). If the temperature of the heated surface is below the minimum temperature, some wetting of the wall may occur resulting in an appreciable fraction of the droplets being evaporated (Wachters [14]). At temperatures above the minimum temperature only dry collisions can take place (collisions where a vapor blanket is always present between surface and droplet). Little heat transfer takes place to small droplets which resist deformation and bounce back soon following a dry collision (Wachters [14], Bennett [20]). However the dry collisions disturb the boundary layer thus improving the wall-vapor heat transfer. Larger droplets are much more deformable and tend to spread considerably thus improving both the wall-vapor and vapor-droplet heat exchange (Cumo [19], Wachters [14]). This spreading may lead to a breakup into many smaller droplets if the impact velocity is sufficiently high (McGinnis [16]). The vapor film thickness separating the stagnated droplets from the heated surface is difficult to estimate but must be greater than the mean free path of the vapor molecules in order to physically separate the liquid from the heated surface.

Attempts to evaluate the direct heat flux to the droplets due to interaction with the heated surface have resulted in the postulation of many simplifying assumptions, e.g. Bailey [21], Groeneveld [22], Plummer [23]. These assumptions may be questionable when applied to liquid deficient cooling. However, due to lack of direct measurement of droplet-wall interaction during forced-convective post-dryout conditions no other approach can be taken.

Inverted Annular Flow. In the inverted annular flow regime few entrained droplets are present as the bulk of the liquid is in the form of a continuous liquid core which may contain entrained bubbles. At dryout the continuous liquid core becomes separated from the wall by a low viscosity vapor layer which can accommodate steep velocity gradients. However, the velocity distribution across the liquid core is fairly uniform. Once a stable vapor blanket has formed, the heat is transferred from the wall to the vapor and subsequently from the vapor to the wavy liquid core. Heat transfer across the wavy vapor-liquid interface takes place by forced convective evaporation. This mode of heat transfer is much more efficient than the single phase convective heat transfer between smooth wall and vapor; hence it is assumed that the bulk of the vapor is at or close to the liquid core temperature (i.e. saturation temperature). The low-viscosity, low-density vapor flow experiences a higher acceleration than the dense core flow. This results in an increased velocity differential across the interface (which may lead to liquid entrainment from the wavy interface). It may also lead to more interaction of the liquid core with the heated surface through dry collisions and will increase the turbulence level in the vapor annulus. The resulting increase in wall-vapor and wall-core heat transfer will lower the wall temperature; if the wall temperature drops below the minimum film boiling temperature rewetting may occur. Rewetting can also occur at higher temperatures if it is caused by a propagating rewetting front (Thompson [17]).

Slug Flow Film Boiling. Slug flow film boiling is usually encountered at low flows and void fractions which are too high to support inverted annular film boiling but too low to support dispersed flow film boiling. In tubes, it is formed just downstream of the inverted annular flow region when the liquid core breaks up into slugs of liquid in an otherwise vapor matrix. The prediction of the occurrence of slug flow in position and time during bottom flooding ECC is important because considerable downstream cooling is obtained from the resulting dispersed flow long before the quench front or collapsed liquid front arrives.

Several theories for the breakup of inverted annular flow into slug flow have been proposed. Data of Chi [24] suggest that the liquid core will break up into slugs which are equal in length to the most unstable wavelength of interfacial waves. Subcooling tends to stabilize the liquid-vapor interface, and thus inhibits the formation of slug flow. Smith [25] measured the location of slug flow as the point of minimum heat transfer coefficient in the film boiling region. In doing so, he is suggesting that the core is broken up by the hydrodynamic forces of the vapor on the liquid. If the vapor velocity is high enough to break up the liquid core then it is also high enough to considerably improve the heat transfer coefficient. Kalinin [26] observed another possible mechanism for the onset of slug flow in their transient tests. Immediately after the introduction of liquid to their test section, the sudden increase in vapor volume due to vapor generation at the leading edge of the liquid caused a back pressure which decelerated the flow. The higher pressure and lower flow rate caused a decrease in vaporization and the flow surges forward. This cycle was repetitive with a liquid slug separating from the liquid core with each cycle.

FORCED CONVECTIVE TRANSITION BOILING

Experimental Studies

The most widely used system in forced convective boiling studies is a heat flux controlled system where the heat output of an electrically heated element is increased gradually. Such a system however does not permit the measurement of transition boiling data except at high flows and high vapor qualities (Fung [27]). Instead, a variety of temperature controlled systems have been used in transition boiling studies.

The earliest reported forced convective transition boiling study (Ellion [13]) utilized a 2.5 cm OD annulus, centrally heated by an electrical tubular heater and cooled internally by a stabilizing fluid to avoid dryout temperature excursions. Although this technique is potentially very promising, the choice of stabilizing fluids which have sufficiently high heat transport properties is limited. The same is true for systems where the heat is supplied directly by circulating fluids. Both McDonough [28] and Ramu [29] used such systems using liquid metals. Peterson [30] used a more novel approach: in his forced convective study, heat was supplied by an electrically heated platinum wire whose temperature was controlled by electronic feedback. More recently, transition boiling data have been derived from temperature-time transients during quenching of high thermal inertia test sections. Iloeje [31] obtained transition boiling data for water at high pressure from a thick Inconel test section while Cheng [32], Newbold [33] and Fung [34] have done so for atmospheric pressure using a thick short copper test section. Newbold [33] and Fung [34] indicated that some axial conduction was present in their test section due to rewetting being initiated at the inlet and/or outlet of their test section. To eliminate this, Newbold installed guard heaters on both sides of their test section.

A search of the literature produced only nine studies dealing with forced convective

transition boiling. Table 1 summarizes the studies; they all suffer from serious shortcomings and cover only narrow ranges of conditions. The data are not considered sufficiently accurate and plentiful to serve as a basis of deriving a correlation. The parametric trends have been deduced from the data (Groeneveld [41]). In general, an increase in mass flux increases the transition boiling heat flux and shifts the wall superheat at the minimum heat flux to higher temperatures. The effect of an increase in subcooling is similar but the effect of quality is less clear: it is expected that at low wall superheats an increase in quality will have a negative effect on the transition boiling heat flux while at higher wall superheats the reverse is true.

Table 1: Transition Boiling Data of Water in a Forced Convective System

GEOMETRY	REFERENCE	RANGE OF DATA				COMMENTS
		P MPa	$G \times 10^3$ $kgm^{-2}s^{-1}$	$\phi \times 10^{-2}$ $kW.m^{-2}$	Subcooling (°C) or Quality	
Annulus 0.64 cm ID 6.35 cm OD	Ellion [73]	0.110-0.413	0.33-1.49	1.47-1.96	28-56°C	ϕ - controlled system with stabilizing fluid, L_H = 7.62 cm
Tube De = 0.386 cm	McDonough et al. [28]	5.51 8.27 13.78	0.27-2.04	0.32-3.78	Subcooled and low quality	NaK used as heating fluid. T_w inferred from heat transfer corr'n for NaK. Data no longer available.
Annulus 0.013 cm ID 1.21 cm OD	Peterson [30]	0.101	0.64-1.93	0.41-1.99	saturated	Heat flux controlled by electronic feedback, L_H = 5.08 cm
Tube De = 1.25 cm	Plummer [23]	6.89	0.07-0.34	0.06-0.27	X = 0.30 - 1.00	Transient test L_H = 10.16 cm
Annulus 1.37 cm ID 2.54 cm OD	Ramu & Weisman [29]	0.172-0.206	0.02-0.05	0.03-0.26	X = 0 - 0.500	Hg used as heating fluid. X not reported. Limited range in T_w
Rod Bundles De = 1.27 cm	Westinghouse FLECHT Cadeck et al. [64]	0.103-0.620	0.05-0.25	0.01-0.27	0-78°C	Transient test. ΔT_{sub} or X unknown.
Tube De = 1.27 cm	Cheng & Ng [32]	0.103	0.19	0.016-0.158	0-26°C	Transient & steady state test, high inertia. Copper block, L_H = 10.16 cm
Tube De = 1.27 cm	Fung [34]	0.101	0.068-1.35	0.008-1.89	0-76°C	Similar tests to Cheng & Ng [32]
Tube De = 1.27 cm	Newbold et al. [33]	0.303	0.016-1.25	0.016-0.942	0-80°C	Similar tests to Cheng & Ng [32] however guard heaters were employed to reduce axial conduction

Prediction Methods

Despite the scarcity of transition boiling data, a large number of correlations have been proposed (Table 2). They may be divided into three groups:

(i) Correlations containing boiling and convective components, e.g. Ramu [36], Mattson [37] and Tong [38]. These correlations usually have the form

$$h = A \exp(-B\Delta T_s) + \frac{k_v}{De} a Re_v^b Pr_v^c$$

where the first term represents the boiling component (which becomes insignificant at high wall superheats) and the second term represents the convective component. The correlations are usually claimed to be valid both in the transition boiling and film boiling region.

(ii) Phenomenological correlations e.g. Iloeje [39]; Tong and Young [40]. These correlations are based on a physical model of heat transfer in the transition boiling region. Because of an inadequate physical understanding they still contain many empirical constants.

(iii) Empirical correlations e.g. Ellion [13], Berenson [9] and McDonough [28]. These correlations all have a very simple form and generally cannot be extrapolated outside the range of data on which they are based. Some of these correlations are based on the conditions at the boiling crisis (CHF and T_{CHF}).

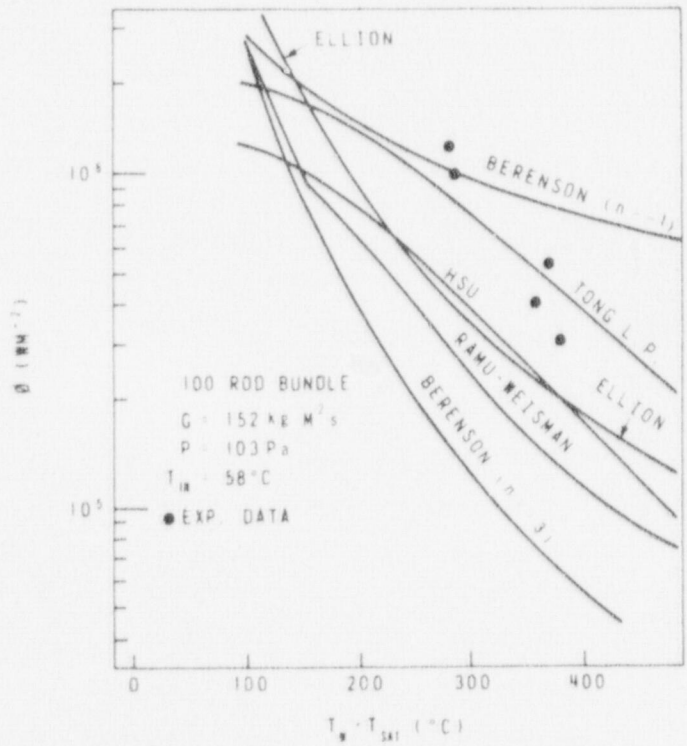

FIG. 3. COMPARISON OF TRANSITION BOILING CORRELATIONS WITH FLECHT DATA

Table 2: Transition Boiling Correlations for Water

EQUATIONS AND REFERENCES	RANGE OF APPLICABILITY FOR WATER					COMMENTS
	P MPa	$G \times 10^{3}$ kg m^{-2} s^{-1}	Subcooling °C or Quality	T_w °C	Geometry (De)	
$\phi = 4.562 \times 10^{11} \times \Delta T_s^{-2.4}$ Ellion [13]	0.110 - 0.413	0.33 - 1.49	28 - 56°C		Annulus (5.72 cm)	Based on data obtained in steady state tests with 7.5 cm heated length and a secondary stabilizing fluid
$\frac{CHF - \phi}{T_w - T_{CHF}} = 730e^{576/p}$ McDonough [28]	5.51 - 13.79	0.2 - 2.04	0 - 0.64	T_{CHF} - 554	Tube (0.38 cm)	$30 \leq L/D \leq 62$. Based on data from a heat flux controlled system
$\frac{\phi}{CHF} = \left(\frac{\Delta T_s}{T_{CHF} - T_s}\right)^n$ Berenson [9]						Pool boiling correlation: n = -3 (Peterson [30]) n = -1 (Groeneveld [41])
$h_{TB \text{ or } FB} = 7000 \exp(-0.008\,\Delta T_s) + 0.023 \frac{k_v}{De} \exp\left(-\frac{190}{\Delta T_s}\right) \left(\frac{C_{pv}}{k}\right)_f^{0.4} \left[\frac{DeG}{\mu_f}\left(X_e \frac{\rho_f}{\rho_g} + (1 - X_e)\frac{\rho_f}{\rho_f}\right)\right]^{0.8}$ Tong [38]	6.89	0.38 - 5.23		321 - 832		Agrees with data from Quinn [65] and Bennett [20] with rms error = 18%
$h_{TB} = 9000 \exp(-0.0054\,\Delta T_s) + h_{FB} + h_{rad}$ $h_{FB} = 0.023\left(\frac{k_f}{De}\right)\left[\left(\frac{GDe}{\mu_f}\right)\left(X_e \frac{\rho_f}{\rho_g} + (1 - X_e)\frac{\rho_f}{\rho_f}\right)\right]^{0.8}\left(\frac{C_{pv}}{k}\right)_f^{0.4}$ $h_{rad} = 1.73 \times 10^{-9}\left(\frac{1 - 0.6\alpha}{1.25 - 0.15\alpha}\right)\left(\frac{T_w^4 - T_s^4}{T_w - T_s}\right)$ Tong [38]	0.103 - 0.620	0.05 - 0.25	9 - 105°C		49, 100-rod	Correlation of bottom flooding data (FLECHT). Extrapolation outside range is tentatively permitted.
$h_{TB} = h_b + h_c$ $h_b = 0.5\,Sh_m\left[\exp[-.0078(T - T_{CHF})] + \exp[-0.0698(T - T_{CHF})]\right]$ $h_c = 0.023\left(\frac{k_g}{De}\right)\left(\frac{\mu_g}{\mu_w}\right)^{0.14}\left(\frac{C_{pv}}{k}\right)_g^{1/3}\left(\frac{GDeX_e}{\mu_g}\right)^{0.8}\left[1 + \frac{1 - X_e}{X_e}\left(\frac{\rho_g}{\rho_f}\right)\right]^{0.8}$ $h_c = 0.023\left(\frac{k_g}{De}\right)\left(\frac{\mu_g}{\mu_w}\right)^{0.14}\left(\frac{C_{pv}}{k}\right)_g^{1/3}\left(\frac{GDeX_e}{\mu_g}\right)^{0.8}\left[1 + \frac{1 - X_e}{X_e}\left(\frac{\rho_g}{\rho_f}\right)^{2/3}\right]$ $h_c = 0.023\left(\frac{k_g}{De}\right)\left(\frac{\mu_g}{\mu_w}\right)^{0.14}\left(\frac{C_{pv}}{k}\right)_g^{1/3}\left(\frac{GDeX_e}{\mu_g}\right)^{0.8}\left[\frac{0.15 + 0.86\,X_e}{X_e^{0.8}}\right]$ Rahu & Weisman [36]	up to critical	0.31 - 3.49	≥ 0.2 ≥ 0.2 $0 \leq X_e < 0.2$		Tube Annulus Tube & Annulus	Convective component correlation due to Quinn [55]. Boiling component fitted to data of Hench [66], Polomik [67], Cumo [68], Nobel [69] with suppression factor S (due to Chen [70]); h_m based on critical heat flux data of Addoms [71] (pool boiling). At low flow and high quality, they replaced ϕ_{hm} by $\phi_{CHF}/\Delta T_{max}$. ϕ_{CHF} is assumed to be a function of the void fraction only.
$h_{TB \& FB} = 9.09 \times 10^{4} \exp(-0.5\sqrt{\Delta T}) + 20.8\left(\frac{GDe}{\mu_g}\right)^{0.269}\left(\frac{\mu C_p}{k}\right)_g^{3.67} De^{-0.319} k_g^{0.306} X_e^{-0.091}$ $h_{TB \& FB} = 2.93 \times 10^{4} \exp(-0.5\sqrt{\Delta T}) + 1.22\left(\frac{GDe}{\mu_g}\right)^{0.505}\left(\frac{\mu C_p}{k}\right)_g^{4.56} De^{-0.16} k_g^{0.189} X_e^{-0.113}$ Mattson et al. [37]	4.13 - 21.51	0.68 - 5.16	0.1 - 0.99		Tube & Rod bundle	Correlations obtained from regression analysis. 28% rms error. 25.8% rms error

Table 2: Transition Boiling Correlations for Water (cont'd)

EQUATIONS AND REFERENCES	RANGE OF APPLICABILITY FOR WATER					COMMENTS
	P MPa	$G \times 10^{-3}$ kg m^{-2} s^{-1}	Subcooling °C or Quality	T_w °C	Geometry (Dₑ)	
$\phi = C\left(\frac{k\,\partial C p_\ell \rho_\ell T_s^2}{P_\ell h_{fg}}\right)\left(\frac{1-X_e}{X_e}\right)\frac{U_v\sqrt{\tau}}{\delta}\exp\left(-\frac{\Delta T_s}{\Delta T_m}\right)$ $+ \lambda(1-\alpha)\left[1-\exp\left(-\frac{T_s}{T_m}\right)\right]\frac{4k_\ell}{\delta}\left[\left(1+\frac{2\gamma_{mv}}{\delta}\right)\ln\left(1+\frac{\delta}{2\gamma_{mv}}\right)-1\right]\Delta T_s$ $+ 0.023\,\frac{k_g}{De}\left[\frac{GDe}{\mu_g}\left(X_e+(1-X_e)\frac{\rho_g}{\rho_\ell}\right)\right]^{0.8}\left(\frac{\mu C p}{k}\right)^{0.4}\Delta T_s$	6.89	0.41 - 1.70	0.1 - 0.7		Tube	3-step model of dispersed vertical flow heat transfer.
$\gamma_{mn} = \epsilon\left[\frac{\Delta T_s}{\Delta T_m}\Big/\left[1-\exp\left(-\frac{\Delta T_s}{\Delta T_m}\right)\left(1+\frac{\Delta T_s}{\Delta T_m}\right)\right]\right]^{1/3}$						
ΔT_s given by						
$\frac{k_v \Delta T_s}{GDeh_{fg}} = 3.274\times10^{-5}\left[2.93+4.443X_e+0.084\left(\frac{GX_e}{125000}\right)^2 - 7.361\left(\frac{GX_e}{125000}\right)^3\right]\Big/\left(\frac{GDe}{\mu_v}\right)^{0.477}$						
C = correlation constant; evaluated using data in transition boiling region, where the first term dominates.						
A = geometric parameter; can be evaluated from data at high wall superheat and low quality, where the second term dominates.						
Iloeje [39]						
$\phi = \frac{\phi_{FB}}{1-\alpha_{TB}}$	6890	0.41 - 5.16	0.2 - 1.45	$5.56 \le \Delta T_s \le 556$	Tube	Based on data of Bennett [20] and Era et al. [51]. rms error = 13.8%
$\phi_{FB} = 0.023(T_w-T_v)\left[\frac{k_v}{De}\left(\frac{GDe}{\mu}\right)^{0.8}_v\left(\frac{nX_e\frac{\rho_v}{\rho_g}+S(1-nX_e)\frac{\rho_v}{\rho_\ell}}{nX_e+S(1-nX_e)}\right)^{0.8}\left(\frac{\mu Cp}{k}\right)^{0.4}_v\right]T_v$	3.45 - 9.65	0.68 - 4.21	0.15 - 1.10	$5.56 \le T_s \le 556$	Annulus & rod bundle	Based on data of Groeneveld [73], Polomik [67] and Bennett et al. [74]. rms error = 29.2%
$n = 1.0 + \left(\frac{dn}{dX_e}\right)(X_e - X_1)$						
$n = 1.0$ for $\Delta T_s < 200°F$ or $G/10^6 > 2.5$						
$X_1 = \exp\left[C_3(0.05+G/10^6)^{0.8}\right]$						
$\frac{dn}{dX_e} = C_4(0.05+G/10^6)^{-0.12}$						
for $G/10^6 \le 0.7$ $C_3 = -0.26$; $C_4 = 0.69$						
$0.8 \le G/10^6 \le 2.5$ $C_3 = -0.57$; $C_4 = +0.25$						
$0.7 < G/10^6 < 0.8$ X_1 and $\frac{dn}{dX_e}$ obtained by linear interpolation						
$\alpha_{TB} = \exp\left[-0.012\,\frac{X_e^{2/3}}{\left(\frac{dX_e}{dL}\right)}\left(\frac{\Delta T_s}{100}\right)^{(1+0.0016\,\Delta T_s)}\right]$						
Tong & Young [40]						
$h_{TB} = 0.62\left[\frac{gX_v^2\rho_v(\rho_\ell-\rho_v)h_{fg}}{\Delta T_s \mu_v}\frac{1}{2\pi}\sqrt{\frac{g(\rho_\ell-\rho_v)}{\sigma}}\right]^{1/4} + A\exp(-B\Delta T_s)$	0.103 - 0.620	0.05 - 0.25	12 - 83		100 rod	Correlation based on FLECHT data. Development of h_{TB} based on Taylor's instability. Relations of A and B were plotted by Hsu and correlated by Groeneveld and Tung [41].
$A = 1456P^{0.558}$						
$B = 3.758\times10^{-3}P^{0.1733}$						
Hsu [42]						

Comparison of Data with Correlations

A limited comparison of some of the correlations with th data was carried out by Groeneveld and Fung [41] and Fung [34]. In general, correlation of the low pressure data was not unreasonable *if* a Berenson type correlation was used (i.e. assuming CHF and T_{CHF} are known). A value of the exponent n between -1 and -2 seemed to give the best fit to the data. A comparison of some of the correlations and the FLECHT data is presented in figure 3. Hsu's [42] correlation is tentatively recommended as it is based on simulated fuel bundle data and also agrees with the data of Ellion [13].

INVERTED ANNULAR AND SLUG FLOW FILM BOILING

Experimental Studies

Most of the experiments in these flow regimes have been carried out on cryogenics and refrigerants. Recently, because of the interest in LOCA heat transfer, some of these studies have also been carried out in water. Due to the high CHF in these flow regimes, post-CHF temperatures are very high. Hence experimental data can only be obtained in temperature controlled systems (Smith [25], Ellion [13] or from transient tests (Newbold [33], Cheng [32], Fung [34]).

Table 3 presents a summary of the studies carried out. As in transition boiling, the data obtained in water are not considered reliable but have been used to derive the parametric trends (Gardiner [18]). As expected, the heat transfer coefficient increases with mass flux because of the higher turbulence level and more intense liquid-wall interaction. An increase in subcooling also improves the heat transfer, presumably due to a thinning of the vapor film because of the subcooled liquid absorbing heat to the detriment of evaporation. The effect of wall superheat on the heat transfer coefficient was expected to be insignificant. . ewbold et al. [33], Cheng and Ng [32] and Fung [34], however, observed a constant film boiling heat flux over a wide range of wall superheats (e.g. figure 4) which implies a reduction in heat transfer coefficient with an increase in wall superheat.

Prediction Methods

Because of scarcity of water data at low qualities and subcooled conditions, most proposed correlations are based on cryogenic or refrigerant film boiling data only. The correlations and their range of applicability are tabulated in Table 4. They may be subdivided into:

(i) Correlations applicable to pool boiling and low mass velocities (e.g. Bromley [43], Berenson [44], Andersen [45]). These correlations basically have the form:

$$h_c = A\left[\frac{k_v^3\,\rho_v(\rho_\ell - \rho_v)i'_{fg}}{\mu_v\,\Delta T_{sat}}\right]^{1/4} f(U,\lambda) + h_{rad}$$

which was originally derived by Bromley [43] from Nusselt's classical analysis of filmwise condensation. The latent heat i'_{fg} is usually modified to include the vapor superheat while the velocity effect is included theoretically or empirically through $f(U,\lambda)$ where λ is either equal to the diameter, critical wavelength or the most unstable wavelength.

Table 3: Low Quality Film Boiling Experiments

AUTHORS	GEOMETRY	FLOW CONDITIONS	MAIN OBSERVATIONS
Bromley, LeRoy, and Robbers [75]	Vertical flow over a horizontal cylinder O.D. - 9.8 mm - 12.6 mm - 16.2 mm	N-hexane, CCl_4, benzene, ethyl alcohol were used. Mass fluxes of 0 to 6.56×10^3 $kgm^{-2}s^{-1}$ were tested.	For $U/\sqrt{gD} < 1.0$, h_c is independent of velocity and for $U/\sqrt{gD} > 2.0$, h_c is proportional to $U^{\frac{1}{3}}$.
Murphy, Kermode, and Zahradnik [76]	Horizontal plate	Hexane, benzene, and methanol were used. Mass fluxes of 0.67×10^3 to 4.04×10^3 $kgm^{-2}s^{-1}$ were tested.	Noted a moderate increase in the heat transfer coefficient with velocity.
Rankin [77]	Vertical tube I.D. - 26.9 mm length - 1.22 m	Freon-113 and methanol at mass fluxes of 0.36×10^3 to 4.04×10^3 $kgm^{-2}s^{-1}$	No effect of velocity in film boiling region.
Dougall and Rohsenow [47]	Vertical tube I.D. - 10.2 mm - 4.6 mm length - 386 mm	0.45×10^3 to 1.11×10^3 $kgm^{-2}s^{-1}$ Freon-113	No effect of velocity on film boiling.
Motte and Bromley [78]	Vertical flow over horizontal cylinders O.D. - 9.8 mm - 12.6 mm - 16.2 mm	$0 - 6.56 \times 10^3$ $kgm^{-2}s^{-1}$ of N-hexane, CCl_4, benzene, and ethyl alcohol with subcoolings of 0 - 45°C	Subcooling increased the heat transfer coefficient by as much as a factor of 4. The effect of subcooling increased with increased velocity.
Kalinin [26]	Downward flow in a vertical tube I.D. - 4 mm to 20 mm length - 100 mm	$6.32 \times 10^3 - 18.9 \times 10^3$ $kgm^{-2}s^{-1}$ of nitrogen with 0 - 38°C subcoolings in transient tests.	Tenfold increase in heat transfer at highest subcooling over saturated conditions. Threefold increase in heat flux over mass flux range tested.
Ellion [13]	Upward flow in a vertical annulus O.D. - 63.5 mm I.D. - 6.4 mm length - 76.2 mm	0.336×10^3 to 1.53×10^3 $kgm^{-2}s^{-1}$ of water with 28°C to 56°C subcooling.	No effect of subcooling or velocity on film boiling heat transfer.
Fung [34]	Upward flow in a vertical tube I.D. - 12.7 mm length - 101.6 mm	0.068×10^3 to 1.35×10^3 $kgm^{-2}s^{-1}$ of water with 0 - 76°C subcoolings in transient tests.	Heat flux increased fourfold at highest subcooling over saturated conditions. Heat flux increases tenfold at highest flow.
Cheng and Ng [32]	Upward flow in a vertical tube I.D. - 12.7 mm length - 57.15 mm	0.19×10^3 $kgm^{-2}s^{-1}$ of water at subcooling of 0 - 26°C in transient tests.	Heat flux increased sixfold for highest subcooling. Noted a sudden dip in the boiling curve near the minimum film boiling temperature at 26°C subcooling.
Newbold [33]	Vertical tube upward and downward flow. I.D. - 10 mm length - 77 mm	0.016×10^3 to 1.245×10^3 $kgm^{-2}s^{-1}$ of water in transient tests.	Order of magnitude increase in wall heat flux over mass flux range tested.
Smith [25]	Vertical tube I.D. - 12.5 mm length - 1.22 m	0.025×10^3 to 0.152×10^3 $kgm^{-2}s^{-1}$ of water.	Too few data points at the same subcoolings and pressure to draw any conclusions on velocity effect.

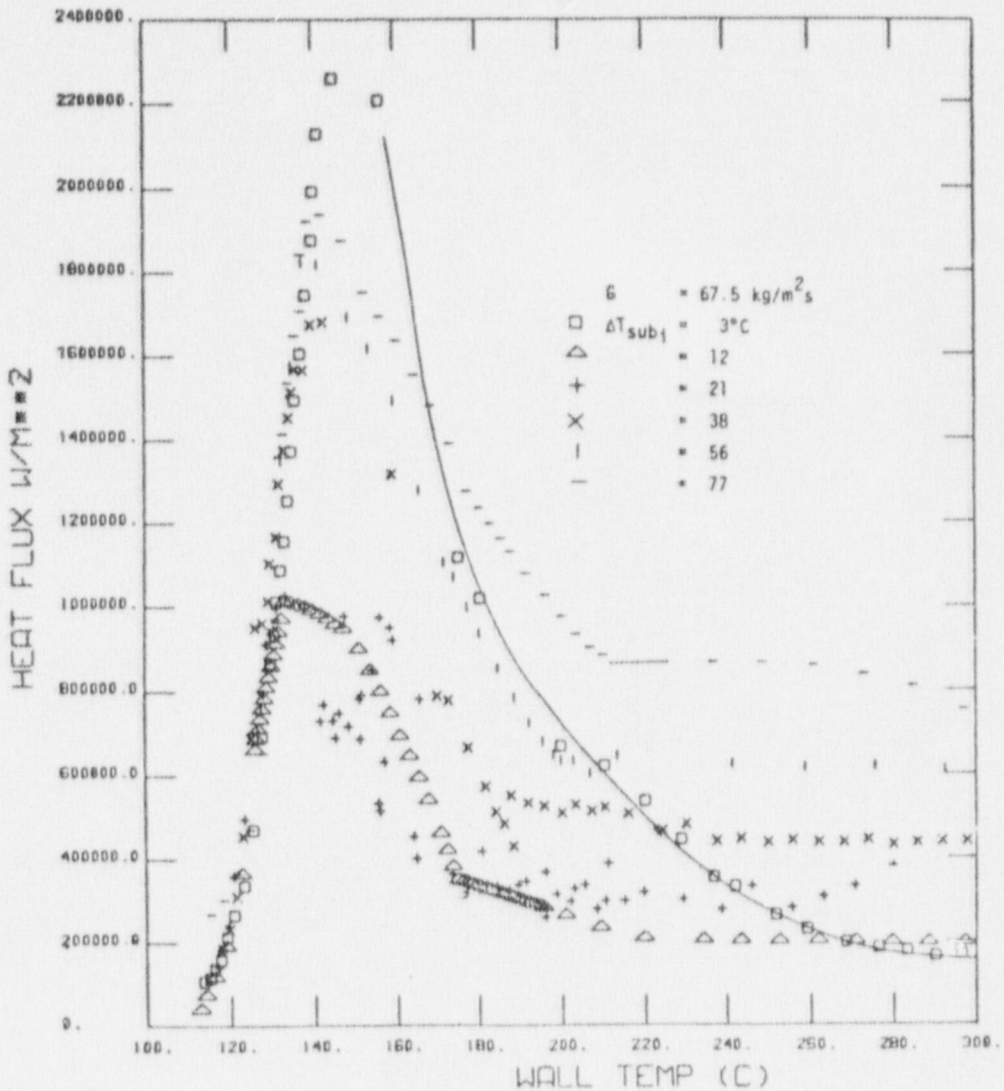

FIG. 4. THE EFFECT OF SUBCOOLING ON THE BOILING CURVE AT A MASS FLUX OF 67.5 kg $m^{-2} s^{-1}$ AND A PRESSURE OF 0.1 MPa (FROM FUNG [34])

(ii) Modified McAdams type correlations e.g. Kalinin [46]. These correlations are basically of the form

$$Nu = a\,Re^{b}\,Pr^{c}\,.F$$ where F is often a function of quality or sheath temperature.

(iii) Phenomenological prediction methods, based on mechanisms governing this type of heat transfer. Examples of this are Dougall-Rohsenow's [47] model which used a universal velocity distribution in the vapor flow, Chi [48] who used a time-averaged pool boiling and convective boiling correlation to represent heat transfer during slug flow.

Table 4: Low Quality and Subcooled Film Boiling Correlations

AUTHORS	EQUATION	RANGE OF APPLICABILITY					COMMENTS
		TEST FLUID	GEOMETRY	PRESSURE MPa	FLOW RATE $kgm^{-2}s^{-1}$	SUBCOOLING °C OR QUALITY	
Bromley [75,79]	$h = h_{FB} + 3/4\ h_{rad}$ $h_{FB} = 0.62\left[\frac{k_v^3 g \rho_v (\rho_\ell - \rho_v) h'_{fg}}{D \mu_v \Delta T_s}\right]^{1/4}$ $h_{rad} = \frac{5.67 \times 10^{-8} (T_w^4 - T_s^4)}{\left(\frac{1}{\varepsilon_w} + \frac{1}{\varepsilon_\ell} - 1\right) \Delta T_s}$ $h'_{fg} = h_{fg}\left(1 + \frac{0.4\ Cp\ \Delta T_s}{h_{fg}}\right)^2$	Nitrogen water n-pentane benzene carbon tetra-chloride ethyl alcohol	Horizontal carbon cylinders OD = 6.4 mm = 9.5 mm = 12.7 mm	Not given	Pool boiling	Saturated	Pool film boiling from external surfaces. Laminar theory.
Berenson [44]	$h_{FB} = 0.425\left[\frac{k_v^3 g \rho_v (\rho_\ell - \rho_v) h'_{fg}}{\mu_v \Delta T_s \sqrt{\frac{\sigma}{g(\rho_\ell - \rho_v)}}}\right]^{1/4}$		Horizontal surface		Pool boiling	Saturated	Theory only.
Sivieur and Ede [80]	$q_{total} = q_v + q_L$ $q_v = 0.613 \frac{k}{D} \Delta T_s \left[\frac{g \rho_v (\rho_\ell - \rho_v) h'_{fg}}{\nu_v k \Delta T_s}\right]^{1/4} + q_{rad}$ $q_L = 0.57 \frac{k}{D} \Delta T_{sub} [Gr\ Pr^2]$ $Gr = g \frac{\beta_\ell \Delta T_{sub} D^3}{\nu^2}$	Water water plus detergent	Horizontal cylinders OD = 3.2 mm = 6.4 mm	0.101	Pool boiling	0 - 90°C	Correlates their data well over the entire range of sub-coolings.
Anderson et al. [45]	$h_C = C_1\left[\frac{k_v^3 h_{fg}^2 g^3 (\rho_\ell - \rho_v)^4 \beta^4}{\nu_v^4 \Delta T_s^2 D}\right]^{1/10}$ $0.3321 \le C_1 \le 0.5498$				L.w flow rat.s	Saturated	Gives slightly higher heat transfer coefficient than Berenson's equation for $\Delta T_{sat} > 200$°C Theory only.
Ellion [13]	$h = \frac{4}{3}\left[\frac{g \rho_\ell \rho_v \nu_v^3 h'_{fg}}{\pi^2 \Delta T_s L \mu_v}\right]^{1/4} + q_{rad}$	Water	Vertical annulus OD = 63.5 mm ID = 6.4 mm length = 76.2 mm	0.11 - 0.41	(0.336 - 1.53) $\times 10^3$	28°C - 56°C	
Kalinin et al. [46]	a) Inverted Annular Flow i) automodel region $Nu = 0.0012\left[\frac{GDe}{\mu_\ell}\right] Pr^{0.4}\left[1 + 1.22 \exp\left(-0.038 \frac{z}{D}\right)\right]$ ii) non-automodel region $Nu = 0.0078\left(\frac{\rho_g U_v 2\delta_v}{\mu_g}\right)^{0.75} Pr_g F$ $F = \left[1 + (3 \times 10^{-6})\varphi + 1.3 \exp(-4 \times 10^{-6}\varphi)\right]$ $\varphi = \frac{Cp_g \Delta T_s}{h_{fg}}\left(\frac{\rho_g GDe}{\mu_g}\right)^{0.7}$ b) Slug Flow $St_v = 39\ Re_v^{-0.25}\left[1 + 0.25 \exp\left(-0.05 \frac{z}{D}\right)\right]$ $St_v = \frac{q}{\rho_g U_{\ell 1} Cp_v (T_w - T_s)}$ $Re_v = \frac{\rho_g U_{\ell 1} De}{\mu_g}$	Nitrogen	Downward flow in a vertical tube ID = 4 mm to 20 mm length = 100 mm	0.61 - 2.13	(6.32 - 18.9) $\times 10^3$	0 - 38°C	Model required to evaluate the film thickness
Dougall and Rohsenow [4]	$Nu = \frac{\frac{\rho_v De}{\mu_v}\sqrt{\frac{\tau_w}{\rho_v}}}{\int_n^{y^+} \frac{dy^+}{1 + Pr \frac{\varepsilon}{\nu}}}$	Freon-113	Vertical tube ID = 10.2 mm and 4.6 mm length = 381.0 mm	0.101	(0.45 - 1.11) $\times 10^3$	Exit quality up to 10%	

Groeneveld [22] and Kaufman [49] developed a semi-theoretical model predicting variation of local parameters such as vapor velocity, liquid velocity, film thickness, etc. These models are not in their final form because of lack of data to verify that the model's assumptions are correct.

Comparison of Data with Correlations

The pool film boiling case has been well researched and one can predict heat transfer coefficients with a good deal of confidence. For flows over external surfaces, Hsu [42] has shown that Berenson's [44] correlation employing Bromley's [43] empirical constant of 0.62 gave reasonable agreement with the FLECHT data. Caution should be exercised, though, in applying this correlation to cases of high velocities or subcooled liquids. The correlations, proposed to fit data obtained with flowing cryogenic or refrigerant fluids, may not be valid for low quality film boiling in water. The void fractions of the data upon which these correlations are based are not well documented and the form of the correlations suggest that they may only be suitable for dispersed flow film boiling.

Most correlations predict heat transfer coefficients which are approximately independent of wall superheat while recent results have shown the heat flux in the film boiling region to remain constant over a fairly wide range of wall superheats. Further work remains to be done to incorporate this feature in the correlations.

LIQUID DEFICIENT HEAT TRANSFER

Experimental Studies

Heated surface temperatures in the liquid deficient regime are usually much lower than those obtained in the inverted annular flow regime, especially if the temperatures are obtained at high flows, high pressures and high qualities. Hence experiments can be carried out on the simple heat flux controlled systems such as direct electrical heating of a sheath without excessive danger of test section overheating. Table 5 summarizes the reported experiments. Most of the experimental effort has gone into studies of simple geometries (tubes, annuli); the studies by Bennett [20] and Herkenrath [50] are the most extensive ones.

The data obtained in bundles are analyzed assuming one-dimensional homogeneous flow. Some of these data were obtained from in-reactor experiments; such experiments are very scarce but provide valuable information on sheath thermal behavior. However, caution must be exercised in interpreting post-CHF bundle results, especially from in-reactor tests because of effects of rod spacing devices (e.g. Era [51], methods of thermocouple attachments, limited number of thermocouple locations and uncertainties in axial, radial and peripheral heat flux distribution (in-reactor tests). In a previous paper, Groeneveld [60] has listed a number of reasons such as above, which render the experimental results unsuitable for prediction development.

Prediction Meth

General. Post-dryo temperatures for steady flow can be predicted from a semi-theoretical model or from empirical equations. The semi-theoretical model was initially developed independently by the UKAEA (Bennett [20]) and MIT (Laverty [53]). In this model all parameters are initially evaluated at the dryout location. It is assumed that heat transfer takes place in two steps: (i) from the heated surface to the vapor, and (ii) from the

Table 5: Post-Dryout Data

GEOMETRY	REFERENCE	RANGE OF DATA					COMMENTS
		P MPa	$\phi \times 10^{-3}$ kW m^{-2}	$G \times 10^{-3}$ kg m^{-2}s^{-1}	X	De cm	
Tube	Parker [81]	0.204	0.01 - 0.06	0.05 - 0.10	0.89 - 1.00	2.54	50 cm heated length rewetting of wall?
	Bennett [20]	7.03	0.30 - 1.90	0.40 - 5.30	0.25 - 1.00	1.27	275 cm heated length
	Bailey [21]	16.3 - 18.3	0.08 - 0.80	0.67 - 2.70	0.20 - 1.00	1.28	U-tube
	Keeys [54]	7.03	0.80 - 1.50	0.70 - 4.10	0.15 - 0.90	1.27	Cosine heat flux distribution
	Bishop [82, 83]	17.0 - 21.9	0.30 - 2.00	0.70 - 3.25	0.10 - 0.95	0.254, 0.508	
	Mueller [56]	7.03	0.50 - 0.85	0.70 - 1.00	0.62 - 1.00	1.57	Also measured vapor superheat
	Polomik [67]	7.03	0.55 - 1.10	0.70 - 1.35	0.80 - 1.00	1.57	Also measured vapor superheat
	Brevi [84]	5.09	0.38 - 1.50	0.47 - 3.00	0.40 - 1.00	0.65, 0.93	
	Bertoletti [85, 86]	7.13	0.10 - 1.60	1.00 - 4.00	0.40 - 0.90	0.50, 0.90	Non-steady temperatures
	Era [51]	7.13	0.10 - 1.30	1.10 - 3.00	0.70 - 1.00	1.6	
	Kerkenrath [50]	14.1 - 25.5	0.10 - 2.05	0.70 - 3.25	0 - 1.00	1.0, 2.0	Data in graphical form
	Swenson	21.1	0.28 - 0.57	0.95 - 1.35	0.20 - 0.90	1.07	
	Schmidt [88]	21.9	0.32 - 0.85	0.42	0.10 - 0.90	0.8	Data in graphical form vertical and horizontal flow
	Lee [89]	14.3 - 18.3	0.30 - 1.40	1.00 - 4.00	0.30 - 0.70	0.9, 1.3	
	Miropol'skiy [90]	4.08 - 22.4	0.25 - 1.10	1.00 - 2.00	0.20 - 1.00	0.8	Data must be derived from graphs
	Farman [91]	15.5	2.0 - 3.47	1.36 - 3.40	0.009 - 0.989	1.27	Transient blowdown tests
	Janssen [92]	0.71 - 7.13	0.03 - 1.00	0.13 - 1.00	0.60 - 1.60	1.26	
Annulus	Polomik [93]	5.60 - 9.88	0.60 - 2.20	1.00 - 2.56	0.15 - 1.00	0.152, 0.305	
	Polomik [94]	7.03	0.75 - 2.30	0.35 - 2.70	0.15 - 0.65	0.338	Results affected by spacers
	Bennett [58]	3.57 - 7.03	0.60 - 1.80	0.70 - 2.70	0.20 - 1.00	0.33	
	Era [51]	7.13	0.13 - 1.04	0.80 - 3.80	0.30 - 1.00	0.20, 0.50	Effects of spacers was studied
	Era [72]	5.09	0.20 - 0.60	0.60 - 2.20	0.20 - 0.90	0.30	Uniformly and non-uniformly heated
	Groeneveld [73]	4.18 - 8.46	0.50 - 1.40	1.35 - 4.10	0.10 - 0.50	0.405	Two heated sections separated by unheated section
Bundles	Hench [66, 95]	4.18 - 9.88	0.45 - 1.90	0.39 - 2.70	0.20 - 0.90	1.03	2-rod
	Kunsemiller [96]	4.18 - 9.88	0.55 - 1.00	0.39 - 1.35	0.30 - 0.70	1.12	3-rod
	Groeneveld [35]	6.42	0.33 - 1.16	1.10 - 2.20	0.30 - 0.60	0.344	3-rod, effect of crud in-reactor experiment
	Adorni [97]	5.09 - 5.60	0.20 - 1.50	0.80 - 3.80	0.20 - 0.90		7-rod, mainly unsteady temperatures
	Matzner [98, 99]	7.03	0.80 - 2.35	0.70 - 2.70	0.1 - 0.60	0.830	19-rod, mainly unsteady temperatures
	McPherson [100]	11.1 - 22.1	0.60 - 1.45	0.70 - 4.10	0.28 - 0.53	0.780	28-rod, mainly unsteady temperatures
	Matzner [101]	3.46 - 8.46	0.78 - 1.15	0.70 - 1.40	0.23 - 0.38	0.670	19-rod segmented bundle
	Groeneveld [63]	6.93 - 10.4	0.08 - 1.20	0.63 - 1.35	0.35 - 1.00		36-rod, in-reactor experiment

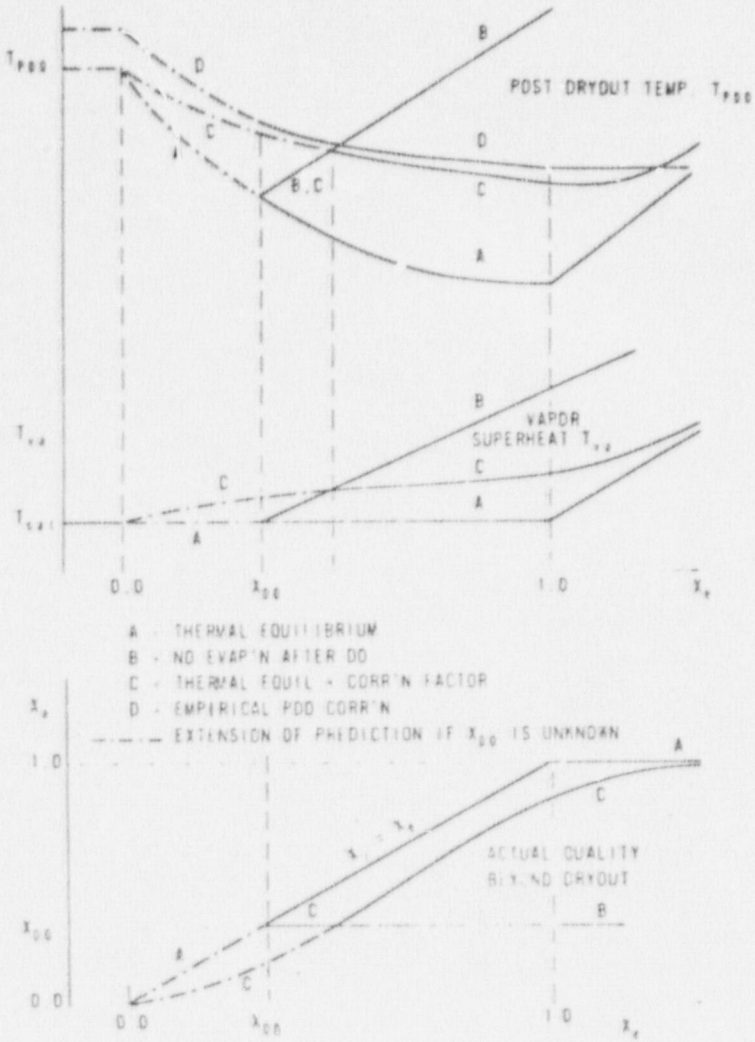

FIG. 5. VARIOUS PREDICTIONS FOR POST-DRYOUT PARAMETERS

vapor to the droplets. The heated channel is subdivided axially and the axial gradients in droplet diameter, quality, vapor velocity and droplet velocity are calculated at each node. Using a heat balance, the vapor superheat can then be evaluated at each node. The conditions at the downstream nodes are found by stepwise integration along the heated channel. The wall temperature is finally found from the vapor temperature using a superheated steam heat transfer correlation. Bennett's approach agrees with post-dryout measurements obtained in steam-water at 70 bar in uniformly and nonuniformly heated tubes (Keeys [54]). Bailey [21], Groeneveld [22], and Plummer [23] have suggested improvements in the original model by including droplet-wall interaction, by permitting a gradual change in average droplet diameter due to the breakup of droplets and by including vapor flashing for large pressure gradients.

Empirical post-dryout correlations may be subdivided as follows; their relative predictions are shown in figure 5.

Thermal Equilibrium. These are correlations which assume that the liquid is in thermal equilibrium with the vapor, and the heated surface is cooled by forced convection to the vapor only. These correlations are basically forced convective correlations where the vapor velocity is evaluated by assuming either homogeneous flow (i.e., S = 1, Dougall [47] or by using a suitable slip ratio correlation (e.g., Quinn [55]):

$$Nu_v = a \left[\frac{\rho_v \cdot U_v \cdot De}{\mu_v} \right]^b (Pr_v)^c$$

where

$$U_v = \frac{GX}{\rho_v \cdot \alpha} = \frac{G}{\rho_v} \left[X + \frac{\rho_v}{\rho_\ell} S(1 - X) \right] \quad \ldots \quad (1)$$

This type of correlation assumes that the vapor is at saturation, i.e. $X = X_e$. This assumption does not agree with experiments (Mueller [56], Polomik [57], Bennett [58]) except for the following cases:

(i) at high mass flows where the liquid-vapor heat exchange is very efficient

(ii) near the dryout location where the vapor has had insufficient time to become superheated

(iii) in the inverted annular flow regime.

This type of correlation is useful since it predicts the lower boundary for the post-dryout temperature.

No Evaporation after Dryout. These are correlations which assume that no evaporation takes place in the post-dryout region, and the heated surface is cooled by forced convection to the vapor only. Although here the same forced convective correlation is used as above, the predicted sheath temperature is much higher since the vapor becomes progressively more superheated. The degree of vapor superheat can be determined from a heat balance. The no evaporation assumption also results in the Reynolds number remaining virtually constant in the post-dryout region. This type of correlation is pessimistic except at lower flows (Bennett [20]); however it can be used to predict an upper boundary for the heated surface temperature.

Thermal Nonequilibrium. These are correlations which predict the degree of thermal nonequilibrium. Values for the actual vapor temperature or actual quality in the post-dryout region can be generated from existing post-dryout data provided the assumption of forced convective cooling only of the heated wall in the post-dryout region is correct. This approach has been used by Tong [40], Quinn [55], Plummer [23] and Groeneveld [59].

Groeneveld's [59] nonequilibrium prediction method is based on six sets of experimental data and has been found to agree with other sets of data. It also has the correct asymptotic trends: (i) the thermal nonequilibrium gradually disappears when Xe is increased above 100%, (ii) an increase in mass flow reduces the thermal nonequilibrium, (iii) when X_e is negative (subcooled film boiling) X_a becomes small but remain positive. Because of these features its range of applicability is considered wider than other nonequilibrium correlations.

Empirical Forced Convective Post-Dryout Correlations. The correlations of Table 6 are of this type. They generally predict a heat transfer coefficient which is based on the temper-

Table 6: Post-Dryout Correlations

EQUATION AND REFERENCE	RANGE OF APPLICABILITY OF EQUATION				EQUATION AGREES WITH DATA FROM REFERENCE	COMMENTS
	P MPa	$G \times 10^3$ kgm^{-2}s^{-1}	X	GEOMETRY		
1. $Nu_f = 0.00136(Re_f)^{0.853} Pr_f^{1/3}\left(\frac{X}{1-X}\right)^{0.147}\left(\frac{\rho_f}{\rho_g}\right)^{2/3}$ Polomik [93]	5.60 - 10.2	1.00 - 2.45	0.40 - 0.70	Annulus	93	Exponents and coefficients for equations 1 - 3 obtained from least error analysis using data from [93]
2. $Nu_f = 0.416\ Re_f^{0.509} Pr_f^{1/3}\left(\frac{\rho_g}{\rho_f}\right)^{0.208}\left(\frac{1-X}{X}\right)^{0.616}$ Polomik [93]	5.60 - 10.2	1.00 - 2.45	0.40 - 0.70	"	93	
3. $Nu_f = 0.023\ Re_f^{0.262} Pr_f^{1/3}\left[\frac{1-X}{X}\right]^{0.01} \phi^{0.417}\left[\frac{\rho_f}{\rho_g}\right]^{0.091}$ ϕ in Btu/h.ft^2 Polomik [93]	5.60 - 10.2	1.00 - 2.45	0.40 - 0.70	"	93	
4. $Nu_g = 0.00115(Re_g)^{0.9} Pr_g^{0.3}\left[\frac{T_w}{T_s} - 1\right]^{-0.15}$ T in °F Polomik [67]	4.08 - 10.2	0.70 - 2.70	0.20 - 1.00	2-rod	66	Has additional temperature parameter to allow for property variations at the heater wall 120% variation with data from ref. [66]
5. $Nu_g = 0.0039\left[Re_g\left[X + \frac{\rho_g}{\rho_f}(1-X)\right]\right]^{0.9}$ Polomik [67]	4.08 - 10.2	0.70 - 2.70	0.20 - 1.00	"	66	110% variation with data from ref. [66]. Better than above equation.
6. $\phi\left[De^{0.2}/(GX)^{0.6}\right] = C(T_w - T_s)^n$ $n = 1.284 - 0.00317\ G$ $C = \frac{1}{389} e^{0.01665\ G}$ Collier [102]	7.03	> 1.00	0.15 - 1.00	Round tubes and annuli	91, 85	$T_w - T_s$ must be below 200°C.
7. $\phi\left[De^{0.2}/(GX)^{0.6}\right] = 0.018(T_w - T_s)^{0.921}$ Collier [102]	7.03	any components	0.15 - 1.00	"	91, 85	Correlation may be used if either $G < 10^6$ or $T_w - T_s > 200$°C.
8. $Nu_f = 0.0191\ Re_f^{0.8} Pr_f^{1.23}\left[\frac{\rho_g}{\rho_f}\right]^{0.068}\left[X + \frac{\rho_g}{\rho_f}(1-X)\right]^{0.68}$ Bishop [83]	4.08 - 21.9	0.70 - 3.40	0.07 - 1.00	Round tubes	93, 83, 87, 103, 82, 90	
9. $Nu_f = 0.033\ Re_w^{0.8} Pr_w^{1.25}\left[\frac{\rho_g}{\rho_f}\right]^{0.197}\left[X + \frac{\rho_g}{\rho_f}(1-X)\right]^{0.738}$ Bishop [83]	4.08 - 21.9	0.70 - 3.40	0.07 - 1.00		93, 83, 87, 103, 82, 90	
10. $Nu_w = 0.098\left[Re_w\frac{\rho_w}{\rho_g}\left[X + \frac{\rho_g}{\rho_f}(1-X)\right]^{1.5}\right]^{0.5}$ $(Pr_w)^{0.6}\left[\frac{\rho_g}{\rho_f}\right]^{0.50}$ Bishop [82]	16.8 - 21.9	1.35 - 3.40	0.10 - 1.00	"	87, 82, 90	Based on high pressure data.
11. $Nu_w = 0.055\left[(Re_w)\frac{\rho_w}{\rho_g}\left[X + \frac{\rho_g}{\rho_f}(1-X)\right]\right]^{0.82}$ $(Pr_w)^{0.96}\left[\frac{\rho_g}{\rho_f}\right]^{0.36}\left[1 + \frac{26.9}{L/D}\right]$ Bishop [82]	16.8 - 21.9	1.35 - 3.40	0.10 - 1.00	"	82	

Table 6: Post-Dryout Correlations (cont'd)

EQUATION AND REFERENCE	RANGE OF APPLICABILITY OF EQUATION				EQUATION AGREES WITH DATA FROM REFERENCE	COMMENTS
	P MPa	$G \times 10^{-3}$ $kgm^{-2}s^{-1}$	X	GEOMETRY		
12. $T_w - T_{sat} = 1.913\left[\frac{\phi}{G\left(X+\frac{1-X}{4.15}\right)}\right]^2$ Lee [89]	14.2 - 18.2	1.00 - 4.00	0.30 - 0.75	Tubes	89	Based on data obtained on 1.3 cm ID indirectly heated tube
13. $Nu_g = 0.023\left[Re_g\left(X+\frac{\rho_g}{\rho_f}(1-X)\right)\right]^{0.8} Pr_w^{0.8} Y$ $Y = 1 - 0.1\left[\frac{\rho_f}{\rho_g} - 1\right]^{0.4}(1-X)^{0.4}$ Mikropol'skiy [90]	4.05 - 22.5	0.70 - 2.00	0.06 - 1.00	"	87, 88, 90	Factor Y was determined empirically
14. $Nu_g = 0.0088\left(Re_f \frac{K}{G}\right)^{0.84}(Pr_f)^{1/3}\left[\frac{1-X_{DO}}{X-X_{DO}}\right]^{0.134}$ Brevi [104]	5.06	0.50 - 1.00	0.40 - 1.00	"	84	
15. $Nu = 0.06\left[\left[Re_w\left(X+\frac{\rho_g}{\rho_f}1-X\right)\right]\left[\frac{\rho_w}{\rho_g}\right]\left[Pr_w\right]\right]^{0.8}$ $\left(\frac{f}{f_0}\right)^{0.4}\left(\frac{p}{p_c}\right)^{2.7}$ $G_0 = 10^3\ kg\ m^{-2}s^{-1}$ Berkenrath [50]	14.2 - 27.2	0.75 - 4.10	0.10 - 1.00	"	50, 82, 87	
16. $Nu_w = 0.005\left[\frac{De\ U_m\ \rho_w}{\mu_w}\right]^{0.8}(Pr_g)^{0.5}$ Tong [105]	> 14.0	> 0.70	< 0.10	"	82, 103	Design equation. To be used only at low quality or subcooled conditions
17. $Nu_g = 1.604 \times 10^{-4}\left[Re_g\left(X+\frac{\rho_g}{\rho_f}(1-X)\right)\right]^{0.838}$ $Pr_w^{1.81} d^{0.27\xi}\left(\frac{q}{q_{crit}}\right)^{-0.308}$ q in Btu/h.ft^2 Slaughterbeck [61]	4.88 - 20.2	1.05 - 5.30	0.12 - 0.90	"	30, 81, 86	
18. $Nu_g = a\left[Re_g\left(X+\frac{\rho_g}{\rho_f}(1-X)\right)\right]^b Pr_w^c$ $T^d d^e$ q in Btu/h.ft^2 $Y = 1 - 0.1\left[\frac{\rho_f}{\rho_g} - 1\right]^{0.4}(1-X)^{0.4}$						
i) $a = 1.85 \times 10^{-4}$ $b = 1.00$ $c = 1.57$ $d = -1.12$ $e = 0.131$ $a = 1.09 \times 10^{-3}$ $b = 0.989$ $c = 1.41$ $d = -1.15$ $e = 0$	4.86 - 21.8	0.70 - 5.30	0.10 - 0.90	"	20, 51, 82, 83, 85, 86, 87, 88	
ii) $a = 1.30 \times 10^{-2}$ $b = 0.864$ $c = 1.68$ $d = -1.12$ $e = 0.133$ $a = 5.20 \times 10^{-2}$ $b = 0.648$ $c = 1.26$ $d = -1.06$ $e = 0$	5.44 - 10.1	0.80 - 4.10	0.10 - 0.90	Annuli	51, 58, 73, 93	
iii) $a = 7.75 \times 10^{-4}$ $b = 0.902$ $c = 1.47$ $d = -1.54$ $e = 0.132$ $a = 3.27 \times 10^{-3}$ $b = 0.901$ $c = 1.22$ $d = -1.50$ $e = 0$	3.44 - 21.8	0.70 - 5.30	0.10 -0.90	Tubes and Annuli	20, 51, 58, 73, 82, 83, 85, 86, 87, 88	
Groeneveld [60]						
19. $\phi = \phi_{TB} + 0.021(T_w - T_{sat})\cdot\frac{k}{De}\left(\frac{G\ V_m\ De}{\mu_w}\right)^{0.8}(Pr_w)^{0.333}$ ϕ_{TB} transition boiling heat flux V_m ... wall mixture velocity Tong [40]	4.05 - 10.1	0.40 - 5.15	0.2 - 1.45	Tubes	20, 51, 54	Correlation also valid for transition boiling region if ϕ_{TB} reported in [40] is used.

ature difference between wall and saturation. They are simple to use but have a limited range of validity and should not be extrapolated outside the recommended range. If extrapolation is unavoidable, one should check that the predicted temperatures fall between the maximum and minimum post-dryout temperatures as discussed above.

Comparison of Data with Prediction Methods

Theoretical post-dryout models such as those by Bennett [20], Bailey [21], Groenveld [22] and Plummer [23] still require some refinements but may eventually predict post-dryout heat transfer for round tubes with greater accuracy than empirical correlations. The models, however, require reasonably accurate values of the dryout quality, especially at the low mass flows. The usefulness of the models in predicting post-dryout temperatures in annular and bundle geometries may be limited as the film flow on the unheated surface and the flow and enthalpy distribution in partially dry bundles are unkown. Also, the model requires the subdivision of the heated channel length in a large number of nodes, which may be too time consuming for thermal hydraulic computer codes.

Four empirical prediction methods were discussed in the previous section; the methods described under Thermal Nonequilibrium are considered the most accurate. They have a much wider range of applicability than the post-dryout correlations of Table 6 but are more difficult to use. Figure 5 shows schematically the relative temperature predictions of the four prediction methods. Note that curve A, based on the "thermal equilibrium after dryout" assumption represents a lower boundary while curve B, based on the "no evaporation after dryout" assumption represents an upper boundary for the post-dryout temperature.

Most correlations of Table 6 are based on only a few sets of data covering a fairly narrow range of experimental data. The data sets (Table 5) contain many data that are not reliable. The sources of errors have resulted in post-dryout temperature measurements lower than what this author considers to be fully developed film boiling. In the derivation of equation 18 (Groeneveld [60]) care was taken that the data subject to possible errors were not included. This could be the reason why Groeneveld's correlations seem conservative compared to some other post-dryout correlations (Slaughterbeck [61]).

DISCUSSION

State-of-the-Art

Forced Convective Transition Boiling. Table 1 shows that the available data cover only narrow ranges of conditions; of the available data sets, none can be considered sufficiently reliable to be used for developing a correlation. Caution must be exercised when using the correlations of Table 2 since (i) the correlations do not agree with each other, and (ii) their data base is highly questionable. In comparing data with correlations differences of an order of magnitude were frequently encountered. A lack of understanding of the physical mechanisms governing forced convective transition boiling does not yet permit the development of an analytical heat transfer model.

The scarcity of data is primarily due to the difficulty in measuring transition boiling data. The latest approach of using high thermal inertia test sections made of copper is promising but still requires further refinement to ensure a uniform axial heat flux distribution.

Inverted Annular Flow and Slug Flow Film Boiling. The situation in this heat transfer regime is only slightly better as visual studies on cryogenics and refrigerants have helped

our understanding of the mechanisms governing this type of heat transfer. Still reliable data for water are lacking because of the complexity of using temperature controlled systems. Another possible approach is the so-called hot patch technique; it has been used by this author (Groeneveld [62]) to measure post-dryout temperatures in Freon-12.

The prediction methods cannot be expected to be accurate for water except at low flows where use of the pool boiling correlations seems reasonable. Present correlations also do not adequately account for the effect of subcooling and flow. For the inverted annular flow regime the development of an analytical model seems feasible, provided details of the velocity distribution in the liquid and vapor phase can be obtained.

Liquid Deficient Regime. During the past ten years much progress has been made in understanding the physical mechanisms governing this type of heat transfer. In an ideal experimental setup such as a vertical, uniformly heated round tube, semi-theoretical models have been reasonably successful in predicting the post-dryout temperature distribution. These models require empirically derived constants; they are generally considered useful especially for predictions outside the data base provided the assumed physical mechanisms are still valid.

Table 5 shows that, even in this relatively well studied post-CHF heat transfer regime, data are nonexistent at low flows, low pressures and low qualities. This again is due to the excessive high post-CHF temperatures encountered when using the conventional heat flux controlled system. Despite the many suggested correlations, no satisfactory method of predicting post-CHF temperatures is available at these conditions, even in simple geometries.

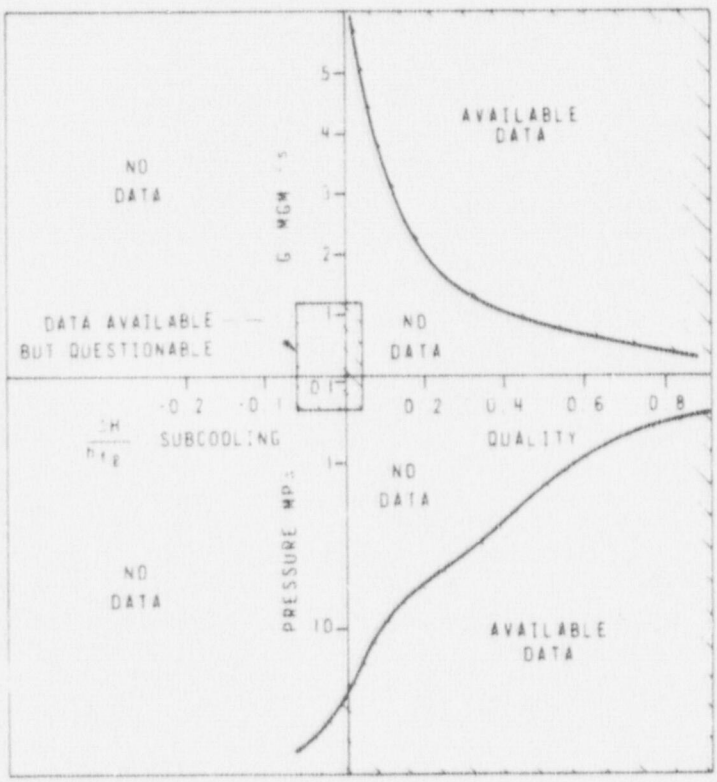

FIG. 6. RANGE OF AVAILABLE FILM BOILING DATA

Post-CHF Heat Transfer in Rod Bundles

Most post-CHF experiments have been carried out on simple geometries such as tubes or annuli (e.g., see Tables 1, 3, 5.) Experimentation in bundle geometries is much more cumbersome because of (i) large and expensive loop facilities, (ii) extensive instrumentation of the bundle, and (iii) increased likelihood of heater failure. Direct application of post-CHF test results to bundle geometries would be warranted if it were possible to predict local flow conditions throughout the bundle. However present subchannel codes are not yet capable of predicting the local flow and enthalpy in partially dry bundles.

Because of questionable correlations, especially in the transition boiling and subcooled film boiling regime, the use of experimental data rather than correlations is advisable. The lack of available film boiling data is illustrated in figure 6: except for data at high pressure, high flows and reasonably high qualities, virtually no data are available. Caution must be exercised when using correlations in the region where no data are available.

Prediction methods based on tube data have frequently been found to overestimate sheath temperatures in fuel bundles. This is not surprising as

(i) Tubes do not contain rod spacing devices (warts, grid spacers) which usually result in improved downstream heat transfer (e.g., Era [51]). Frequent grid spacers (short spacer pitch) also prevent high vapor superheats, thus reducing sheath temperatures.

(ii) Partially dry bundles could result in a subchannel type oscillation due to large differences in friction pressure gradients in wet and dry subchannels (e.g., Groeneveld [63]).

(iii) Film boiling experiments in bundles are often terminated at a power level just above the dryout power to reduce the chance of heater failure. At such low power levels film boiling heat transfer is not yet fully developed (Groeneveld [63]).

Virtually all post-CHF correlations are based on steady-state data while frequently the correlations are applied to transient conditions. Post-CHF heat transfer is expected to be somewhat higher during fast transients as compared to steady-state conditions because of the higher CHF, more intense mixing and low vapor superheat.

CONCLUSIONS AND FINAL REMARKS

1. Post-CHF heat transfer correlations developed for the liquid deficient regime can be used with reasonable confidence except at low flows and low pressures. Correlations for the transition boiling region, and for the low quality or subcooled film boiling region should be suspected because of the lack of a reliable data base.

2. Present thermohydraulic reactor analysis usually ignores the transition boiling heat transfer mode. Instead, it is assumed that, during reflood the film boiling mode will suddenly be replaced by the nucleate boiling mode (or vice versa during dryout occurrence). In both cases the assumption that film boiling rather than transition boiling takes place will result in an overprediction of the calculated surface temperature.

3. Stable film boiling can only be maintained if the heated surface temperature is above the minimum film boiling temperature. The minimum film boiling temperature, however, is not constant but depends on the properties of the liquid, the surrounding atmosphere, and on the heated surface properties. The velocity, impact angle and liquid mass approaching the heated surface also affect this temperature.

4. In general, rewetting of a heated surface can only occur if the wall temperature is

below the minimum film boiling temperature. If a liquid front exists somewhere on the heated surface, then conduction from the dry to the wet surface can be very efficient in reducing the dry surface temperature locally and permitting the liquid rewetting front to propagate.

5. Improvement in the post-CHF temperature prediction in bundles may be made if the subchannel flow and quality could be predicted. However present subchannel codes need extensive modification before being applied to partially dry bundles.

6. To remove the uncertainty in the prediction of post-CHF heat transfer the following studies need to be carried out:

– measurement of vapor superheat or degree of nonequilibrium during film boiling in tubes

– measurement of liquid temperature (subcooling) during film boiling in tubes

– development of analytical heat transfer model for inverted annular flow film boiling

– measurement of boiling curve at low pressures, low flows and subcooled conditions.

REFERENCES

[1] Berenson, P. J., "Experiments in Pool-Boiling Heat Transfer," *Int. J. Heat Mass Trans.*, Vol. 5, 1962, pp. 985-999.

[2] Zuber, N., "Hydrodynamic Aspects of Boiling Heat Transfer," Atomic Energy Commission Report AECU-4439, 1959.

[3] Kutateladze, S. S. and Borishanskii, V. M., "A Concise Encyclopedia of Heat Transfer," Pergamon Press, 1966.

[4] Ruckenstein, E., "On Transition Boiling Heat Transfer from a Horizontal Surface," *Rev. Roumaine Phys., Acad. Rep. Populaire Romaine*, Vol. 9, No. 1, 1964, pp. 63-73.

[5] Bankoff, S. G. and Mehra, V. S., "A Quenching Theory for Transition Boiling," *I. & E. C. Fundamentals*, Vol. 1, No. 1, 1962, pp. 38-48.

[6] Stock, B. J., "Observations on Transition Boiling Heat Transfer Phenomena," ANL-6175, (TID-4500, 15th ed.), AEC Research and Development Report, 1960.

[7] Westwater, J. W. and Santangelo, J. G., "Photographic Study of Boiling," *Ind. end Eng Chem.*, Vol. 47, 1955, pp. 1605-1610.

[8] Hesse, G., "Heat Transfer in Nucleate Boiling, Maximum Heat Flux and Transition Boiling," *Int. J. Heat Mass Trans.* Vol. 16, 1973, pp. 1611-1627.

[9] Berenson, P. J., "Transition Boiling Heat Transfer from a Horizontal Surface," MIT Technical Report No. 17, 1960.

[10] Collier, J. G., "Convective Boiling and Condensation," McGraw-Hill, London, 1972.

[11] Tong, L. S., "Two Phase Flow and Boiling Heat Transfer," John Wiley & Sons, 1965.

[12] Hewitt, G. F. and Hall-Taylor, N.S., "Annular Two-Phase Flow," Pergamon Press, Oxford, 1970.

[13] Ellion, M. E., "A Study of the Mechanism of Boiling Heat Transfer," California Institute of Technology, Report JPL-MEMO-20-88, 1954.

[14] Wachters, L. H. J., *De Warmte Overdracht von een Hete Wand Naar Druppels in de Sferoidale Toestand*, Ph.D. Thesis, Technological University, Delft, 1965.

[15] Pedersen, C. O., "An Experimental Study of the Dynamic Behavior and Heat Transfer Characteristics of Water Droplets Impinging Upon a Heated Surface, *Int. J. Heat Mass Trans.*, Vol. 13, 1970, pp. 369-381.

[16] McGinnis, F. K. and Holman, J. P., "Individual Droplet Heat-Transfer Rates for Splattering on Hot Surfaces," *Int. J. Heat Mass Trans.*, Vol. 12, 1969, pp. 95-108.

[17] Thompson, T. S., "On the Process of Rewetting a Hot Surface by a Falling Liquid Film,"

Atomic Energy of Canada Limited Report AECL-4516, 1973.

[18] Gardiner, S. R. M. and Groeneveld, D. C., "Film Boiling Heat Transfer at Low Qualities and Subcooled Conditions: A Literature Survey," Atomic Energy of Canada Limited, to be published as an AECL Report, 1977.

[19] Cumo, M. and Farello, G. E., "Heated Wall Droplet Interaction for Two Phase Flow Heat Transfer in Liquid Deficient Region," *Proceedings Symposium on Two Phase Flow Dynamics*, Eindhoven, Vol. II, 1967, pp. 1325-1357.

[20] Bennett, A. W., Hewitt, G. F., Kearsey, H. A. and Keeys, R.K.F., "Heat Transfer to Steam Water Mixtures Flowing in Uniformly Heated Tubes in which the Critical Heat Flux has been Exceeded," AERE-R-5373, 1967.

[21] Bailey, N. A., *The Interaction of Droplet and Forced Convection in Post Dryout Heat Transfer at High Subcritical Pressures*, European Two-Phase Flow Group Meeting, Rome, 1972.

[22] Groeneveld, D. C., "The Thermal Behaviour of a Heated Surface at and Beyond Dryout," Atomic Energy of Canada Limited Report AECL-4309, 1972.

[23] Plummer, D. N., Griffith, P. and Rohsenow, W. M., "Post-Critical Heat Transfer to Flowing Liquid in a Vertical Tube," *Presented at the 16th National Heat Transfer Conference*, 76-CSME/CSChE-13, St. Louis, 1976.

[24] Chi, J. W. H., "Slug Flow and Film Boiling of Hydrogen," ASME 65-WA/HT-32, 1965.

[25] Smith, T. A., *Heat Transfer and Carryover of Low Pressure Water in a Heated Vertical Tube*, M. Sc. Thesis, MIT, 1974.

[26] Kalinin, E. K., et al., "Heat Transfer in Tubes with Rod Regime in the Case of Flow Boiling of a Subcooled Liquid," *Cocurrent Gas-Liquid Flow*, Plenum, New York, 1969, pp. 497-525.

[27] Fung, K. K., Groeneveld, D. C. and Hooper, F. C., "Forced Convective Transition Boiling," *Proc. the 6th Canadian Congress of Applied Mechanics, Vancouver, 1977.*

[28] McDonough, J. B., Milich, W. and King, E. C., "An Experimental Study of Partial Film Boiling Region with Water at Elevated Pressures in a Round Vertical Tube," *Chem. Eng. Prog. Symp., Ser.* Vol. 57, No. 32, 1961, pp. 197-208.

[29] Ramu, K. and Weisman, J., "Transition Boiling Heat Transfer to Water in a Vertical Annulus," *Presented at the National Heat Transfer Conference*, San Francisco, 1975.

[30] Petersen, W. C., Aboul Fetouh, M. M. and Zaalouk, M.G., "Boiling Curve Measurements from a Controlled Forced Convection Process," *Proc. Brit. Nucl. Eng. Society, Conference on Boiler Dynamics and Control in Nuclear Power Stations*, London, 1973.

[31] Iloeje, O. C., Plummer, D. N., Griffith, P. and Rohsenow, W. M., "An Investigation of the Collapse and Surface Rewet in Film Boiling in Forced Vertical Flow," ASME 73-WA/HT-20, 1973.

[32] Cheng, S. C. and Ng, W., "Transition Boiling Heat Transfer in Forced Vertical Flow Via a High Thermal Capacity Heating Process," *Letters in Heat Transfer*, Vol. 3, 1976, pp. 333-342.

[33] Newbold, F. J., Ralph, J. C. and Ward, J. A., *Post Dryout Heat Transfer Under Low Flow and Low Quality Conditions*, Paper presented at the European Two Phase Flow Group Meeting, Erlangen, 1976.

[34] Fung, K. K., "Forced Convective Transition Boiling," M.Sc. Thesis, University of Toronto, 1977.

[35] Groeneveld, D. C., Thibodeau, M., and McPherson, G. D., "Heat Transfer Measurements on Trefoil Fuel Bundles in the Post Dryout Regime – With Data Tabulation," Atomic Energy of Canada Limited Report AECL-3414, 1970.

[36] Ramu, K. and Weisman, J., "A Method for the Correlation of Transition Boiling Heat Transfer Data," *Proceedings of the Fifth International Heat Transfer Conference*, Tokyo, Vol. IV, B4.4, 1974.

[37] Mattson, R. J., Condie, K. G., Bengston, S. J. and Obenchain, C. F., "Regression Analysis of Post-CHF Flow Boiling Data," *Proceedings of the Fifth International Heat Transfer Conference*, Tokyo, Vol. IV, B3.8, 1974.

[38] Tong, L. S., "Heat-Transfer Mechanisms in Nucleate and Film Boiling," *Nucl. Eng. and Des.*, Vol. 21, 1972, pp. 1-25.

[39] Iloeje, O. C., Plummer, D. N., Rohsenow, W. M. and Griffith, P., "A Study of Wall Rewet and Heat Transfer in Dispersed Vertical Flow," MIT Technical Report 72718-92, 1974.

[40] Tong, L. S. and Young, J. D., "A Phenomenological Transition and Film Boiling Heat Transfer Correlation," *Proceedings of the Fifth International Heat Transfer Conference*, Tokyo, Vol. IV, B3.9, 1974.

[41] Groeneveld, D. C. and Fung, K. K., "Forced Convective Transition Boiling: Review of Liter-

ature and Comparison of Predictive Methods," Atomic Energy of Canada Limited Report AECL-5543, 1976.

[42] Hsu, Y. Y., Private communication, 1975.

[43] Bromley, L.A., "Heat Transfer in Stable Film Boiling," *Chem. Eng. Progr.*, Vol. 46, 1950, pp. 221-227.

[44] Berenson, P. J., "Film Boiling Heat Transfer from a Horizontal Surface," *J. of Heat Trans.*, Vol. 83, 1961, pp. 351-358.

[45] Andersen, J. G. H., et al., "Low Flow Film Boiling Heat Transfer on Vertical Surfaces – Part I: Theoretical Model – Part II: Empirical Formulations and Application to BWR-LOCA Analysis," *Presented at the 16th National Heat Transfer Conference*, AIChE-52, St. Louis, 1976.

[46] Kalinin, E. K., et al., "Investigation of Film Boiling in Tubes with Subcooled Nitrogen Flow," *Presented at the Fourth International Heat Transfer Conference*, B4.5, Paris, 1970.

[47] Dougall, R. S. and Rohsenow, W. M., "Film Boiling on the Inside of Vertical Tubes with Upward Flow of the Fluid at Low Qualities," MIT Report No. 9079-26, 1963.

[48] Chi, J. W. H., "Slug Flow and Film Boiling of Hydrogen," *J. of Spacecraft and Rockets*, Vol. 4, 1967, pp. 1329-1332.

[49] Kaufman, J. M., "Post Critical Heat Flux Heat Transfer to Water in a Vertical Tube," M.Sc. Thesis, MIT, 1976.

[50] Herkenrath, H., et al., "Wärmeübergang an Wasser bei Erzwungener Strömung in Druckbereich von 140 bis 250 bar," EUR-3658d, 1967.

[51] Era, A., "Heat Transfer Data in the Liquid Deficient Region for Steam-Water Mixtures at 70 kg/cm^2 Flowing in Tubular and Annular Conduits," CISE R-184, 1967.

[52] Groeneveld, D. C., "Forced Convective Heat Transfer to Superheated Steam in Rod Bundles," Atomic Energy of Canada Limited Report AECL-4450, 1973.

[53] Laverty, W. F. and Rohsenow, W. M., "Film Boiling of Saturated Liquid Nitrogen Flowing in a Vertical Tube," *J. of Heat Transfer*, Vol. 89, 1967, pp. 90-98.

[54] Keeys, R. K. F., Ralph, J. C. and Roberts, D. N., "Post Burnout Heat Transfer in High Pressure Steam-Water Mixtures in a Tube with a Cosine Heat Flux Distribution," AERE-R6411, 1971.

[55] Quinn, E. P., "Physical Model of Heat Transfer Beyond the Critical Heat Flux," GEAP-5093, 1966.

[56] Mueller, R. E., "Film Boiling Heat Transfer Measurements in a Tubular Test Section," EURAEC-1871/GEAP-5423, 1967.

[57] Polomik, E. E., "Transition Boiling, Heat Transfer Program, Final Summary Report on Program for Feb/63-Oct/67," GEAP-5563, 1967.

[58] Bennett, A. W., "Heat Transfer to Mixtures of High Pressure Steam and Water in an Annulus," AERE-R4352, 1964.

[59] Groeneveld, D. C. and Delorme, G. G. J., "Prediction of Thermal Nonequilibrium in the Post-Dryout Regime," *Nucl. Eng. and Des.*, Vol. 36, 1976, pp. 17-26.

[60] Groeneveld, D. C., "Post-Dryout Heat Transfer at Reactor Operating Conditions," ANS Conf. 730304, 1973, pp. 321-350, also AECL-4513, 1973.

[61] Slaughterbeck, D. C., Ybarrondo, L. J. and Obenchain, C. F., "Flow Film Boiling Heat Transfer Correlations: A Parametric Study with Data Comparisons," ASME 73-HT-50, 1973.

[62] Groeneveld, D. C., "Effect of a Heat Flux Spike on the Downstream Dryout Behavior," *Trans. ASME, J. of Heat Transfer*, Vol. 96, 1974, pp. 121-125.

[63] Groeneveld, D. C. and McPherson, G. D., "In-Reactor Post-Dryout Experiments with 36-Element Fuel Bundles," Atomic Energy of Canada Limited Report AECL-4705, 1973.

[64] Cadeck, F. F., Dominicis, O. P. and Leyse, R. H., "PWR FLECHT Final Report," WCAP-7665, 1971.

[65] Quinn, E. P., "Forced Flow Transition Boiling Heat Transfer from Smooth and Finned Surfaces," GEAP-4786, 1965.

[66] Hench, J. E., "Forced Flow Transition Boiling Experiments in a Two Rod Test Section at High Pressures," ASME 64-WA/HT-44, 1964.

[67] Polomik, E. E., "Transition Boiling Heat Transfer Program, Final Summary Report on Program for February 1963-October 1967," GEAP-5563, 1967.

[68] Cumo, M. and Urbani, G. C., "Anomalies in Post-Dryout Heat Transfer at High Pressures," *Trans. ANS*, Vol. 14, 1971, pp. 245-246.

[69] Nobel, L., "The Heat Transfer Coefficient as a Function of Steam Quality for High-Pressure Once-Through Flow Boiling, with Determination of the Transition Points Between the Regions of

Particular Heat Transfer," EUR-4561, 1970.

[70] Chen, J. C., "A Correlation for Boiling Heat Transfer to Saturated Fluids in Convective Flow," ASME 63-HT-34, 1963.

[71] Addoms, J. N., *Heat Transfer at High Rates to Water Boiling Outside Cylinders*, D.Sc. Thesis, MIT, 1948.

[72] Era, A., Gaspari, G. P., Protti, M. and Zavatarelli, Z., "Post Dryout Heat Transfer Measurements in an Annulus with Uniform and Non-Uniform Axial Heat Flux Distribution," European Two Phase Group Meeting, Riso, 1971.

[73] Groeneveld, D. C., "An Investigation of Heat Transfer in the Liquid Deficient Regime," Atomic Energy of Canada Limited Report AECL-3281, 1969.

[74] Bennett, A. W., Kearsey, H. A. and Keeys, R. K. F., "Heat Transfer to Mixtures of High Pressure Steam and Water in an Annulus," Part VI, AERE-R-4352, 1964.

[75] Bromley, L. A., LeRoy, N. R. and Robbers, J. A., "Heat Transfer in Forced Convective Film Boiling," *Ind. Eng. Chem.*, Vol. 45, 1953, pp. 2639-2646.

[76] Murphy, C. D., Kermode, R. I. and Zahradnik, R. L., "Forced Convection Film Boiling Heat Transfer," *Fourth International Heat Transfer Conference*, B4.8, Paris, 1970.

[77] Rankin, S., "Forced Convection Film Boiling Inside Vertical Pipes," Ph.D. Thesis, University of Delaware, 1961.

[78] Motte, E. I. and Bromley, L. A., "Film Boiling of Flowing Subcooled Liquids," *Ind. and Eng. Chem.*, Vol. 49, 1957, pp. 1921-1928.

[79] Bromley, L. A., "Effect of Heat Capacity of Condensate," *Ind. Eng. Chem.*, Vol. 44, 1952, pp. 2966 2969.

[80] Siviour, J. B. and Ede, A. J., "Heat Transfer in Subcooled Pool Film Boiling," *Fourth International Heat Transfer Conference*, B3.12, Paris, 1970.

[81] Parker, j. D. and Grosh, R. J., "Heat Transfer to a Mist Flow," ANL-6291, 1962.

[82] Bishop, A. A., Sandberg, R. O. and Tong, L. S., "High Temperature Supercritical Pressure Water Loop. Part V: Forced Convection Heat Transfer to Water After the Critical Heat Flux at High Subcritical Pressures," WCAP-2056, (Pt. 5), 1964.

[83] Bishop, A. A., Sandberg, R. O. and Tong, L. S., "Forced Convection Heat Transfer at High Pressure After the Critical Heat Flux," ASME-65-HT-31, 1965.

[84] Brevi, R., Cumo, M., Palmieri, A. and Pitimada, D., "Heat Transfer Coefficient in Post Dryout Two Phase Mixtures," European Two Phase Group Meeting, Karlsruhe, June, 1969.

[85] Bertoletti, S., "Heat Transfer and Pressure Drop with Steam Water Spray," CISE R-36, 1961.

[86] Bertoletti, S., "Heat Transfer to Steam-Water Mixtures," CISE R-78, 1964.

[87] Swenson, H. S., Carver, J. R. and Szoeke, G., "The Effects of Nucleate Boiling Versus Film Boiling on Heat Transfer in Power Boiler Tubes," ASME 61-WA-201, 1961.

[88] Schmidt, K. R., "Thermodynamic Investigations of Highly Loaded Boiler Heating Surfaces," AEC-TR-4033, 1960.

[89] Lee, D. H., "Studies of Heat Transfer and Pressure Drop Relevant to Sub-Critical Once-Through Evaporators," IAEA-SM-130/56, *IAEA Symp. on Progress in Sodium-Cooled Fast Reactor Engineering*, Monaco, 1970.

[90] Miropol'skiy, Z. L., "Heat Transfer in Film Boiling of a Steam Water Mixture in Steam Generating Tubes," *Teploenergetika*, Vol. 10, 1963, pp. 49-53.

[91] Farman, R. F. and Cermak, J. O., "Post DNB Heat Transfer During Blowdown," WCAP-9005/3, 1975.

[92] Janssen, E. and Kervinen, J. A., "Film Boiling and Rewetting," NEDO-20975, 1975.

[93] Polomik, E. E., Levy, S. and Sawochka, S. G., "Heat Transfer Coefficients with Annular Flow During Once Through Boiling of Water to 100% Quality at 800, 1000, and 1400 psi," GEAP-3703, 1961.

[94] Polomik, E. E., "Deficient Cooling," 7th Quarterly Report, GEAP-10221-7, 1971.

[95] Hench, J. E., "Multi Rod (Two Rod) Transition and Film Boiling in Forced Convection to Water at 1000 psi," GEAP-4723, 1964.

[96] Kunsemiller, D. F., "Multi-Rod, Forced Flo Transition and Film Boiling Measurements," GEAP-5073, 1965.

[97] Adorni, N., "Heat Transfer Crisis and Pressure Drop with Steam Water Mixtures: Experimental Data with Seven Rod Bundles at 50 and 70 kg/cm^3," CISE R-170, 1966.

[98] Matzner, B., "Basic Experimental Studies of Boiling Fluid Flow and Heat Transfer at

Elevated Pressures," Columbia University Monthly Progress Report MPR-XIII-2-63, 1963.

[99] Matzner, B. and Neill, J. S., "Forced Flow Boiling in Rod Bundles at High Pressures," DP-857, 1963.

[100] McPherson, G. D., et al., "Dryout and Post-Dryout Behaviour of a 28-Element Fuel Bundle," American Nuclear Society Winter Meeting, Miami Beach, 1971.

[101] Matzner, B., Casterline, J. E. and Kokolis, S., "Critical Heat Flux and Flow Stability in a 9 ft. 19 Rod Test Section Simulating a String of Short Discrete Rod Bundles," Columbia University Topical Report No. 10, 1968.

[102] Collier, J. G., "Heat Transfer and Fluid Dynamic Research as Applied to Fog Cooled Power Reactors," Atomic Energy of Canada Limited Report AECL-1631, 1962.

[103] Bishop, A. A., Efferding, L. E. and Tong, L. S., "A Review of Heat Transfer and Fluid Flow of Water in the Supercritical Region and During 'Once-Thru' Operation," WCAP-2040, 1962.

[104] Brevi, R., et al., "Post-Dryout Heat Transfer with Steam/Water Mixtures," *Trans. Am. Nucl. Soc.*, Vol. 12, 1969, pp. 809-811.

[105] Tong, L. S., "Film Boiling Heat Transfer at Low Quality or Subcooled Region," *Proceedings 2nd Joint USAEC-EURATOM Two Phase Flow Meeting*, Germantown, 1964, Report CONF-640507, p. 63.

APPENDIX II

TABLES OF TRANSIENT POST-CHF DATA (Yadigaroglu [1975])

(a) Bundle Data

(b) Single Channel Data

(c) References

(a) Transient Post-CHF Data in Rod Bundle (Yadigaroglu [1975])

Reference	Bundle Geometry*	Heater Rod Design **	Vessel geometry	Pressure psia(bar-a)	Initial max rod surface temperature °F(°C)	Peak power generation kW/ft(kW/m)	Inlet coolant temperature † °F(°C)	Flooding rate in./s(mm/s)	Remarks
PWR-FLECHT [5-12]	7x7 and 10x10 bundles d=0.422(10.7) p=0.563(14.3) ℓ=12(3.66) Simulates PWR bundle	F: Nichrome or Kanthal/BN ss-and zr-clad cosine apf=1.65 rpf=1.10	4.2x4.2 in. (107x107 mm) and 5.889 x 5.889 in. (150x150 mm) heated flow housing	15-90 (1-6.2)	800-2200 (430-1200)	0.69-1.40 (2.27-4.6) decays	Subcooling = 16-189 (9-105)	0.6-10 (15-457) constant and variable in two steps	Flow blockages also simulated
PWR-FLECHT low clad temperature tests [14]	10x10 bundle d=0.422(10.7) p=0.563(14.3) ℓ=12(3.66) Simulates PWR bundle		5.889x5.889 in.(150x150 mm) heated flow housing	19-60 (1.3-4.1)	253-754 (123-401)	0.7- 1.2 (2.3-4) decays	139-171 (59-77)	1-6(25-150) constant and variable in two or three steps	Used FLECHT-SET Phase-A Bundle
PWR-FLECHT Top injection Tests [14]				14.7,18.0 (1,1.24)	1100,1400 (593,760)	0.4-0.7 (1.3-2.3) decays	82-190 (28-82)	15.35 gpm (0.95,2.2 litre/s)	
PWR-FLECHT -SET Phase A [14]				19-62 (1.3-4.3)	712-1402 (378-761)	0.4-1.0 (1.32-3.3) decays	153-195 (67-91)	Cold flooding rate variable in two steps: 9 and 1 or 4.5 and 1 (230 and 25 or 115 and 25)	Simulated PWR primary system with one loop and no steam generator
PWR-FLECHT-SET Phase B1 [16]				20,60 (1.4,4.1)	940,1100 (505,595)	0.74, 84,1.05 (2.4,2.8,3.5) decays	150,235,270 (65,113,132)	9 and 1 (230 and 25)	Simulated entire PWR primary system
BWR-FLECHT [59,62-66]	7x7 bundle d=0.570(14.5) p=0.738(18.75) ℓ=12(3.66) simulates BWR/5 bundle	F:Nichrome /MgO ss-clad cosine apf:1.37 rpf:1.21	5.273x5.278 in. (134x134 mm) insulated flow channel	15-300 (1-20.7)	Transient Tests 1300-2150 (700-1180)	0.41-0.665 (1.35-2.18) decays	100 (38)	0.63-6.05 (16-153) constant	Include steady-state reflooding and combined bottom-reflooding and spray cooling tests
				atm	Steady-state Tests	0.042-0.55 (0.14-1.8)			

(a) cont'd.

Reference	Bundle Geometry*	Heater Rod Design**	Vessel geometry	Pressure psia(bar-a)	Initial max rod surface temperature °F(°C)	Peak power generation kW/ft(kW/m)	Inlet coolant temperature † °F(°C)	Flooding rate in./s(mm/s)	Remarks
SECHT I and II [68]	37-rod (square pitch) d=0.58(14.7) p=0.75(19.0) ℓ=3(0.915)	F:Nichrome /Mgo ss-clad uniform	6.065 in. (154 mm) ID pipe	atm	1330-2509 (720-1376)	? constant	100-158 (38-70)	0.9-3.6 (23-92)	All SECHT tests were essentially constant reflooding-rate experiments
SECHT-III [58]	37-rod (square pitch) d=0.57(14.5) p=0.75(19.0) ℓ=6(1.83)	F:Nichrome /Mgo ss-clad uniform		atm	600-2000 (315-1095)	0,0.081,.019 (0,0.25,0.62) constant	100,200 (38,93)	0.45-7.2 (11-183)	
SECHT-IV [69]	37-rod (square pitch) d=0.58(14.7) p=0.75(19.0) ℓ=6(1.83)	F:Nichrome/ Mgo Zr-clad uniform		atm	1000-1800 (540-980)	0.19 (0.62) constant	100 (38)	1.8 (46)	Comparison between stainless-steel and zircaloy-clad heaters
FHUST [71]	3x3 d=0.440(11.2) p=0.580(14.7) ℓ=2.5(0.76)	F: ?/Mgo ss-clad uniform	2.7in(69mm) ID glass cylinder	atm					Visualization tests.
	7x7 d=0.495(12.6) p=0.650(10.5) ℓ=3(0.915)	F: ?/Mgo inconel-clad uniform	6.5x6.5 in (165x165mm) flow housing	atm	1000-1800 (540-980)	0-0.47 (0-1.55) constant	75-200 (24-93)	0.53-8.5 (13-216)	Essentially Constant-flooding-rate experiments
Chalk River Nat'l Lab, Thompson [72]	18-rod CANDU-type cluster d=0.775(19.7) p=0.805-0.815 (20.4-20.7) ℓ=6.3(1.92)	F:chromalox /Mgo ss-clad uniform	~ 4in(100mm) ID pressure tube flow housing	atm	300-1200 (150-650)	0.12-0.49 (0.4-1.6) constant	40,160 (5,71)	1-9 (25-228)	Bundle inversion and forced-reflooding tests

(a) cont'd.

Reference	Bundle Geometry*	Heater Rod Design**	Vessel geometry	Pressure psia(bar-a)	Initial max rod surface temperature °F(°C)	Peak power generation kW/ft(kW/m)	Inlet coolant temperature † °F(°C)	Flooding rate in./s(mm/s)	Remarks
FIAT-SORIN, Campanile and Pozzi [73]	21 rods (square pitch) d=0.386(9.8) p=0.507(12.9) ℓ=3.89(1.184)	S: inconel uniform	3.06 in (77.8 mm) ID insulated flow housing	atm	Transient Tests: 1470-1830 (800-1000)	0.12-0.63 (0.39-2.1) constant	?	0.2,0.4,0.6 (5.10,15)	Include steady-state reflooding experiments. Conditions for 2300°F maximum cladding limit searched
					Steady-State Tests:	0.5-1.0 (1.5-3.3)			
SIEMENS A.G., Riedle and Winkler [74]	340 rods (square pitch) d=0.423(10.75) p=0.563(14.3) ℓ=9.5(2.900) Simulates Siemens PWR bundle	F: ?/Mgo inconnel-clad cosine apf: 1.43 rpf: #1 (3 zone)	Flow channel of octagonal shape surrounding the bundle	15-87 (1-6	930-1470 (560-800)	0.42-0.84 (1.38-2.77) constant	77-149 (25-65)	1.2-5.1 (30-130)	Heated bundle is parallel with downcomer; bottom and combined top-and bottom-reflooding tests; investigated effect of discharge line restriction.
Hitachi Ltd, Ogasawara et al [76]	7x7 bundle d=0.570(14.5) p=0.738(18.75) ℓ=12(3.66) simulates BWR/5 bundle	F: Nichrome ss-clad cosine apf #1 rpf=1.24 (4-zone)	5.278x5.278 in.(134x134 mm)flow housing	atm	Transient Tests: 600-1280 (315-693)	0.13-0.33 0.42-1.26) decays	59-131 (15-25)	1.06-4.5 (27-115)	Include steady-state reflooding tests
					Steady-state tests:	0.009-0.535 (0.03-1.76)	86-194 (30-90)		

*d = rod OD in. (mm)
p = pitch in. (mm)
ℓ = heated length ft (m)

**
S: skin-heated rods
F: filament-type heaters (Filament/insulation)
ss: stainless steel cladding
zr: zircaloy cladding
apf: axial peaking factor
rpf: radial peaking factor
Uniform or cosine axial heat flux distribution

† or subcooling when indicated

(b) Single Channel Transient Post-CHF Data (Yadigaroglu [1975])

Reference	Heated Channel Geometry *	Heater Design **	Pressure psia(bar-a)	Initial Max Surface Temperature °F (°C)	Peak Power Generation kW/ft (kW/m)	Inlet Coolant temperature † °F (°C)	Flooding Rate in./s (mm/s)	Remarks
Siemens, Schneider and Thomas [74,75]	Tube d_o=0.543(13.8) ℓ=9.8(2.985)	S: Inconel 625 t=0.0236(0.6) 0.079 in. (2mm) thick Al_2O_3 jacket pressed on heater. Uniform	14.5, 51, 73 (1, 3.5, 5)	1020, 1290, 1470 (550, 700, 800)	0.56, 0.66 (1.84, 2.18) constant and stepwise decayed power tests	~120 (~50)	Cold flooding rate 1.7, 3.4, 5.1 (43, 85, 130)	Bottom and top-reflooding tests. Downcover and simulated containment volume included in apparatus. Oscillations observed
CISE Martini and Premoli [61]	Tube d_o=0.828(21.0) ℓ=13.2(4.0)	S: Stainless steel t=0.079(2.0) Uniform	atm	727 - 1252 (386 - 678)	0.72 - 0.88 (2.4 - 2.9)	77 - 194 (25 - 90)	2 - 16 (50 - 400)	
	Annulus d_i=0.530(13.5) d_o=0.828(21.0) ℓ^o=13.2(4.0)	S: Stainless steel External surface heated only t=0.079(2.0) Uniform	atm	1160 - 1360 (630 - 740)	0.67 - 0.78 (2.2 - 2.25)	82 - 196 (28 - 91)	2 - 40 (50 - 1000)	Pressure drop oscillations observed in spite of forced flooding-rate condition.
			68 - 290 (4.7 - 20)	1330 - 1470 (720 - 800)	0.68 - 1.07 (2.25 - 3.5)	84 - 304 (29 - 151)	8 - 16 (200 - 400)	Two quench fronts always observed
Grenoble, Andreoni and Courtaud [78,79]	Annulus d_i=0.787(20) d_o=1.18(30) ℓ^o=3.3(1.0)	Heated rod in unheated annulus S: Stainless steel Uniform	atm	750 - 1650 (400 - 900)	0.19 - 1.15 (0.63 - 3.8)	68 - 194 (20 - 90)	0.8 - 7 (20 - 180)	
	d_i=0.787(20) d_o=1.2(30) ℓ^o=11.8(3.6)		atm	750 - 1650 (400 - 900)	0.57 - 1.15 (1.9 - 3.8)	68 - 194 (20 - 90)	1 - 7 (25 - 180)	
	d_i=.402(10.2) d_o=.787(20) ℓ^o=13.2(4.0)	F: Kanthal/MgO Inconel clad Uniform	atm	750 - 1300 (400 - 700)	0.29 - 0.49 (0.96 - 1.6)	~68 (~20)	2 - 7 (50 - 180)	
Grenoble, Andreoni, Courtaud and Dervaz [80]	Tube d_o=0.539(13.7) ℓ=10.7(3.275)	S: Inconel t=0.17(4.4) Uniform	(14.5,43.5, 87) (1,3,6)	570,1100,1650 (300,600,900)	0.39,0.65, 0.91 (1.29,2.15, 3.0)	Inlet:Subcooling 36, 90, 144 (20, 50, 80)	2.0,3.0,4.7, 7.0 (50,75,120, 179)	
Central Electricity Generating Board, White and Duffy [77]	Annulus d_i=0.56(14.2) d_o= 0.76(19.3) ℓ^o=1.50(.457) silica shroud	F: Stainless steel Boron nitride t=0.025(0.635) Uniform	atm	752, 1292, 1832 (400, 700, 1000)	0.59 (1.93)	68, 140	0.4 - 7.3 (11 - 186)	Test section in parallel with downcomer; variable test section. Outlet resistance (range from K=15 to 26,000) Oscillation observed Comparison to forced-flooding rate experiments.

*d_i= rod OD in. (mm) d_o= annulus ID in. (mm) ℓ=heated length ft (m)

**S: Skin-heated rods t=heater(clad) thickness in. (mm)
F: filament-type heaters (Filament/Insulation)
Uniform or cosine axial heat flux distribution

† or inlet subcooling when indicated

(c) References - APPENDIX II

5. J.C. Haire and G.F. Brockett, "Pressurized Water Reactor - Full Length Emergency Cooling Heat Transfer (PWR - FLECHT) Tests Project," IN-1386 (April 1970).

6. J.L. O'Brien, Jr. (ed.), "Full-Length Emergency Cooling Heat Transfer Tests (FLECHT) Conceptual Design," WCAP-7200 (May 1968).

7. J.O. Cermak, et al., "PWR FLECHT Final Test Plan," WCAP-7228 (January 1969).

8. J.O. Cermak, et al., "PWR FLECHT GROUP I TEST REPORT," WCAP-7435 (January 1970).

9. J.H. Berlinghoff, J.F. Mellor, and A.P. Suda, "PWR FLECHT Interim Materials Evaluation Report," WCAP-7444 (January 1970).

10. F.F. Cadek, et al., "PWR FLECHT Group II Test Report," WCAP-7544 (September 1970).

11. F.F. Cadek, et al., "PWR FLECHT (Full Length Emergency Cooling Heat Transfer) - Final Report," WCAP-7665 (April 1971).

12. F.F. Cadek, et al., "PWR FLECHT Final Report Supplement," WCAP-7931 (October 1972).

14. J.A. Blaisdell, L.E. Hochreiter, and J.P. Waring, "PWR FLECHT-SET Phase A Report", WCAP-8238 (December 1973).

16. J.P. Waring, et al., "PWR FLECHT-SET Phase B1 Data Report", WCAP-8431 (December 1974).

58. C.M. Moser and R.W. Griebe, "SECHT III - An Experimental Investigation of Top and Bottom Flooding of a Nuclear Bundle Simulator," IN-1355 (February 1970).

59. F.A. Schraub and J.E. Leonard, "Core Spray and Core Flooding Heat Transfer Effectiveness in a Full-Scale Boiling Water Reactor Bundle," APED 5529 (June 1968).

61. R. Martini and A. Premoli, "Bottom Flooding Experiments with Simple Geometries under Different E.C.C. Conditions," Energia Nucleare, 20, 540 (1973).

62. J.C. Haire and G.F. Brockett, "Boiling Water Reactor - Full Length Emergency Cooling Heat Transfer (BWR-FLECHT) Test Project" IN-1385 (June 1970).

63. J.D. Duncan and J.E. Leonard, "Response of a Simulated BWR Fuel Bundle Cooled by Flooding Under Loss-of-Coolant Conditions," GEAP-10117 (December 1969).

64. J.D. Duncan and J.E. Leonard, "BWR Standby Cooling Heat Transfer Performance Under Simulated Loss-of-Coolant Conditions between 15 and 300 psia," GEAP-13190 (May 1971)

65. J.D. Duncan and J.E. Leonard, "Emergency Cooling in BWR's Under Simulated Loss-of-Coolant Conditions (BWR-FLECHT Final Report)," GEAP-13197 (June 1971).

66. R.W. Griebe and J.W. McConnell, "Boiling Water Raactor - Full Lenght Emergency Core Cooling Heat Transfer (BWR-FLECHT) Tests Project Final Report on Atmospheric Pressure Stainless Steel Experiments," ANCR-1115 (November 1973).

68. L.D. Schlenker et al., "Interim Report on SECHT Series I and II Tests and Analysis," IDO-17278 (August 1968).

69. J.L. Plum, "SECHT-IV Performance Evaluation of Stainless Steel and Zircaloy-Clad Electrically Powered Heaters," IN-1378 (June 1970).

71. R.T. Jensen, "Experimental Results of the Fuel Heatup Simulation Tests (FHUST) - Emergency Core Cooling Test Series," IN-1390 (September 1970).

72. T.S. Thompson, "Simulated Bottom-Flooding Emergency Cooling of a Close-Spaced Rod Bundle," European Two-Phase Flow Group Meeting, Casaccia (June 6-8, 1972).

73. A. Campanile and G.P. Pozzi, "Low Rate Emergency Reflooding Heat Transfer Tests in Rod Bundle," Proceedings of the CREST Specialist Meeting on Emergency Core Cooling for Light Water Reactors, Garching/München, October 18-20, 1972, MRR 115, Volume 1.

74. K. Riedle and F. Winkler, "ECC-Reflooding Experiments with a 340-Rod Bundle," Proceedings of the CREST Specialist Meeting on Emergency Cooling for Light Water Reactors, Garching/Munchen, October 18-20, 1972, MRR 115, Volume 1.

75. Schneider and Thomas, "Further Development of the Technology of Light Water-Cooled Reactors - Project 2b - Cooling Conditions of the Reactor Core in the Case of the Maximum Credible Accident During Refilling by the Safety Feed System - Final Report," AEC-tr- 7396 (February 1973).

76. H. Ogasawara, S. Kashiwai and Y. Takashima, "Cooling Mechanism of the Low Pressure Coolant Injection System of Boiling Water Reactors and Other Studies on the Loss-of-Coolant Accident Phenomena," Topical Meeting on Water Reactor Safety, Salt Lake City, Utah, March 26-28, 1973, CONF-730304, pp. 351-370.

77. E.P. White and R.B. Duffey, "A Study of the Unsteady Flow and Heat Transfer in the Reflooding of Water Reactor Cores," Central Electricity Generating Board Report RD/B/N3134 (September 1974).

78. D. Andréoni, "Refroidissement de Secours des Réacteurs Nucléaires," Note TT No. 404, Centre d'Etudes Nucléaires de Grenoble (April 1972).

79. D. Andréoni and M. Courtaud, "Study of Heat Transfer During the Reflooding of a Single Rod Test Section," Proceedings of the CREST Specialist Meeting on Emergency Core Cooling for Light Water Reactors, Garching/München, October 18-20, 1972, MRR 115, Volume 1.

80. D. Andréoni, M. Courtaud and R. Deruaz, "Heat Transfer during the Reflooding of a Tubular Test Section," European Two-Phase Flow Meeting, Harwell, 3-7 June 1974.